Reliability-Based Design in Geostructural Engineering

by

Nico de Koker

Dissertation presented for the degree of Doctor of Philosophy in Civil Engineering in the Faculty of Engineering at Stellenbosch University

Supervisor:	Prof. P.W. Day
Co-supervisor:	Prof. C. Viljoen

December 2018

Declaration

By submitting this dissertation electronically, I declare that the entirety of the work contained therein is my own, original work, that I am the sole author thereof (save to the extent explicitly otherwise stated), that reproduction and publication thereof by Stellenbosch University will not infringe any third party rights and that I have not previously in its entirety or in part submitted it for obtaining any qualification.

This dissertation includes three original papers published in peer-reviewed journals. The development and writing of the papers were the principal responsibility of myself and declarations are included in the dissertation indicating the nature and extent of the contributions of co-authors.

Date: ......December 2018..........

i

Abstract

Current standards used in South African geotechnical design practice follow the partial factor limit states design approach. Although partial factors used in this approach are calibrated for standardised target reliability levels, the approach does not take direct account of the probability of failure. Probabilistic reliability analysis provides additional insight to practitioners, making for potentially more optimal geotechnical structures.

The technical committee responsible for drafting the South African geotechnical design standard has been requested by representatives of the geotechnical community to consider including standardised guidelines to reliability based geostructural design. As background research towards compiling the pre-normative report for such a set of guidelines, the use of reliability analysis in geostructural design needs to be considered in the context of the following problems.

Firstly, the reliability analysis techniques appropriate to different geostructural design problems – a design standard can only be successful if the analysis methods are sufficiently accurate, robust, and practical to apply. Secondly, the appropriate statistical descriptions of the various model parameters – reliability analysis of civil structures is extrapolatory by nature, and so is very sensitive to the choice of functional form (distribution) and the values used to constrain its parameters. Thirdly, the minimum requirements on sample quality – sophisticated reliability analysis techniques have little value if parameter values are based on biased samples that are not representative of the material upon which the structure is to be founded.

This thesis presents a number of studies associated with the issues listed above, from which it is concluded that geostructural design to a target reliability is possible, provided that the resistance model and the statistics describing its parameters are accurate and unbiased. However, it is shown that for this to be achieved, samples consisting of a greater number of specimens than currently used in routine geotechnical practice would be required, while the distribution types used to represent the various geotechnical material parameters should be standardised. Of the range of reliability analysis techniques available, the variants of the first order reliability method (FORM), in combination with an analytical surrogate performance function (response surface) where required, are shown to provide the best balance of transparency, economy, and accuracy.

Oorsig

Geostrukturele ontwerpstandaarde wat tans in die Suid Afrikaanse praktyk gebruik word, volg die parsiële faktor limietstaatontwerp benadering. Hoewel die faktore in dié benadering teen gestandaardiseerde teikenbetroubaarheidsvlakke gekalibreer is, word die faalwaarskynlikheid nie direk in ag geneem nie. Betroubaarheidsanalise en -ontwerp met 'n direkte waarskynlikheidsgrondslag bied die praktisyn dieper stogastiese insig, wat potensieel meer optimale geotegniese struktuurontwerp kan bewerkstellig.

Die tegniese komitee verantwoordelik vir die opstel van die Suid Afrikaanse geotegniese ontwerpstandaard, is deur verteenwoordigers van die geotegniese ingenieursprofessie versoek om die insluiting van gestandaardiseerde riglyne vir betroubaarheidsontwerp te oorweeg. As grondslag vir die verwante konsepverslag is dit nodig om geostrukturele betroubaarheidsontwerp in die konteks van die volgende probleme te oorweeg.

Eerstens, die metodes vir betroubaarheidsanalise van verskeie geostrukturele ontwerpsprobleme – 'n ontwerpstandaard kan slegs suksesvol wees met akkurate, veelsydige, toepasbare analise metodes. Tweedens, die gepaste statistiese beskrywings vir die verskeie modelparameters – betroubaarheidsanalise van siviele strukture is uiteraard ekstrapolerend, en dus baie sensitief vir die keuse van verdelingstipe en parameterwaardes. Derdens, die vereiste steekproefgrootte en -kwaliteit – gevorderde betroubaarheidsanalise is van min nut wanneer parameterwaardes sydig en nie verteenwoordigend van die struktuur se onderliggende grondlaag is nie.

Hierdie tesis bevat 'n stel navorsingstudies gemik op dié vrae, en bevind dat geostrukturele ontwerp teen 'n teikenbetroubaarheidsvlak uitgevoer kan word, mits die weerstandsmodel én die statistiese beskrywing van parameters, akkuraat en onsydig is. Dít is egter slegs moontlik met meer steekproefwaardes as wat tans die norm in die praktyk is, terwyl verdelingstipes vir die verskeie geotegniese parameters gestandaardiseer behoort te word. Uit die verskeidenheid metodes vir betroubaarheidsanalise is bevind dat die verskillende vorme van die lineêre betroubaarheidsmetode ('first order reliability method', FORM), waar nodig gekombineer met 'n vervangde limietstaatfunksie (responsoppervlak), die optimale balans van duidelikheid, doeltreffendheid, en akkuraatheid bied.

Acknowledgements

The origins of this thesis can certainly be said to lie in chance. My research interests had been drifting towards the application of statistics in engineering for a number of months when I found myself in Peter Day's sunny office, discussing his interest in reliability based design. Soon followed a visit to Celeste Viljoen and Johan Retief in Stellenbosch where the idea for this thesis emerged.

However, what cannot be ascribed to chance, was the support and encouragement I received from my parents, Johan and Verelene, during the course of my change in direction. The privilege of being their son has been a stroke of extremely good fortune. I can only hope for a chance to pay it forward to future students and colleagues.

Contents

List of Figures

List of Tables

Acronyms

CDF	Cumulative Distribution Function
DA	Design Approach
EN	European Standard (Europäische Norm)
FEA	Finite Element Analysis
FORM	First Order Reliability Method
FOSM	First Order Second Moment
ISO	International Organisation for Standardisation
JCSS	Joint Committee on Structural Safety
LMFD	Load and Material Factor Design
LRFD	Load and Resistance Factor Design
LSD	Limit States Design
NR-FORM	Newton-Raphson FORM
PDF	Probability Distribution Function
PEM	Point Estimate Method
pfLSD	Partial Factor Limit States Design
pRBD	Probabilistic Reliability Based Design
RBD	Reliability Based Design
RS-FORM	Response Surface FORM
SAICE	South African Institution of Civil Engineering
SANS	South African National Standard
SPT	Standard Penetration Test
WSD	Working Stress Design

Chapter 1

Reliability in Geostructural Design Standards

1.1   Introduction

Engineering design has, as its primary goal, the development of safe solutions that are economical, efficient, robust, and practical. Indeed, maintaining this balance remains one of the primary drivers of innovation in engineering research.

Starting from the earliest attempts at structural design, the principal means of ensuring safety has been to overcompensate for the most severe expected loading conditions by means of safety factors. Historically, this approach has also inadvertently compensated for flawed theoretical descriptions of mechanics used in structural design (e.g. Galilei, 1638; Petroski, 1994). However, with progressive experience and improvements in design methodology, reasonably robust values for safety factors emerged (Meyerhof, 1995). This design philosophy is embodied in the permissible stress method, in which a single safety factor is used.

By accounting for reasonable upper/lower limits on loads, this use of a factor of safety can be intuitively understood to decrease the probability of failure of the design. The statistical interpretation of safety factors was formalised with the development of mathematical statistics, as part of the theory for structural reliability (Freudenthal, 1947; Freudenthal and Gumbel, 1953; Pugsley, 1955).

In this probabilistic context the inefficiency of using a single factor of safety in design also becomes apparent. Multiple failure modes are generally associated with designs of realistic complexity, each with a unique ensemble of relevant load cases and controlling material properties. Partial factor limit states design (pfLSD; Figure 1.1) attempts to address this discrepancy by associating unique factors with each load and/or material resistance property, to reflect the likelihood of variation in their values.

However, pfLSD does not account for variations in the probability of failure with changes in the parameters used in the assessment of load and resistance. As a result, design scenarios for distinct parameter values will satisfy reliability requirements only in the sense of exceeding a minimum acceptable level of reliability (Phoon *et al.*, 2011).

The current South African loading standard (SANS 10160-1:2010), which is based on the Eurocode specification (EN 1990:2002; EN 1991:2002; EN 1997:2004), uses pfLSD methods in which partial factors are applied to individual load components and resistance parameters. While the standard provides guidance on the factors to be used for loading during the design of geostructures, there is not currently a standard covering the material resistance or the geostructural design itself. Some practitioners use EN 1997:2004 for this purpose, although it is not optimised for South African reliability requirements.

While pfLSD remains a margin of safety method, it combines practical experience with reliability analyses to determine factor magnitudes (Holicky *et al.*, 2010). Because EN 1990:2002 and SANS 10160:2010 have a strong foundation in reliability through probabilistically informed parameter calibration, they are often referred to as semi-probabilistic codes.

An alternative to these adjusted safety margin design approaches, is to base the optimal design directly on a target probability of failure, i.e. base the design decisions directly on a calculation of the reliability level, instead of indirectly via pre-calibrated partial factors.

This approach, probabilistic reliability-based design (pRBD), is currently not frequently used in geostructural design practice, but has been extensively explored in the research literature (e.g. Phoon *et al.*, 2003; Phoon, 2008*b*; Phoon and Ching, 2015). While factors such as computational burden and inertia of expertise certainly play a role, the absence of provisions for the technique in national standards is, no doubt, also a contributor – designers choosing to follow a methodology not codified in national standards have less legal protection should failure occur, be it due to errors in the design or elsewhere.

Through the Geotechnical Division of the South African Institution of Civil Engineering (SAICE), the South African geotechnical community has decided to adopt EN 1997:2004, with a new national annex, as geotechnical design code citepDay2017a. Notable interest was also expressed for inclusion of the pRBD methodology in the future standard. General principles for standardised reliability based design are given by ISO 2394:2015. The intention of this project is to provide the bulk of the background research necessary for the development of the pre-normative report necessary to realise this process.

The emphasis of this design standard would be the resistance capacity of structures in a geotechnical context (spread footings, piles, retaining walls, slopes). Other problems commonly dealt with by geotechnical engineers (settlement, consolidation, seep, filtration) are not included in its scope. This thesis therefore uses the term 'geostructural engineering' to differentiate this structural focus of the design process under consideration.

1.2 Reliability-Based Design in Geotechnical Loading and Design Standards

The current specifications for structural loading used in South Africa (SANS 10160:2010), provides a set of partial factor values, with associated combination factors, for the various loading types considered in South African design practice. The code is based on the Eurocodes (EN 1990:2002; EN 1997:2004), which provides a common framework within which individual EU countries base their detailed design specifications in the form of National Annexes.

The Eurocode has a strong reliability basis, derived from the guidelines for structural reliability and risk management detailed in ISO 2394:2015, and the specifications set forward by the Joint Committee on Structural Safety (JCSS) probabilistic model code (JCSS, 2008a).

ISO 2394:2015 identifies target reliability levels for different combinations of cost and consequences of failure, expressed either in terms of an annual probability of failure, or in terms of a 50-year lifetime for the structure. Both EN 1997:2004 and SANS 10160:2010 parameterise the specified partial factors to target reliability levels using the techniques of reliability analysis discussed in the preceding section. These values are supplemented by extensive experiential input, with the result that the codes differ in their base target levels: a reliability index of $\beta = 3.0$ is deemed sufficient for South African conditions (Retief and Dunaiski, 2010), compared to the more conservative value of $\beta = 3.8$ used in the Eurocodes (Gulvanessian, 2010). This difference in target β values is one of the primary reasons why a South African national annex to EN 1997:2004 would be preferable to using, say, the NA to BS EN 1997:2004.

These codes are not unique in having a direct foundation in reliability. The loading specifications in use in the USA (ASCE 7:2002; AASHTO:2002), and Canada (CHBDC CSA S6:2000) are similarly founded on the principles of reliability. However, while all these codes are reliability-based, they do not provide guidelines on the application of probabilistic techniques to directly assess the reliability of a design. The only available guidance for the application of probabilistic reliability techniques in geotechnical and structural design is given in Appendices D and E of ISO 2394:2015, with the primary aim of partial factor calibration, rather than direct applications in design.

The progressive increase in the extent to which structural loading standards have a reliability basis is facilitated by the increase in the availability of quantitative data and historical records. It is therefore not surprising that the first infrastructure safety standard to directly apply probabilistic reliability calculations was recently announced, providing safety standards for flood barriers in the Netherlands (Jonkman and Schweckendiek, 2015).

This trend is reflected in the geotechnical design literature, where notable interest in pRBD is evident (e.g. Christian *et al.*, 1994; Duncan, 2000; Phoon, 2008b; Phoon and Ching, 2015).

1.3 Probabilistic Reliability-Based Design

Although pfLSD is routinely applied in geotechnical practice, it does have a number of limitations that suggest the utility an alternative approach would provide. The choice of parameter values used in the design (characteristic values), is inconclusive for many geotechnical problems. This problem is compounded when the same property has both stabilising and destabilising effects in different parts of a geostructure (e.g. retaining walls). Furthermore, the probability of failure depends on the parameter values assumed, so that partial factor values are calibrated to meet minimum reliability requirements across a range of parameter values. As a result, design solutions are seldom optimal for a given site. The pfLSD paradigm also poses a challenge when practitioners are faced with unusual problems that fall outside the scope of loading, material parameters, and risk profile assumed in calibration of these codes. In addition, because the method treats all elements in a system as independent, it provides no means of analysing redundancy or interaction of failure modes.

As a result of the large degree of uncertainty and variability present in describing the properties of the soil upon which a structure is to be founded, the use of statistics in the design process has long been of interest to geotechnical engineers (Duncan, 2000; Baecher and Christian, 2003). Early studies based reliability analyses on relatively simple techniques (e.g. Christian *et al.*, 1994; Duncan, 2000), in which crude assumptions regarding the distribution of parameters are made. As the reliability levels that characterise civil structures correspond to relatively small failure probabilities ($10^{-3} - 10^{-4}$), these techniques end up making very large extrapolations using overly simplified representations. As a result, their estimates of failure probability are often off by multiple orders of magnitude (fortunately towards the conservative side Barratt and Day, 2016), to the extent that the utility of the results is questionable.

More recent studies of geotechnical reliability adopted the analysis techniques developed in structural engineering, notably the first order reliability method (FORM, Hasofer and Lind, 1974; Rackwitz and Fiessler, 1978), with more reasonable results (e.g. Forrest and Orr, 2011; Pereira and Caldeira, 2011). Indeed, FORM is the primary method used by structural engineers for reliability-based partial factor calibration (ISO 2394:2015; JCSS, 2008*a*; Holicky *et al.*, 2010; Holicky and Retief, 2005).

The extent to which a given reliability method provides an accurate answer can be determined by comparison to the reliability determined using the Monte-Carlo technique. The simple utility of the Monte-Carlo technique for determining the failure probability for closed form geostructural problems is well known (Baecher and Christian, 2003). To clarify, in closed form problems the resistance capacity can be determined analytically, while non-closed form problems require the use of iterative numerical solution methods. In principle, Monte Carlo provides the most direct determination of the probability of fail-

ure, yet its suitability as a geostructural design tool is limited for non-closed form problems, as it requires in excess of 10^5 resistance capacity evaluations, a number which increases significantly when higher levels of reliability are specified (e.g. Phoon, 2008*a*, see Chapter 2).

While alternative schemes have been proposed (e.g. Simpson *et al.*, 1981; Honjo *et al.*, 2010; Ching and Phoon, 2011), the pfLSD framework used in EN 1990:2002 and SANS 10160:2010 makes use of the concept of a 'characteristic' value – effectively reflecting a confidence level-based bound on the expected value of the parameter in question. With geotechnical parameters often showing large variability (Vanmarcke, 1977; Phoon *et al.*, 1995; Phoon and Kulhawy, 1999), and the nature of geotechnical failure reflecting integration over these variations along the failure plane, judgement in the choice of the characteristic values is left to the practitioner.

Both partial factor and probabilistic design techniques require the statistical nature of parameters to be well understood, notably the variable soil properties that contribute to determination of the resistance capacity. This point is not emphasised often enough: the statistical parameters, which are chosen based on samples taken from site, have a notable effect on the final design and, by association, the extent to which its true reliability conforms to the target value.

1.4 Standardising Reliability Based Geostructural Design

As noted in Section 1.1, the technical committee responsible for drafting the South African geotechnical design standard has been requested by representatives of the South African geotechnical community to consider including a reliability based design option (Day, 2017*a*). Successfully compiling such a design standard option would require greater insight and guidelines on the following factors.

1. Identifying appropriate reliability analysis techniques. As noted above, a number of different techniques have been developed, offering varying degrees of tradeoff between accuracy, computational effort, and computational complexity. A design standard can only be successful if the analysis methods are sufficiently accurate, robust, and practical to apply.

2. Establishing the appropriate statistical descriptions of the various model parameters. Reliability analysis of civil structures is extrapolatory by nature, and so is very sensitive to the choice of functional form (distribution) and its parameters used.

3. Determining the minimum requirements on sample quality. The data used to determine parameter statistics are only as accurate as the samples

from the stratum in question will allow. Sophisticated reliability analysis techniques are worthless if parameter values are based on biased samples that are not representative of the material upon which the structure is to be founded.

Five research chapters will explore these issues, and are presented in Chapters 3 to 7. Chapter 2 provides a brief review of the necessary statistical foundations and an overview of reliability theory.

The performance of reliability analysis is assessed in Chapter 3 for a variety of benchmark geostructural problems, after which Chapter 4 considers the merits of an ongoing debate on the design of eccentrically loaded spread footings from a reliability perspective. Both Chapters 3 and 4 consider closed-form descriptions of the assessment of failure; Chapter 5 builds on this work by exploring the suitability of the various analysis techniques for slope stability, a very common non-closed form geostructural problem.

The parameters used in reliability analysis are considered in Chapter 6 in the context of Bayesian updating as a potential means of augmenting the typically small sample sizes that are routinely used in geotechnical practice, in an effort to provide clarity on the extent to which prior knowledge can be incorporated into parameter values. With the small sample sizes identified as a particular obstacle to accurate parameter values, decision theory and risk analysis are applied in Chapter 7 to determine how large the sample size needs to be for reliability based design to be meaningful.

Finally, Chapter 8 summarises the findings of these research studies into a set of guidelines to be considered for assembly of a reliability based geostructural design standard.

1.5   Scope of the Study

Structural reliability is a broad field of research. This thesis primarily considers the viability of a standardised set of guidelines for the application of reliability in geostructural design in practice. To limit the discussion to the most salient factors, a number of topics that are either primarily academic interest, or insufficiently developed in a geotechnical context, are not considered in great detail. Most notably, these include:

1. An extensive consideration of the bias and lack of precision in resistance models. However, the limitations to standardisation introduced by model uncertainty, will be discussed in Chapter 8.

2. Direct applications of load test data in reliability determinations. Instead the focus will be the various physics-based resistance models used in geostructural design.

3. Finite-element analyses of geotechnical and geostructural problems, including problems where spatial variation of the subsurface is modeled in a random fields context.

4. Problems where multiple failure modes are comparably critical, and similarly, systems-type problems where the failure multiple components are involved.
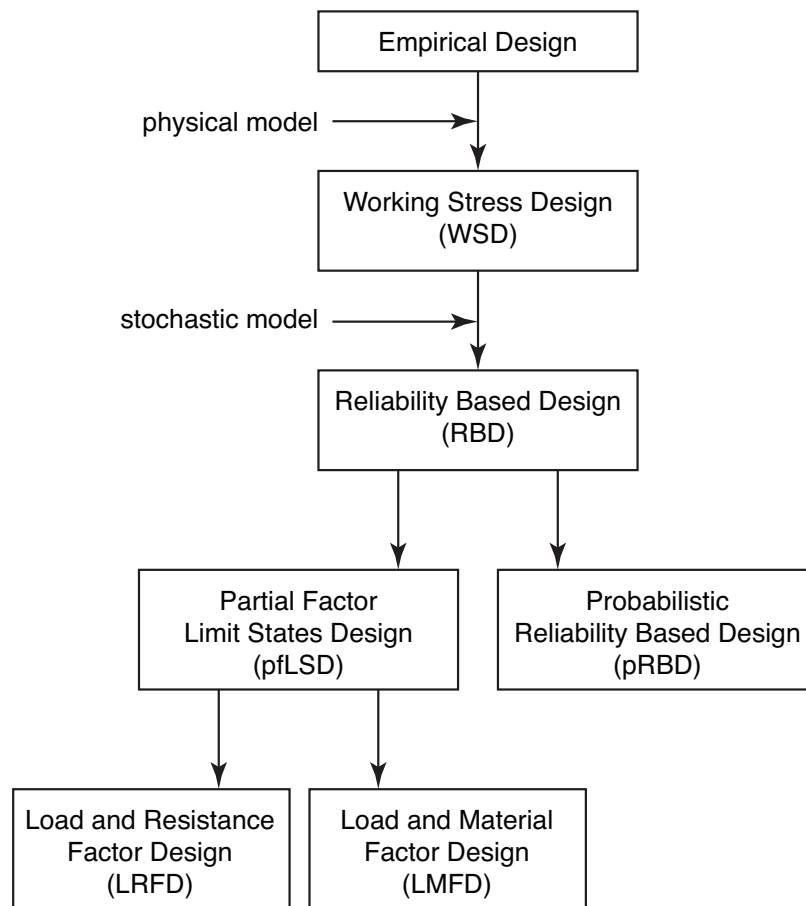
Figure 1.1: Hierarchy of design methodologies. Both pfLSD and pRBD have a reliability foundation.

Chapter 2

Review of Mathematical Statistics for Reliability Analysis

Notation

a, b, d	constant values
$\mathbf{C}$	covariance matrix
E	load effect
$E()$	expected value operator
$F()$	cumulative density function
$f()$	probability density function
$g()$	generic function
g	performance function
$\mathbf{L}$	lower triangular matrix
n	number of values
N	number of dimensions or variables
$P()$	probability operator
p, p_f	probability, probability of failure
R	resistance capacity
$\mathbf{R}$	correlation matrix
$\mathbb{R}$	the set of real numbers
u	uncorrelated standard normal variable
$\mathbf{u}$	uncorrelated standard normal vector
u^*	design point in standard normal space
$V()$	variance operator
X	generic random variable
x	instance of a random variable
$\mathbf{x}$	vector of random variable values
Z	standard normal random variable
z	instance of a standard normal random variable

α	level of confidence
α_i	direction cosine of ith component of u^*
β	reliability index
$\Gamma()$	gamma function
γ_e	Euler-Mascheroni constant, $0.577216\ldots$
δ	coefficient of variation
ϵ	tolerance
ζ	scale parameter of the Γ distribution
η_α	interval factor corresponding to confidence α
κ	shape parameter of the Γ distribution
λ	measure of location
μ	mean
μ	vector of mean values
ν	number of degrees of freedom
ξ	measure of spread
ρ	correlation coefficient
σ	standard deviation
σ	vector of standard deviation values
$\Phi()$	standard normal cumulative distribution function
$\sim \Gamma$	gamma distributed
$\sim$ Gumbel	Gumbel distributed
$\sim$ LN	log-normally distributed
$\sim$ N	normally distributed
$\sim$ Uni	uniformly distributed

2.1   Introduction

The research chapters in this thesis assume that the reader has a reasonable background knowledge of statistics. The intention of this chapter is to give an overview of the statistical concepts relevant to reliability analysis, and to explain the basic framework of the theory of reliability. A number of texts provide deeper discussions of the various concepts. Montgomery and Runger (2014) and Hald (1952) provide very good introductions to statistics relevant to research in engineering and physical sciences. Ang and Tang (1984) focus more specifically on concepts around failure in structural engineering. Ditlevsen and Madsen (1996) and Harr (1987) specifically discuss the theory of reliability. Press *et al.* (2007) gives a clear and accessible discussion of the numerical implementation of the various functions and algorithms associated with reliability analysis.

2.2   Review of Basic Concepts

Probability as an expected fraction – Probability is a central concept in the description of uncertainty. In a technical context it is most readily described as the fraction of trial events that meet a predetermined criterion. That is

$$p = \frac{n_{\text{success}}}{n_{\text{total}}}, \tag{2.1}$$

with the immediate implication that $0 \leq p \leq 1$.

Random variable – A variable measure with outcomes or values that are stochastic, i.e. not deterministic. Any random variable will be characterised by (i) point parameters, and (ii) a distribution function. To satisfy the requirement of probability values, the variable must also have a defined range of possible values it can take, though this does not have to be limited to a finite set.

Population vs. sample – If a set of random variable values includes all its possible realisations, that set is the *population*. In general, it is not possible or not practical to determine the entire population. Instead, it is characterised by taking a *sample*. It is important that the sample be representative of the population. This is most readily achieved by ensuring that a sample is random, i.e. not influenced by bias on the part of the sampler.

Statistical notation – When dealing with random variables, it is customary to use greek letters to denote population parameters, and roman letters for sample parameters. Capitals denote the random variable as a stochastic entity, and lower case indicates a specific realisation of the random variable.

Parameters of a random variable – Point parameters that summarise the characteristics of a random variable include measure of location (mean μ) and measures of dispersion (standard deviation σ, variance σ^2). Though often treated as fixed, these are random variables as well, for which values are estimated using sample statistics ($\overline{x}$ and s^2).

Distribution functions of a continuous random variable – Distribution of the random variable defined in terms of relative probability, expressed via the $f(x)$, probability density function (PDF), such that

$$P(a \leq X \leq b) = \int_a^b f(x)dx, \tag{2.2}$$

and $F(x)$, the cumulative distribution function (CDF),

$$F(x) = P(X \leq x) = \int_{-\infty}^x f(x')dx'. \tag{2.3}$$

Expected value of a random function – The most likely value a function of a random variable can take is defined in terms of the PDF

$$E(g(x)) = \int_{-\infty}^{\infty} g(x)f(x)dx. \tag{2.4}$$

Two special cases are $g(x) = x$, from which follows the mean $E(x)$, and $g(x) = (x - \mu)^2$, which gives the variance $V(x)$. This implies that

$$V(x) = E(x^2) - E(x)^2, \tag{2.5}$$

and that

$$E(x + y) = E(x) + E(y), \qquad V(x + y) = V(x) + V(y). \tag{2.6}$$

Intervals of a random variable – A confidence interval gives a one- or two-sided bracket on the values a random variable can take with a given amount of confidence. Let X be some random variable with μ and σ known. We are interested in the range of possible values X can take. With a $1 - \alpha$ level of confidence, upper- or lower bounds (one sided) on the value of X are

$$x_\alpha = \mu + \eta_\alpha \sigma = \mu \left(1 + \eta_\alpha \delta\right), \qquad \delta = \sigma/\mu \tag{2.7}$$

Bayesian vs. frequentist views of statistics – There are two interpretations of the mathematical description of uncertainty. The frequentist view considers the sample as a random instance of a fixed (defined, but unknown) population distribution, while the Bayesian perspective recognises the sample as known information, and the population description as uncertain.

2.3 Distributions of Random Variables

2.3.1 Distributions for Geostructural Reliability

A number of distribution types will be used in the research chapters to follow. For reference, their definitions are summarised below. Note the notation '$\sim$', which is shorthand for 'is distributed as'.

Continuous Uniform Distribution – All values of a random variable X in the range $[a, b] \in \mathbb{R}$ has equal probability density.

$$X \sim \mathrm{Uni}(a, b), \qquad a \leq x \leq b, \tag{2.8}$$

$$f(x) = 1/(b - a), \tag{2.9}$$

$$F(x) = (x - a)/(b - a), \tag{2.10}$$

$$E(x) = \tfrac{1}{2}(a + b), \qquad V(x) = \tfrac{1}{12}(a - b)^2. \tag{2.11}$$

Normal Distribution – Results from additive or averaging processes.

$$X \sim \mathrm{N}(\mu, \sigma^2), \qquad -\infty < x < \infty, \tag{2.12}$$

$$f(x) = \frac{1}{\sqrt{2\pi\sigma^2}} \exp\left(-\frac{(x - \mu)^2}{2\sigma^2}\right), \tag{2.13}$$

$$F(x) = \frac{1}{2}\left[1 + \mathrm{erf}\left(\frac{x - \mu}{\sqrt{2\sigma^2}}\right)\right]. \tag{2.14}$$

Important Special Case: **Standard Normal Distribution** – If X is a random variable such that

$$X \sim \mathrm{N}(\mu, \sigma^2), \tag{2.15}$$

and Z is a random variable with

$$Z = \frac{X - \mu}{\sigma}, \tag{2.16}$$

then

$$Z \sim \mathrm{N}(0, 1), \qquad -\infty < z < \infty. \tag{2.17}$$

$$f(z) = \frac{1}{\sqrt{2\pi}} \exp\left(-\frac{z^2}{2}\right), \tag{2.18}$$

$$F(z) = \Phi(z) = \frac{1}{2}\left[1 + \mathrm{erf}\left(\frac{z}{\sqrt{2}}\right)\right]. \tag{2.19}$$

Log-Normal Distribution – Results from geometrically averaged processes, and is often used to enforce $X > 0$. If X is a random variable such that

$$\ln X \sim \mathrm{N}(\lambda, \xi^2), \tag{2.20}$$

then

$$X \sim \mathrm{LN}(\mu, \sigma^2), \tag{2.21}$$

where

$$\lambda = \ln\left(\mu / \sqrt{(1 + \delta^2)}\right), \tag{2.22}$$

$$\xi^2 = \ln\left(1 + \delta^2\right), \tag{2.23}$$

$$\delta = \sigma / \mu, \tag{2.24}$$

subject to

$$0 < x < \infty. \tag{2.25}$$

The distribution function is

$$f(\ln x) = \frac{1}{\sqrt{2\pi\xi^2}} \exp\left(-\frac{(\ln x - \lambda)^2}{2\xi^2}\right), \tag{2.26}$$

so that

$$f(x) = \frac{1}{x} f(\ln x). \tag{2.27}$$

Gumbel Distribution – Extreme value distribution for any parent distribution with an exponential tail (see Ang and Tang, 1984, chapter 4). Also referred to as a Type I extreme value distribution.

$$X \sim \text{Gumbel}(\mu, \sigma^2), \qquad -\infty < x < \infty, \tag{2.28}$$

$$f(x) = \frac{1}{\xi} \exp\left[-\frac{x-\lambda}{\xi} - \exp\left(-\frac{x-\lambda}{\xi}\right)\right], \tag{2.29}$$

$$F(x) = \exp\left[-\exp\left(-\frac{x-\lambda}{\xi}\right)\right], \tag{2.30}$$

with

$$\lambda = \mu - \xi\gamma_e, \qquad \xi^2 = (6/\pi^2)\sigma^2, \tag{2.31}$$

where $\gamma_e = 0.577216\ldots$ is the Euler-Mascheroni constant.

Γ Distribution – Relevant to the distribution of the inverse variance $1/\sigma^2$, also called the 'precision'.

$$X \sim \Gamma(\kappa, \zeta), \qquad 0 < x < \infty, \tag{2.32}$$

$$f(x) = \frac{x^{\kappa-1}\exp(-x/\zeta)}{\Gamma(\kappa)\zeta^\kappa}, \tag{2.33}$$

$$F(x) = \frac{\gamma(\kappa, -x/\zeta)}{\Gamma(\kappa)}, \tag{2.34}$$

$$E(x) = \kappa\zeta, \qquad V(x) = \kappa\zeta^2, \tag{2.35}$$

where κ is the shape parameter, ζ is the scale parameter, $\Gamma()$ is the gamma function, and $\gamma()$ is the incomplete gamma function (e.g. McQuarrie, 2003). Note that the χ^2 distribution is a special case of this distribution, with $\kappa = \nu/2$ and $\zeta = 2$, ν being the number of degrees of freedom.

2.3.2 Standard Normal Transformation

Transforming random variables to standard normal space allows application of a variety of statistical tools, and plays a key role in reliability analysis.

Let Z be a standard normal random variable, and let X have any distribution. We require a transformation $X \leftrightarrow Z$, such that

$$P(X \le x) = P(Z \le z), \tag{2.36}$$

which implies the *isoprobabilistic transform*. Setting

$$F(x) = \Phi(z), \tag{2.37}$$

gives

$$z = \Phi^{-1}\left(F(x)\right), \quad x = F^{-1}\left(\Phi(z)\right). \tag{2.38}$$

In some cases analytical equations for this transformation are available; transformations required for reliability analysis are as follows.

Uniform – Transforming between $X \sim \text{Uni}(a, b)$ and $Z \sim \text{N}(0, 1)$:

$$z = \Phi^{-1}\left(\frac{x-a}{b-a}\right), \qquad x = \Phi(z)\left(b-a\right) + a. \tag{2.39}$$

Normal – Transforming between $X \sim \text{N}(\mu, \sigma^2)$ and $Z \sim \text{N}(0, 1)$:

$$z = \frac{x-\mu}{\sigma}, \qquad x = \mu + z\sigma. \tag{2.40}$$

Log-Normal – Transforming between $X \sim \text{LN}(\mu, \sigma^2)$ and $Z \sim \text{N}(0, 1)$:

$$z = \frac{\ln x - \lambda}{\xi}, \qquad x = \exp\left(\lambda + \xi z\right). \tag{2.41}$$

Gumbel – Transforming between $X \sim \text{Gumbel}(\mu, \sigma^2)$ and $Z \sim \text{N}(0, 1)$:

$$z = \Phi^{-1}\left(\exp\left(-\exp\left(-\frac{x-\lambda}{\xi}\right)\right)\right), \qquad x = \lambda - \xi \ln\left(-\ln\left(\Phi\left(z\right)\right)\right). \tag{2.42}$$

2.3.3   Multivariate Distributions

For reliability analysis we will require a description of the simultaneous stochastic behaviour of multiple random variables. The case where each random variable has a non-normal distribution is made tractable by transformation to a multivariate standard normal problem.

The general N-variate normal probability distribution function can be written as

$$f(x_1, \ldots, x_N) = \frac{1}{\sqrt{(2\pi)^N |\mathbf{C}_N|}} \exp\left[-\frac{1}{2}(\mathbf{x} - \boldsymbol{\mu})^T \mathbf{C}_N^{-1}(\mathbf{x} - \boldsymbol{\mu})\right], \tag{2.43}$$

where $\mathbf{C}_N$ is the $N \times N$ *covariance matrix* (see below), $\mathbf{x}$ is the N-sized vector of normal random variables, and $\boldsymbol{\mu}$ is the corresponding vector of their mean values.

Multivariate distributions must account for possible correlation between pairs of variables. Given X and Y, the correlation coefficient for the pair is

$$\rho_{XY} = \frac{\sum(x_i - \mu_X)(y_i - \mu_Y)}{\sqrt{\sum(x_i - \mu_X)^2}\sqrt{\sum(y_i - \mu_Y)^2}}, \tag{2.44}$$

such that $-1 \leq \rho_{XY} \leq 1$. Note, however that it strictly indicates linear dependence. This means that ρ_{XY} is not invariant when transforming to standard normal space. For example, $\rho(x, y) \neq \rho(\ln x, \ln y)$. The importance of this distinction will be explored later in this chapter.

For N random variables, the *correlation matrix* is then $N \times N$ with entries ρ_{ij}. In the bivariate case

$$\mathbf{R} = \begin{bmatrix} 1 & \rho_{XY} \\ \rho_{XY} & 1 \end{bmatrix}, \tag{2.45}$$

which can be combined with individual variance values to obtain the covariance matrix

$$\mathbf{C} = \begin{bmatrix} \sigma_X^2 & \rho_{XY}\sigma_X\sigma_Y \\ \rho_{XY}\sigma_X\sigma_Y & \sigma_Y^2 \end{bmatrix} = \boldsymbol{\sigma}^T \mathbf{R} \boldsymbol{\sigma}. \tag{2.46}$$

Cholesky decomposition of $\mathbf{R}$ gives

$$\begin{aligned} \mathbf{C} &= \boldsymbol{\sigma}^T \mathbf{R} \boldsymbol{\sigma} \\ &= \boldsymbol{\sigma}^T \mathbf{L} \mathbf{L}^T \boldsymbol{\sigma}, \end{aligned} \tag{2.47}$$

where $\mathbf{L}$ is a lower triangular matrix. Then

$$\begin{aligned} (\mathbf{x} - \boldsymbol{\mu})^T \mathbf{C}^{-1} (\mathbf{x} - \boldsymbol{\mu}) &= (\mathbf{x} - \boldsymbol{\mu})^T \left[\boldsymbol{\sigma}^T \mathbf{L} \mathbf{L}^T \boldsymbol{\sigma} \right]^{-1} (\mathbf{x} - \boldsymbol{\mu}) \\ &= \left[\mathbf{L}^{-1} \mathbf{z} \right]^T \left[\mathbf{L}^{-1} \mathbf{z} \right] \\ &= \mathbf{u}^T \mathbf{u}, \end{aligned} \tag{2.48}$$

where $\mathbf{u}$ is a vector of uncorrelated standard normal variables. In the bivariate case, it is straightforward to show $\mathbf{L}$ that

$$\mathbf{L} = \begin{bmatrix} 1 & 0 \\ \rho & \sqrt{1 - \rho^2} \end{bmatrix}. \tag{2.49}$$

Equation 2.48 gives the transformation of a random vector to uncorrelated standard normal space, in which the multivariate distribution function becomes simply

$$f(u_1, \ldots, u_N) = \frac{1}{\sqrt{(2\pi)^N}} \exp \left[-\frac{1}{2} \mathbf{u}^T \mathbf{u} \right]. \tag{2.50}$$

The geometrical interpretation of $\mathbf{u}^T \mathbf{u}$ follows from the Pythagorean theorem: It denotes the squared distance of point $\mathbf{u}$ from the origin in units of standard deviations.

The transformation of the correlated random N-tuple to the uncorrelated representation can be summarised via the following two steps, illustrated in Figure 2.1. First, transform each individual variable to its standard normal equivalent via

$$z_x = \frac{x - \mu_x}{\sigma_x}. \tag{2.51}$$

Next, transform the vector of all z_x values to remove correlation skewing

$$\mathbf{u} = \mathbf{L}^{-1} \mathbf{z}. \tag{2.52}$$

2.3.4   Determining Multivariate Probabilities

Determining multivariate probability in general requires numerical integration in multiple dimensions. However, there are two special cases we can exploit (Figure 2.2).

Case 1: Hypersphere centred on origin – The key observation in this case is that quantiles of the multi-variate normal distribution are χ^2 distributed. For N variables U_i, the probability is then

$$P(\mathbf{u}^T\mathbf{u} \leq d^2) = \chi^2_{\text{CDF}}(d^2, N). \qquad (2.53)$$

Case 2: Infinite half-space bounded by a linear hyperplane – Here the key observation is that the uncorrelated standard normal distribution is invariant under rotation. Marginal distributions of the multi-variate normal distribution are univariate normally distributed, so that

$$P(u_\perp > d) = \Phi(d), \qquad (2.54)$$

where $u_\perp$ is the shortest distance between the hyperplane and the origin.

2.4   Random Numbers

2.4.1   Random Number Generation

The idea of computer generated random numbers is somewhat of a contradiction, as computers are completely deterministic. Algorithms have been developed that generate sequences of numbers that meet the criteria of randomness, notably in terms of distribution and lack of correlation. Notable examples include the linear congruential generator and the Marsenne twister (Press *et al.*, 2007).

These algorithms are nonetheless deterministic, in that starting from a specific seed value will always yield the same sequence of values. If a seed is not explicitly provided, algorithms often use the time and date as a seed. The sequence of values generated by an algorithm is cyclical with a return period (typically around $10^9 - 10^{14}$ values), which is important to keep in mind when generating very large sets of random values.

Pseudo-random number generators yield uniformly distributed values in the interval $[0, 1]$. Values with non-uniform distributions can be simply obtained by an inverse probability transformation (Figure 2.3). Because normally distributed random numbers are so common, most numerical packages and libraries have a separate optimised command built in for their generation.

2.4.2 Correlated random numbers

To obtain N-tuples of correlated random numbers, the transformation in Equations 2.51 and 2.52 is performed in reverse. First generate an N-tuple of uncorrelated standard normal variables $\mathbf{u}$, and apply correlation via

$$\mathbf{z} = \mathbf{L}\mathbf{u}. \tag{2.55}$$

Next transform each variable individually to its desired distribution through the isoprobabilistic transformation equations in Section 2.3.2.

In the bivariate case, one can therefore get correlated normal $[X, Y]$ pairs by applying

$$\begin{bmatrix} z_x \\ z_y \end{bmatrix} = \begin{bmatrix} 1 & 0 \\ \rho & \sqrt{1-\rho^2} \end{bmatrix} \begin{bmatrix} u_x \\ u_y \end{bmatrix}, \qquad x_i = \mu_i + z_i \sigma_i, \tag{2.56}$$

from which follows the direct transformation equations

$$x = \mu_x + u_x \sigma_x, \qquad y = \mu_y + \left(\rho u_x + \sqrt{1-\rho^2} u_y \right) \sigma_y. \tag{2.57}$$

2.4.3 Non-normal correlation

As noted above, the correlation coefficient assumes a linear relationship between X and Y. For non-normal distributions, this linearity does not survive transformation to and from standard normal space. Applying ρ_{XY} in Equation 2.56 may therefore not capture the correlation between $\rho_{U_X U_Y}$. This problem is sometimes addressed by more advanced formulations such as by the use of copulas (Sklar, 1959). However, as ρ values tend to be relatively poorly constrained, it is worth exploring how large an effect transformation really has on correlation values, to see whether more advanced formulations are really required in the problem types to be considered in this thesis.

Illustrated in Figure 2.4 are the correlation coefficients determined numerically from 10^5 random pairs via Equation 2.44, as a function of the standard normal correlation coefficient used to generate the pairs. When both random variables are log-normally distributed, the actual correlation coefficient differs notably from the normal value only at very large negative correlation values and high coefficients of variation. The magnitude of the difference is smaller when only one variable is log-normal, but is present for both positive and negative correlations.

This suggests that one can do the transformation in Equations 2.51 and 2.52 with relatively small error, if ρ is not very strong, δ is relatively small, and the parameter distributions are not strongly asymmetrical.

2.5   Reliability Analysis

Reliability analysis is concerned with the margin between the loads to be resisted by a structure, and its capacity to resist them. This margin can be expressed via the *performance function*, defined as

$$g = R - E. \tag{2.58}$$

Failure is taken to occur when $R < E$, that is when $g < 0$, so that the *limit state function* is defined according to the condition

$$g = 0. \tag{2.59}$$

In general, R and E are random variables, so that g will also be a random variable. The probability that $g < 0$ is then the *probability of failure p_f* (Figure 2.5). The associated *reliability index* is given by

$$\beta = -\Phi^{-1}(p_f). \tag{2.60}$$

If the limit state function is linear in standard normal space, this expression for the reliability index is equivalent to its formal definition

$$\beta = \min\left(\sqrt{\mathbf{u}^T\mathbf{u}}\right) \quad s.t. \quad g(\mathbf{u}) = 0. \tag{2.61}$$

The value of p_f should be considered in the context of an associated period of time. The probability of failure in a given year would be lower than the probability of failure during the design lifetime of a structure. Failure probabilities and reliability indices in this thesis will refer to the lifetime of the structure, usually taken as 50 years (ISO 2394:2015).

The likelihood of failure is accurate to the extent that all sources of uncertainty are correctly accounted for. Although this is seldom the case, it still has value in a relative sense if the same assumptions are applied to all cases being considered/compared.

Typical structural and geotechnical engineering reliability values fall in the range $3.0 \leq \beta \leq 4.5$, so that corresponding p_f values fall well into the distribution tails. As a result the value of β determined from statistical parameters depends very strongly on the choice of distribution used. Furthermore, in geotechnical engineering R is generally a nonlinear function of multiple random variables, with the result that g seldom has a simply described distribution function.

Two approaches have been followed to this problem. The first is to approximate the form of $f(g)$ in some way and determine p_f from this approximation. The second is to treat the problem in terms of the individual random variables using multi-variate distributions.

Methods in the first option generally obtain a representation of g in terms of its moments about the mean. These methods include the point estimate

method (PEM), and the first order second moment method (FOSM), as defined about the mean (Ang and Tang, 1984; Baecher and Christian, 2003). Because these methods generally treat the tail of the distribution very poorly, they tend to give very inaccurate p_f values.

Methods in the second option include the first order reliability method (FORM) and Monte-Carlo simulation. These methods are discussed in greater detail below.

2.5.1 Monte Carlo Simulation

Monte Carlo reliability determination is effectively a numerical integration strategy to determine p_f directly. The principle behind it is simple: A multivariate distribution is randomly sampled as described in Section 2.4 a large number of times n_{trial}. For each trial, the value of g is determined, and the fraction of points for which $g < 0$ counted. The probability of failure is then simply

$$p_f = n_{g<0}/n_{\text{trial}}. \tag{2.62}$$

The error in the proportion p_f determined using a total of n trials follows from the binomial distribution as

$$\epsilon = z_\alpha \sqrt{\frac{1 - p_f}{p_f n_{\text{trial}}}}. \tag{2.63}$$

This can be rearranged to get the number of trials required for a confidence interval with width corresponding to a required tolerance

$$n_{\text{trial}} = \frac{z_\alpha^2}{\epsilon^2} \frac{1 - p_f}{p_f}. \tag{2.64}$$

Based on this relation, simulations for typical geostructural p_f values would require

$$n_{\text{trial}} = 1.54 \times 10^6 \text{ when } p_f = 1/1000, \ \beta = 3.1, \tag{2.65}$$

$$n_{\text{trial}} = 1.54 \times 10^7 \text{ when } p_f = 1/10000, \ \beta = 3.7, \tag{2.66}$$

for $\epsilon = 5\%$ and a confidence limit of 95%.

Direct application of Monte Carlo in reliability determination is therefore rather wasteful and inefficient. A number of techniques exist to reduce the number of required trials, including importance sampling and Markov chain Monte Carlo (Honjo, 2008), and subset simulation (e.g. Au and Wang, 2014). While these techniques are required when evaluation of the performance function is time consuming, direct Monte Carlo is sufficient for the problems considered in this thesis.

2.5.2   First Order Reliability Method

Consider the multi-variate distribution describing the set of model parameters. The distribution for each is specified separately, together with internally consistent correlation pairs.

The point on the limit state function where the value of $f()$ is the highest is interpreted as the most likely combination of parameters for which failure would occur. This point is referred to as the *design point* (Figure 2.6). In U space this point is where the limit state function is closest to the origin and tangent to the contours of $f(\mathbf{u})$. If the limit state function is linear in standard normal space, the problem reduces to a simple 1D normal distribution problem, as discussed in Section 2.3.4 (Figure 2.7).

FORM determines p_f by replacing the limit state function with its tangent at the design point. This approximation tends to be quite accurate, as the increasing deviation from the linear tangent coincide with much smaller f values.

FORM obtains the reliability by finding the design point via

$$\beta = \min\left(\sqrt{\mathbf{u}^T\mathbf{u}}\right) \quad s.t. \quad g(\mathbf{u}) = 0, \tag{2.67}$$

and then determines the probability of failure as

$$p_f = \Phi(-\beta). \tag{2.68}$$

In the special case where $R \sim \mathrm{N}$, $E \sim \mathrm{N}$, and correlation is absent, it can be shown from the definition in Equation 2.67, that

$$\beta = \frac{\mu_R - \mu_E}{\sqrt{\sigma_R^2 + \sigma_E^2}}. \tag{2.69}$$

More generally, β is often determined via a Newton-like algorithm, sometimes referred to as the HLRF algorithm for its developers (Hasofer and Lind, 1974; Rackwitz and Fiessler, 1978), the details of which can be found in Ang and Tang (1984). The direction cosines α_i of the individual variables used in the algorithm also provide an indication of the sensitivity of β to each variable. To illustrate, let the design point $\mathbf{u}^*$ have components

$$u_i^* = -\alpha_i\beta, \tag{2.70}$$

in which

$$\alpha_i = \frac{\partial g(\mathbf{u}^*)/\partial u_i}{\sqrt{\sum\left[\partial g(\mathbf{u}^*)/\partial u_i\right]^2}}, \tag{2.71}$$

so that

$$\sum \alpha_i^2 = 1. \tag{2.72}$$

2.5.3   Model Uncertainty

The model used in determining the resistance R is invariably a simplified representation of the true behaviour of the system, either because a more exact description is not practical, or because the underlying physics is not sufficiently well understood for a more accurate model to be available.

A common method to account for this model uncertainty is via a multiplicative model factor (e.g. Melchers, 1999),

$$M = R_{\text{true}}/R_{\text{model}}, \qquad (2.73)$$

where R_{true} represents the 'true' resistance capacity, usually obtained from a series of controlled laboratory or field tests. Although M is generally be dependent on the other model parameters, data seldom allows this effect to be accurately captured.

Mean values of M different from 1.0 imply that the model is biased. For example, $M > 1$ implies that the model is conservative. If distribution parameters for M are known, it can be included in the reliability analysis by rewriting the performance function as

$$g = MR - E. \qquad (2.74)$$
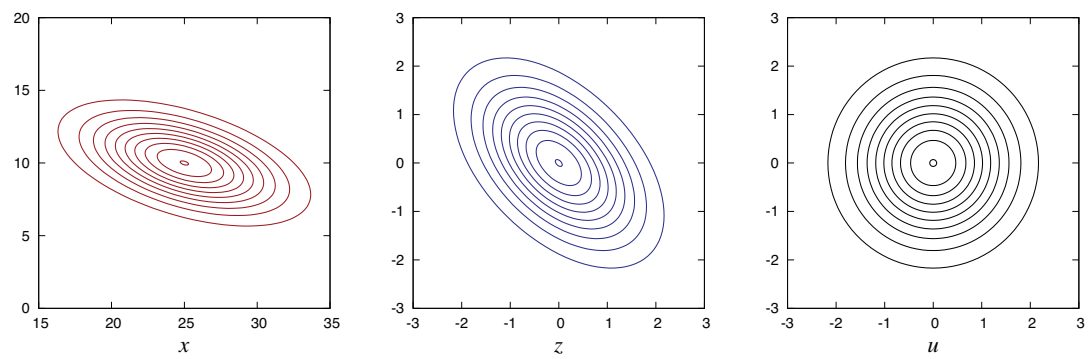
Figure 2.1: Bivariate transformation between parameter space **x** and uncorrelated standard normal space **u**.
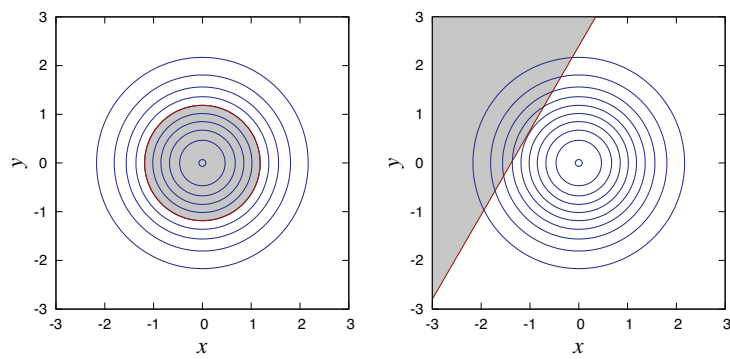
Figure 2.2: Two special cases for which multivariate probabilities can be easily determined. (left) Quantiles of a multivariate normal distribution, and (right) infinite half-space bounded by a hyperplane.
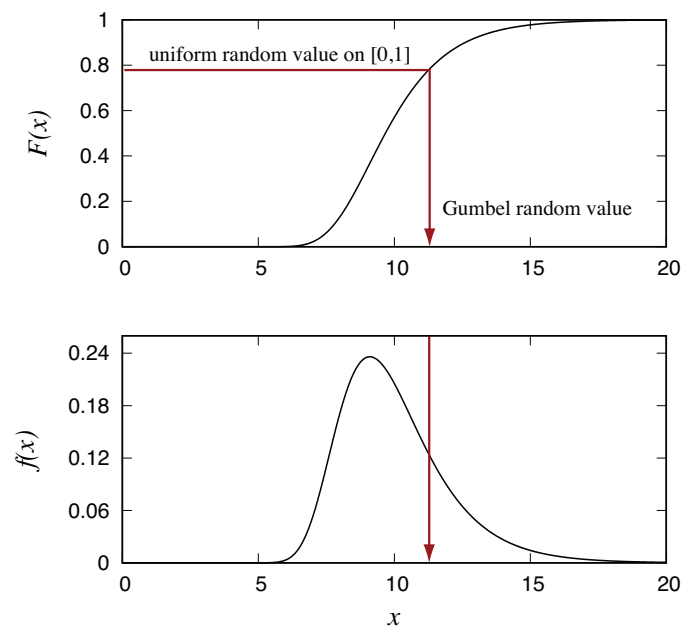
Figure 2.3: Obtaining Gumbel distributed random numbers from continuous uniform random numbers on interval [0,1].
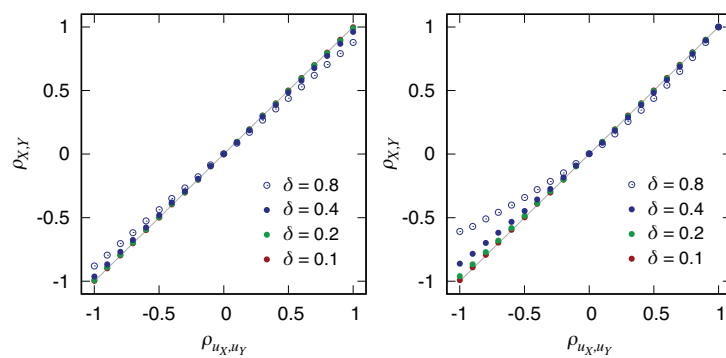
Figure 2.4: Comparison of the standard normal correlation used to generate correlated random numbers, and the numerically determined correlation of the transformed coordinates. (left) $X \sim N$, $Y \sim LN$; (right) $X \sim LN$, $Y \sim LN$
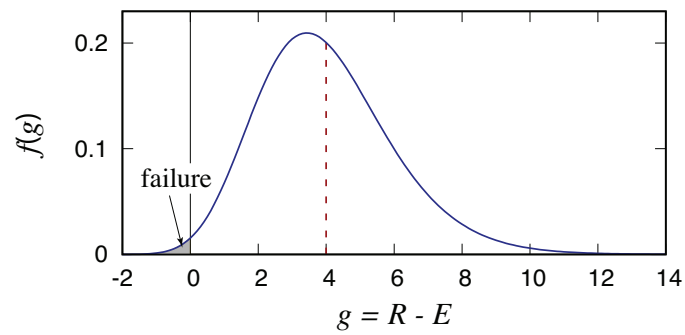
Figure 2.5: The reliability problem requires the probability of failure to be determined, with $g < 0$ as failure criterion.
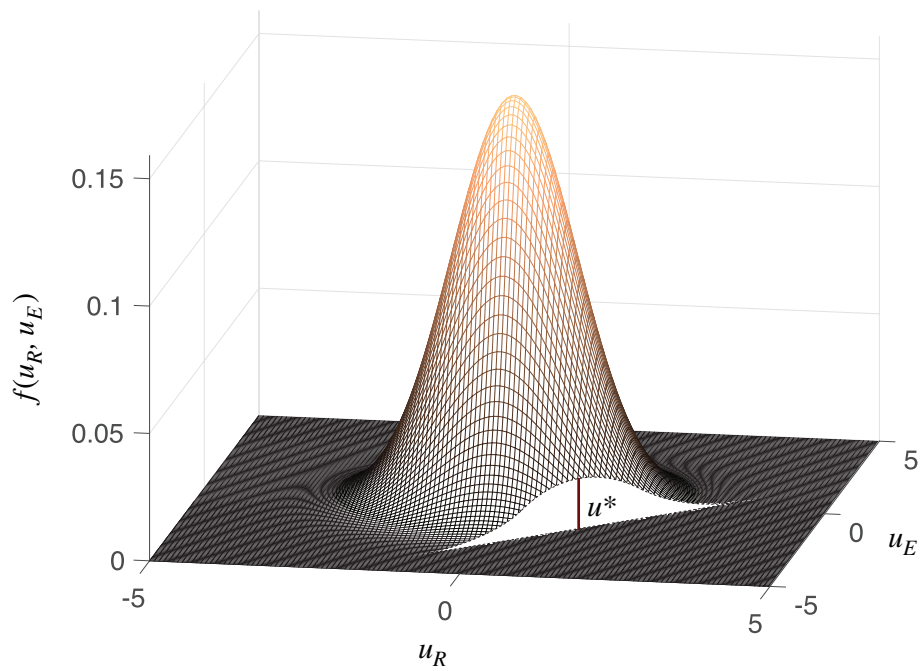
Figure 2.6: The design point u^* (indicated by vertical line) is located where the multivariate density function reaches a maximum value on the limit state function $g = 0$ (denoted by the vertical white plane).
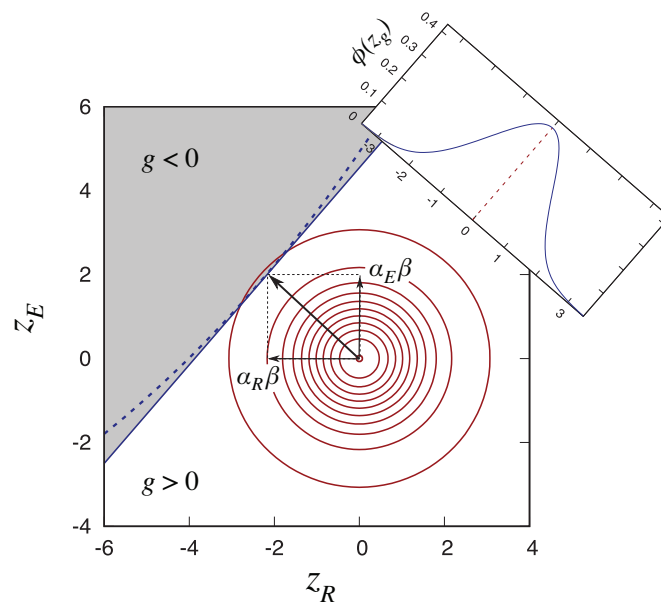
Figure 2.7: Geometrical illustration of FORM, which represents the limit state function as the tangent hyperplane at the design point.

Chapter 3

Assessment of Reliability Based Design for a Spectrum of Geotechnical Design Problems

Nico de Koker, Peter Day

Summary

Reliability analyses were performed for a set of benchmark problems consisting of footings, piles and retaining walls, each designed according to the limit states design method outlined in EN 1990:2002 and EN 1997:2004. Close correspondence was found between reliability index values from Monte Carlo calculations to those from the first-order reliability method, which affirms the latter's utility in reliability based design. These results further show relatively uniform reliability indices among the variety of problems considered, and are somewhat lower than the target reliability of $\beta = 3.8$ specified by the Eurocodes. Finally, the analyses illustrate the robustness of the limit states design approach implemented in EN 1997:2004, but highlight the importance of choosing reasonably conservative characteristic parameter values, as well as the need for caution when designing for ground where the friction angle in particular shows a high degree of variance.

Notation

A	area
a	anchor position
B	dimension determined from limit states design
c_{v}	coefficient of variation
E	applied load or action
e	eccentricity
G	permanent load
g	performance function
H	horizontal load
h	height
i_q, i_γ	inclination factors
K	pressure coefficient
L	dimension determined from limit states design
M_x	moment
N	bearing capacity coefficient
$P(x)$	cumulative distribution function for x
p	probability
Q	imposed point/line load
q	imposed distributed load
R	resistance capacity
$\mathbf{R}$	correlation matrix with elements ρ_{ij}
s_q, s_γ	shape factors
t	thickness
V	vertical load
W	weight
w	width
x	random variable of any distribution
$\overline{x}$	sample mean for x
$\mathbf{z}$	standard normal random variable
$\mathbf{z}_d$	standard normal design point
$\mathbf{z}_d^{\mathrm{T}}$	standard normal design point
β	reliability index
γ	soil density
γ_e	Euler-Mascheroni constant
γ_x	partial factor for property x
η_{k}	characteristic multiplier
λ	statistical measure of centrality
μ	mean
ξ	statistical measure of spread
Φ	standard normal cumulative distribution function
ϕ	friction angle
Ψ_0	combination factor

Subscripts

a	active
b	bearing, base, bottom part
d	design point
f	footing
H	horizontal
i, j	1, 2, 3 and so on
k	characteristic value
p	passive
q	surcharge
s	sliding, side
t	top part
V	vertical

3.1 Introduction

Uncertainty regarding the nature of the subsurface is inherent to geotechnical engineering. Sound foundation design can often benefit from the use of multiple avenues through which to evaluate the final design decisions.

Reliability analysis has been applied in structural and geotechnical engineering for many years, providing the basis for the formulation and calibration of limit states design (LSD) codes, such as the Eurocodes. Despite the fact that limit states design is now an international norm, the perceived obscurity of the method, multiplicity of approaches and openness to interpretation impede widespread adoption of the method. As a result, some practitioners are electing to continue using working stress design (WSD) methods while, at the other end of the spectrum, others are advocating greater reliance on reliability based design (RBD) methods.

Reliability based design techniques use target values for the probability of failure directly to determine the geometric and strength requirements of the structure under design. In the past 10 years, these methods have become sufficiently accessible to serve as practical tools in a geotechnical design office, rather than being confined to research applications. In order to assess the suitability of reliability based design in geotechnical applications, the breadth of application and design data requirements must be considered, and the comparison of results to current practice assessed.

In this manuscript, LSD solutions are obtained for a range of common geotechnical problems; these are then evaluated in the context of WSD and RBD. Some of the limitations and merits of the various design methods are highlighted by comparing results for a set of benchmark design problems solved using LSD to the corresponding factors of safety and reliability levels.

3.2 Theoretical Background

3.2.1 Reliability Specification

The current set of specifications for structural and geotechnical loading given by the Eurocodes (EN 1990:2002; EN 1997:2004, and the associated British national annexes, NA to BS EN 1990:2002; NA to BS EN 1997:2004), have a strong reliability basis, derived from the guidelines for structural reliability detailed in ISO 2394:2015, and the specifications set forward by the Joint Committee on Structural Safety (JCSS, 2008*b*).

EN 1990:2002 identifies target reliability index values of $\beta = 3.3 - 4.7$ (failure probabilities of $p_{\text{fail}} = 10^{-3} - 10^{-5}$ in a fifty year reference period) depending on the consequences of failure. For the class of structures in which failure would have considerable impact, the standard recommends a target value of $\beta = 3.8$ (Gulvanessian and Holicky, 2005).

National annexes to the Eurocodes provide values for LSD partial factors calibrated to these target reliability levels, supplemented by extensive empirical and experiential input (Gulvanessian, 2010; Harris and Bond, 2010).

3.2.2 Reliability Analysis

Consider a reliability problem in which n variables have meaningful uncertainty, for which failure occurs when the performance function g becomes negative. The reliability index β for this problem may be viewed as the multidimensional equivalent of the one dimensional measure in units of standard deviations from the mean to the boundary of the $g < 0$ domain (Hasofer and Lind, 1974). That is

$$\beta = -\Phi^{-1}(p_{\text{fail}}), \tag{3.1}$$

where Φ is the cumulative distribution function of the standard normal distribution.

The definition of β effectively casts the boundary of the failure domain ($g = 0$) as a linear plane. The first order reliability method (FORM, Rackwitz and Fiessler, 1978) formalises this definition in its geometrical definition of β, generalized to account for correlation. Denoting the "design point" $\mathbf{z}_{\text{d}}$ as the point on this domain boundary in standard normal space where the probability density is at a maximum, β is simply the distance to the origin,

$$\beta = \sqrt{\mathbf{z}_{\text{d}}^T \mathbf{R}^{-1} \mathbf{z}_{\text{d}}}, \tag{3.2}$$

where $\mathbf{R}$ is the correlation matrix with elements ρ_{ij}.

For x_i not necessarily normally distributed, z_i is obtained by performing the transformation (Hald, 1952),

$$z_i = \Phi^{-1}\left(P_i(x_i)\right), \tag{3.3}$$

where P_i is the cumulative distribution function for x_i, and Φ is the standard normal cumulative distribution function. Analytical expressions for the transformations and their inverses, are summarised in Table 3.1 for the distribution types used in this study.

Equation 3.3 and its inverse are used extensively in the numerical calculations in this study: Monte Carlo calculations use N sets of randomly generated n-dimensional standard normal variables **z**, each of which is transformed to x-space by means of the appropriate inverse transform (Table 3.1). In the FORM calculations, the performance function is determined in x-space, while the minimisation of β occurs in z-space.

3.2.3   Limit States Design

Although the limit states design approach aims to account for differences in the characteristic uncertainty of individual parameters, it only treats the target reliability values outlined by ISO 2394:2015 in an implicit and indirect sense. The method adjusts the characteristic value of each parameter x_k via partial factors γ_x, calibrated to target reliabilities as noted previously.

The characteristic value of a parameter is chosen to reflect a conservative confidence interval on the mean,

$$x_k = \overline{x}\left(1 + \eta_k c_v\right),\tag{3.4}$$

where $\overline{x}$ is the estimator of the mean μ, and the coefficient of variation c_v allows estimation of the standard deviation as $c_v\overline{x}$. Though spatial variability of soil can be difficult to account for (eg. Ching and Phoon, 2013), the multiplier η_k is usually selected by the designer (Schneider, 1997; EN 1997:2004), taking into account the number of test results available and the extent to which the occurrence of the ultimate limit state (i.e. failure) is dependent on the average rather than a minimum/maximum value of the parameter.

3.3   Investigation Methodology

3.3.1   Problems Analysed

The problems analysed were based on those selected by Orr *et al.* (2005) as benchmark problems for the current Eurocode limit states design specification. Only problems with closed-form solutions were used, the solution required in each case being a dimension that determines the adequacy of the structure such as the width of a footing or the length of a pile. Tables 3.2 and 3.3 illustrate each of the problems that are considered and provide the salient loading and geometrical parameters.

A single soil type was chosen for the purposes of this study, namely a cohesionless sand with a deep water table. As a result, there are only two

material parameters to be considered, namely friction angle ϕ' and density γ (Table 3.4). Mean values of these parameters are such that characteristic values $\phi'_{\mathrm{k}} = 32°$ and $\gamma_{\mathrm{k}} = 20$ kN/m^3 are one standard deviation below the mean, except where otherwise stated.

The statistical distributions, coefficients of variation, and ratios of characteristic to mean loading are based on Retief and Dunaiski (2010) and Phoon and Kulhawy (1999) (Table 3.4). Characteristic values for the imposed loads reflect 95% upper bounds. That is, $x_{\mathrm{k}} = P^{-1}(0.95)$, for which η_{k} is determined via Equation 3.4. As soil properties are mobilized over the full slip surface, a lower bound of 1σ below the mean values is chosen for the characteristic values. That is, $\eta_{\mathrm{k}} = -1.0$. Ultimate limit state partial factor values are taken as specified in NA to BS EN 1990:2002 and NA to BS EN 1997:2004.

3.3.2   Load Capacity Evaluation

3.3.2.1   Strip and Square Footings (Examples A, B, C)

For the foundation structures, parameter value combinations that yield bearing failure are identified by negative values of the performance function,

$$g = R_{\mathrm{b}} - E_{\mathrm{v}} < 0, \tag{3.5}$$
$$E_{\mathrm{v}} = G_V + Q_V + W_{\mathrm{f}},$$
$$R_{\mathrm{b}} = A'_{\mathrm{b}} q_{\mathrm{b}},$$

where E_{v} is the total vertical action (effect), R_{b} is the vertical component of the resistance force associated with bearing capacity q_{b} at foundation level, $A'_{\mathrm{b}} = B'L'$ the effective area, and the self-weight of the footing $W_{\mathrm{f}} = \gamma_{\mathrm{conc}} DA'$. The density of concrete is taken as $\gamma_{\mathrm{conc}} = 24$ kN/m^3.

The moment due to horizontal load Q_H acting across the width of the foundation at height h results in a reduced effective width,

$$B' = B - 2e_B, \tag{3.6}$$
$$e_B = M_x/E_{\mathrm{v}},$$
$$M_x = Q_H(h + D).$$

$L = B$ for square footings, and $L = \infty$ for strip foundations.

The bearing capacity is obtained as

$$q_{\mathrm{b}} = \gamma' D N_q i_q s_q + \tfrac{1}{2}\gamma' B' N_\gamma i_\gamma s_\gamma, \tag{3.7}$$
$$N_q = \exp\left(\pi \tan \phi'\right) \tan^2\left(\tfrac{\phi'}{2} + 45°\right),$$
$$N_\gamma = 2\left(N_q - 1\right) \tan \phi',$$

with shape factors s_q and s_γ, and inclination factors i_q and i_γ determined using the equations in Annex D of EN 1997:2004.

With overburden weight at founding level $W_e = \gamma DA'$, the factor of safety is

$$FoS = \frac{R_b - W_e}{E_v - W_e}. \tag{3.8}$$

In a similar way, sliding failure is present when

$$
\begin{aligned}
g = R_s - E_h &< 0, \tag{3.9}\\
E_h &= Q_H,\\
R_s = \tan\phi'(G_V &+ W_f),
\end{aligned}
$$

where E_h is the total horizontal action, and R_s is the resistance load against sliding.

The factor of safety against sliding follows as

$$FoS = \frac{R_s}{E_h}. \tag{3.10}$$

3.3.2.2 Piles (Example D)

Resistance provided by a pile is a combination of shear resistance along the sides and bearing at its base. The performance function indicates failure when

$$
\begin{aligned}
g = R_p - E_v &< 0, \tag{3.11}\\
E_v = G_V + Q_V &+ W_f,\\
R_p = R_b &+ R_s,
\end{aligned}
$$

with R_b R_s the vertical bearing and shear resistance. Following Vesic (1967) and Meyerhof (1976), as presented in Poulos and Davis (1980), we set $\phi'_1 = 0.75\phi'$, and limit the skin resistance to a constant value below critical depth z_c. That is,

$$
\begin{aligned}
R_b &= \sigma_{vb} A_b N_q, \tag{3.12}\\
R_s &= \sigma_{vs} \tan\phi' \left(1 - \sin\phi'\right) \left(\tfrac{1}{2} A_{s1} + A_{s2}\right),\\
\sigma_{vb} &= \gamma'L, \qquad \sigma_{vs} = \gamma' z_c,\\
A_b = \pi d^2/4, \qquad A_{s1} &= \pi d z_c, \qquad A_{s2} = \pi d\left(L - z_c\right),\\
z_c/d &= \max\left[(0.3\phi'_1 - 3.5), \, (2.6\phi'_1 - 87.9)\right].
\end{aligned}
$$

The associated factor of safety is

$$FoS = \frac{R_p - W_e}{E_v - W_e}. \tag{3.13}$$

3.3.2.3   Gravity Retaining Walls (Example E)

For the chosen example, failure occurs in bearing below the base, which is treated as a strip footing (Example A), with a reduced effective width B' due to moments acting on the base,

$$B' = B - 2e, \tag{3.14}$$
$$e = M_\text{t}/V_\text{t},$$
$$M_\text{t} = M_\text{w} + M_\text{s} + M_{Vq} + M_{Hq} + M_\gamma,$$
$$V_\text{t} = W_\text{b} + W_\text{w} + W_\text{s} + V_q.$$

Vertical loads result from the self-weight of the base (W_b), wall (W_w), and fill (W_s), as well as the surcharge over the base (V_q) if present. Horizontal loads result from the active pressure from the fill weight (H_γ) and surcharge (H_q). These are obtained as

$$W_\text{b} = tB\gamma_\text{conc}, \qquad W_\text{w} = w(D-t)\gamma_\text{conc}, \tag{3.15}$$
$$W_\text{s} = (D-t)(B-w)\gamma',$$
$$V_q = (B-w)q, \qquad H_q = qK_\text{a}D,$$
$$H_\gamma = \tfrac{1}{2}K_\text{a}\gamma'D^2,$$

where the active pressure coefficient is

$$K_\text{a} = \frac{1 - \sin\phi'}{1 + \sin\phi'}. \tag{3.16}$$

Taking moments about the centre of the base,

$$M_\text{w} = W_\text{w}(B-w)/2, \qquad M_\text{s} = -W_\text{s}w/2, \tag{3.17}$$
$$M_{Vq} = -V_q w/2, \qquad M_{Hq} = H_q D/2,$$
$$M_\gamma = H_\gamma D/3.$$

3.3.2.4   Embedded Retaining Walls (Examples F, G)

Failure of an embedded retaining wall occurs when there is a loss of moment equilibrium about a pivot point: In the simple embedded wall, the pivot is close to the toe of the wall; for an anchored/propped wall, it is at the level of the anchor or prop. The performance function and associated factor of safety are taken to reflect the balance between active (destabilising) and passive (resisting) moments M_a and M_p,

$$g = M_\text{p} - M_\text{a}, \qquad FoS = \frac{M_\text{p}}{M_\text{a}}. \tag{3.18}$$

For the simple embedded wall, horizontal loads due to active pressure behind the wall (H_a), passive pressure in front (H_p), and the surcharge (H_q) are

$$H_\mathrm{a} = \tfrac{1}{2}\gamma' \left(L + h\right)^2 K_\mathrm{a}, \tag{3.19}$$
$$H_\mathrm{p} = \tfrac{1}{2}\gamma' L^2 K_\mathrm{p},$$
$$H_q = q_V \left(L + h\right) K_\mathrm{a},$$

where K_a and K_p are the active and passive pressure coefficients

$$K_\mathrm{a} = \frac{1 - \sin \phi'}{1 + \sin \phi'} = \frac{1}{K_\mathrm{p}}. \tag{3.20}$$

Moments about the toe of the wall are then

$$M_\mathrm{p} = \tfrac{1}{3}H_\mathrm{p}L, \tag{3.21}$$
$$M_\mathrm{a} = \tfrac{1}{2}H_q \left(L + h\right) + \tfrac{1}{3}H_\mathrm{a} \left(L + h\right).$$

In practice the calculated value of L is extended by 20% in design to allow for the actual pivot point located somewhat above the toe, $L_\mathrm{design} = 1.2L$.

For the anchored wall, the failure mechanism is modeled by assuming active stress conditions behind the wall (below anchor level) and passive conditions in front. Horizontal loads are therefore (subscripts t and b indicate regions above and below the anchor, respectively)

$$H_\mathrm{pt} = \tfrac{1}{2}\gamma' a^2 K_\mathrm{p}, \tag{3.22}$$
$$H_\mathrm{ab1} = \gamma' \left(L + h - a\right) a K_\mathrm{p},$$
$$H_\mathrm{ab2} = \tfrac{1}{2}\gamma' \left(L + h - a\right)^2 K_\mathrm{a},$$
$$H_\mathrm{pb} = \tfrac{1}{2}\gamma' L^2 K_\mathrm{p},$$
$$H_{q\mathrm{t}} = q_V a K_\mathrm{p},$$
$$H_{q\mathrm{b}} = q_V \left(L + h - a\right) K_\mathrm{a}.$$

Moments about the anchor are

$$M_\mathrm{p} = \tfrac{1}{2}H_{q\mathrm{t}}a + \tfrac{1}{3}H_\mathrm{pt}a + H_\mathrm{pb}\left(\tfrac{2}{3}L + h - a\right), \tag{3.23}$$
$$M_\mathrm{a} = \left(L + h - a\right)\left[\tfrac{1}{2}H_{q\mathrm{b}} + \tfrac{1}{2}H_\mathrm{pb1} + \tfrac{2}{3}H_\mathrm{pb2}\right].$$

3.3.3   Method of Analysis

Basic analysis of each geotechnical example problem is performed as follows. For a given soil characterised by mean values $\overline{\phi'}$ and $\overline{\gamma}$, and a specified set of mean loading values $\overline{G}$ and $\overline{Q}$ or $\overline{q}$, the characteristic parameter and load values are obtained using Equation 3.4.

Next, using these characteristic values of loads and material properties, the minimum required dimension (B or L) is determined using limit states design (EN 1990:2002 and EN 1997:2004, design approach 1, combination 2). Safety factors for this design are determined for resistance capacities calculated from the characteristic and mean parameter values.

Finally, the reliability index β for this optimal LSD design is calculated. This is done using both the FORM technique as well as Monte Carlo calculations with $N = 10^6$ trials. For an actual $\beta = 3.5$, theory indicates that $N = 10^6$ Monte Carlo trials can be expected to estimate β with a 95% confidence interval of 3.50 ± 0.03.

Following the initial calculations at the reference mean values, the response of β and FoS to parameter value variations is explored. To do this, mean parameter values for $\overline{\phi}'$, $\overline{\gamma}$, and $\overline{Q}_V$ are systematically varied, and the limit states design optimisation and reliability determination just outlined repeated.

Partial factors used in the limit states design component are included in Tables 3.2 and 3.3. Note that for piles the material parameters are not factored. Instead, partial resistance factors are applied to the individual resistance terms in Equation 3.11 directly,

$$R_{\mathrm{p}} = R_{\mathrm{b}}/\gamma_{\mathrm{Rb}} + R_{\mathrm{s}}/\gamma_{\mathrm{Rs}}. \tag{3.24}$$

3.4   Results

A summary of the minimum dimensions required by limit states design, corresponding factors of safety for these designs determined for characteristic and mean parameter values, reliability indices determined using the FORM and Monte Carlo methodologies, and corresponding design points, is presented in Table 3.5.

Figure 3.1 illustrates the reliability calculations in three dimensional parameter space (four dimensional in Example C), with the marginal probability distribution function contours and planes of intersection of the performance function. Figures 3.2-3.4 compare the partial variation of β and FoS values for the respective examples over reasonable ranges of parameter values and coefficients of variation. For the plots on the left in each figure, all parameters are kept at their reference values used in the preceding calculations, and one of $\overline{\phi}'$, $\overline{\gamma}$, or $\overline{Q}_V$ (or $\overline{q}_V$) is varied systematically. Similarly plots on the right are obtained by keeping all parameters and their variation coefficients at the reference values, and systematically adjusting the variation coefficient of each of ϕ', γ, or Q_V.

3.5   Discussion

3.5.1   Limit States Design

The starting point for the above analyses was an EN 1997:2004 compliant, partial factor limit states design solution to each of the seven common geotechnical problems shown in Tables 3.2 and 3.3.

At the reference parameter values (Tables 3.2 - 3.4), the corresponding reliability indices match closely over the wide range of problems considered (footings, piles and retaining structures). β values do not show a strong dependence on parameter values, so that this correspondence among problem types is maintained across the ranges of parameter values explored (Figures 3.2 - 3.4).

The relative independence of β on problem type and parameter values supports the robustness of the limit states design approach implemented in EN 1997:2004. However, while the index values correspond to the lower end of the ISO 2394:2015 recommendations, the values are somewhat below the EN 1990:2002 target value of $\beta = 3.8$.

Comparison of the β values for Examples B and C indicates that including Q_H in the LSD design results in a somewhat more conservative result, reflecting the intended function of the combination factor. However, for $\Psi_0 = 1.0$, $\beta = 3.828$ for Example C (compared to 3.720 for $\Psi_0 = 0.7$) suggesting that the combination factor only partly brings about the desired economy.

The similarity of reliability indices across problem types is present at the parameter level as well, where the ratios of characteristic values to design point values show remarkable correspondence (Figure 3.5). This correspondence reflects the similar performance function geometry of the different problem types (Figure 3.1). The low β values may therefore simply reflect characteristic values that are insufficiently conservative. Indeed, using $\eta_k = -1.25$ for ϕ' yields a $\beta = 3.6 - 3.8$.

The decrease of β with $\overline{\phi}'$ for the pile example reflects the large variation of pile LSD length over the same spectrum. At low $\overline{\phi}'$ values, very long piles are required to provide sufficient shear area to resist the axial loads, an effect exacerbated by Vesic's limitation on skin resistance with depth (Vesic, 1967). Partial resistance factors γ_{Rb} and γ_{Rs} are intended to restore this balance, but under-compensate at low $\overline{\phi}'$ values (Figure 3.6).

In contrast to the relatively modest variation in reliability index, the factors of safety obtained from WSD analyses vary widely for different problem types, and strongly across the range of soil properties considered (Tables 3.2-3.4). This supports the now well-established realisation that the factor of safety is a poor measure of the reliability of a structure. The contrast between characteristic and mean value factors of safety reflects FoS values increasing away from the failure surface ($g = 0$, where FoS=1.0), and illustrates the need for conservative characteristic values when factors of 2.0-3.0 are used with WSD

for geotechnical problems.

Increasing the coefficient of variation of ϕ' results in a notable decrease in β. However, changes in the variation coefficient of the other parameters do not have the same effect in all cases. This can be understood as a balance of two competing effects: A higher standard deviation would decrease the β value (Equation 3.2), but would also result in more a conservative characteristic value (Equation 3.4) and a higher β value. Because β is most sensitive to changes in $\overline{\phi'}$, the more conservative ϕ'_k value does not always compensate for the effect of higher than expected variance in soil properties on the reliability index. Caution should be exercised when using the recommended partial material factors for limit states design methods in ground where the friction angle shows a high degree of variance.

3.5.2 Reliability Based Design

Reliability indices computed via FORM correspond very closely with the Monte Carlo results in each of the problems considered, with differences of less than 2.3%. Monte Carlo reliability calculations provide failure probabilities directly, so that the agreement verifies the utility of FORM as a suitable technique for reliability based geotechnical design problems.

The gradient-based FORM algorithm required fewer than 10 iterations to locate the design points (convergence tolerance 10^{-6}), compared with the $N = 10^6$ trial calculations required by the Monte Carlo calculations. This reduced number of iterations makes implementing FORM for non-closed form geotechnical problems a viable option. Spreadsheet applications of FORM for problems with closed-form geotechnical solutions (e.g. Low and Phoon, 2015) are already available that could make FORM a useful design office tool, although they use numerical search algorithms requiring far more (around 100) performance function evaluations.

One of the limitations of the reliability analyses described in this manuscript is the assumption that a single value of a material parameter applies at all points in the soil mass and over the full extent of the failure surface. Consider, for example, the effect of variations in the friction angle ϕ' in the case of the pile foundation in Example D. The assumption made in both the FORM and Monte Carlo analyses is that the same $\overline{\phi'}$ applies throughout, i.e. for the calculation of both end bearing and shaft resistance. Thus, although variations in the strength of the ground are taken into account, the spatial variations and the degree to which these variations will be "averaged out" along the length of the failure surface are not described. Figure 3.2 illustrates this effect: $\overline{\phi'}$ values increasing with depth would result in shorter piles and β values closer to the target range.

In this respect, the approach used in limit states design appears more appropriate for pile design, as the characteristic values used can be selected to

account of the degree to which the occurrence of the limit state is affected by the average or local properties of the ground.

3.6 Conclusion

Reliability indices were determined for limit states designed footings, piles and retaining walls using Monte Carlo and FORM techniques. Analyses establish the utility of FORM as an economical reliability based design technique for a broad selection of geotechnical problem types. Our results further illustrate the robustness of the limit states design approach implemented in EN 1997:2004 over the range of expected values of both material and loading parameters, while indicating the importance of choosing reasonably conservative characteristic parameter values, especially when designing for ground where the friction angle in particular shows a high degree of variance.

Table 3.1: Equations for transformation of variable x to and from standard normal space (z). Note: $\gamma_e = 0.577216\ldots$ is the Euler-Mascheroni constant.

$x \sim \mathrm{N}(\mu, \sigma)$	$z = \frac{x-\mu}{\sigma}$
	$x = \mu + z\sigma$
$x \sim \mathrm{LN}(\mu, \sigma)$	$z = \frac{\ln x - \lambda}{\xi}$
	$x = \exp\left(\lambda + \xi z\right)$
	$\lambda = \ln\left(\mu\right) - \frac{1}{2}\xi^2$
	$\xi = \sqrt{\ln\left(1 + \left(\frac{\sigma}{\mu}\right)^2\right)}$
$x \sim \mathrm{Gumbel}(\mu, \sigma)$	$z = \Phi^{-1}\left(\exp\left(-\exp\left(\frac{\lambda-x}{\xi}\right)\right)\right)$
	$x = \lambda - \xi\ln\left(-\ln\left(\Phi\left(z\right)\right)\right)$
	$\lambda = \mu - \xi\gamma_e$
	$\xi = \frac{\sqrt{6}}{\pi}\sigma.$

Table 3.2: Loading and geometrical parameters for the four foundation example problems.

Example A: Vertically Loaded Strip Footing
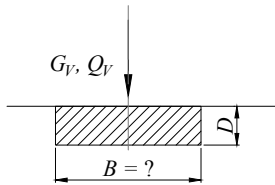
$$\overline{G} = 900 \text{ kN/m} \qquad \gamma_G = 1.0 \quad \gamma_{\phi'} = 1.25$$
$$\overline{Q}_V = 412.5 \text{ kN/m} \quad \gamma_Q = 1.3 \quad \gamma_\gamma = 1.0$$
$$Q_{Vk} = 600 \text{ kN/m}$$

$$D = 0.8 \text{ m}$$

Example B: Vertically Loaded Square Footing
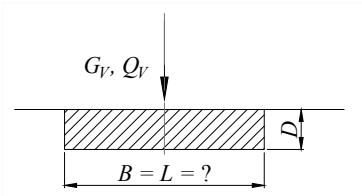
$$\overline{G} = 3000 \text{ kN} \qquad \gamma_G = 1.0 \quad \gamma_{\phi'} = 1.25$$
$$\overline{Q}_V = 1375 \text{ kN} \qquad \gamma_Q = 1.3 \quad \gamma_\gamma = 1.0$$
$$Q_{Vk} = 2000 \text{ kN}$$

$$D = 0.8 \text{ m}$$

Example C: Vertically and Horizontally Loaded Square Footing
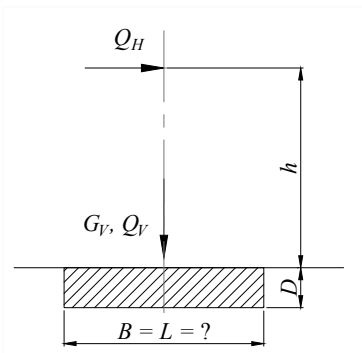
$$\overline{G} = 3000 \text{ kN} \qquad \gamma_G = 1.0 \quad \gamma_{\phi'} = 1.25$$
$$\overline{Q}_V = 1375 \text{ kN} \qquad \gamma_Q = 1.3 \quad \gamma_\gamma = 1.0$$
$$Q_{Vk} = 2000 \text{ kN} \qquad \Psi_0 = 0.7$$
$$\overline{Q}_H = 207 \text{ kN}$$
$$Q_{Hk} = 400 \text{ kN}$$

$$D = 0.8 \text{ m}$$
$$h = 4.0 \text{ m}$$

Example D: Vertically Loaded Bored Pile
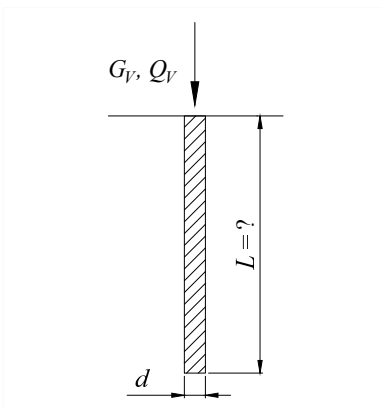
$$\overline{G} = 1200 \text{ kN} \qquad \gamma_G = 1.0 \quad \gamma_{\phi'} = 1.0$$
$$\overline{Q}_V = 412.5 \text{ kN} \qquad \gamma_Q = 1.3 \quad \gamma_\gamma = 1.0$$
$$Q_{Vk} = 600 \text{ kN} \qquad\qquad\qquad \gamma_{Rs} = 1.4$$
$$\qquad\qquad\qquad\qquad\qquad\qquad\quad \gamma_{Rb} = 1.7$$

$$d = 0.6 \text{ m}$$

CHAPTER 3.   GEOSTRUCTURAL RELIABILITY ANALYSIS   **45**

Table 3.3: Loading and geometrical parameters for the three retaining structure example problems.

Example E: Gravity Retaining Wall with a Vertical Surcharge Load
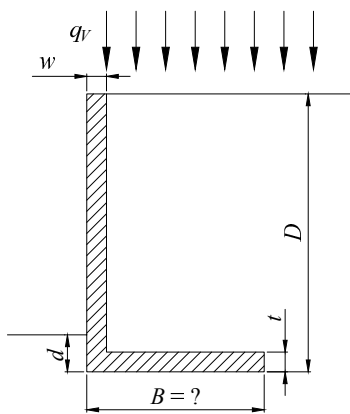
$\overline{q}_V = 13.75 \text{ kN/m}^2 \quad \gamma_q = 1.3 \quad \gamma_{\phi'} = 1.25$

$q_{Vk} = 20 \text{ kN/m}^2 \qquad\qquad\quad \gamma_\gamma = 1.0$

$D = 6.75 \text{ m}$

$d = 0.75 \text{ m}$

$t, w = 0.4 \text{ m}$

Example F: Embedded Retaining Wall
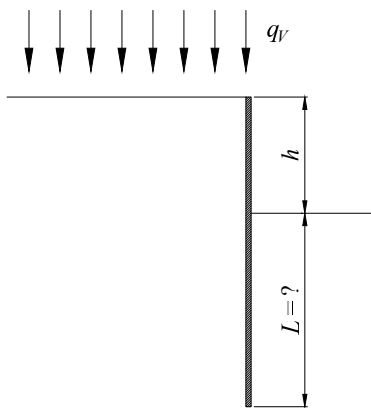
$\overline{q}_V = 6.875 \text{ kN/m}^2 \quad \gamma_q = 1.3 \quad \gamma_{\phi'} = 1.25$

$q_{Vk} = 10 \text{ kN/m}^2 \qquad\qquad\quad \gamma_\gamma = 1.0$

$h = 3.0 \text{ m}$

Example G: Anchored Retaining Wall
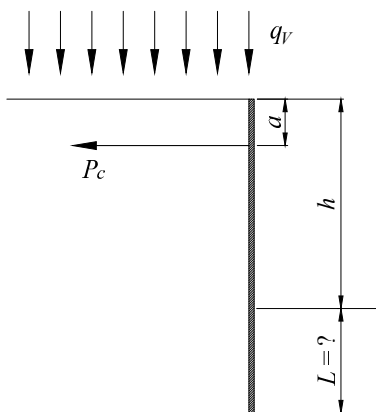
$\overline{q}_V = 6.875 \text{ kN/m}^2 \quad \gamma_q = 1.3 \quad \gamma_{\phi'} = 1.25$

$q_{Vk} = 10 \text{ kN/m}^2 \qquad\qquad\quad \gamma_\gamma = 1.0$

$h = 3.0 \text{ m}$

$a = 0.5 \text{ m}$

Table 3.4: Statistical parameters used for variable action and material properties. Specific values for the imposed loads are given for each example problem in Tables 3.2 and 3.3.

	Distribution	c_v	η_k
Actions			
Q_V	Log-Normal	0.25	1.818
q	Log-Normal	0.25	1.818
Q_H	Gumbel	0.50	1.866
Material Parameters			
ϕ'	Log-Normal	0.1	-1.0[†]
γ	Normal	0.05	-1.0[†]
	Corr. Coeff.: $\rho_{\phi\gamma} = 0.2$		

[†] *For piles, $\eta_\mathrm{k} = -0.5$ for the sides of the shaft. In all other cases:*

$\overline{\gamma} = 21.05 \text{ kN/m}^3$, $\gamma_\mathrm{k} = 20 \text{ kN/m}^3$

$\overline{\phi'} = 35.55°$, $\phi'_\mathrm{k} = 32°$

Table 3.5: Summary of the analysis results at the reference mean parameter values noted in Tables 3.2-3.4.

	LSD Solution	Factor of Safety		Reliability Index β[†]		Design Point			
	B or L	Char	Mean	Monte Carlo	FORM	ϕ'	γ	Q_V, q_V	Q_H
	(meter)					(degrees)	(kN/m^3)	(kN/m, kN, kN/m^2)	
A	3.10	2.50	5.18	3.409	3.486	25.28	19.85	482.6	–
B	3.24	2.45	5.04	3.472	3.497	25.27	19.83	1617	–
C	3.89	2.55	6.54	3.617	3.720	27.57	20.18	1333	626.0
D	16.1	1.56	2.20	3.208	3.218	26.34	19.76	143.6	–
E	3.52	3.12	6.88	3.301	3.326	25.48	20.19	14.95	–
F	4.00	1.63	2.34	3.351	3.398	25.34	20.22	7.71	–
G	2.57	1.25	1.43	3.237	3.242	25.65	20.30	7.29	–

[†]β-values where the correlation between γ and ϕ' is excluded are about 0.1 higher in both FORM and MC.
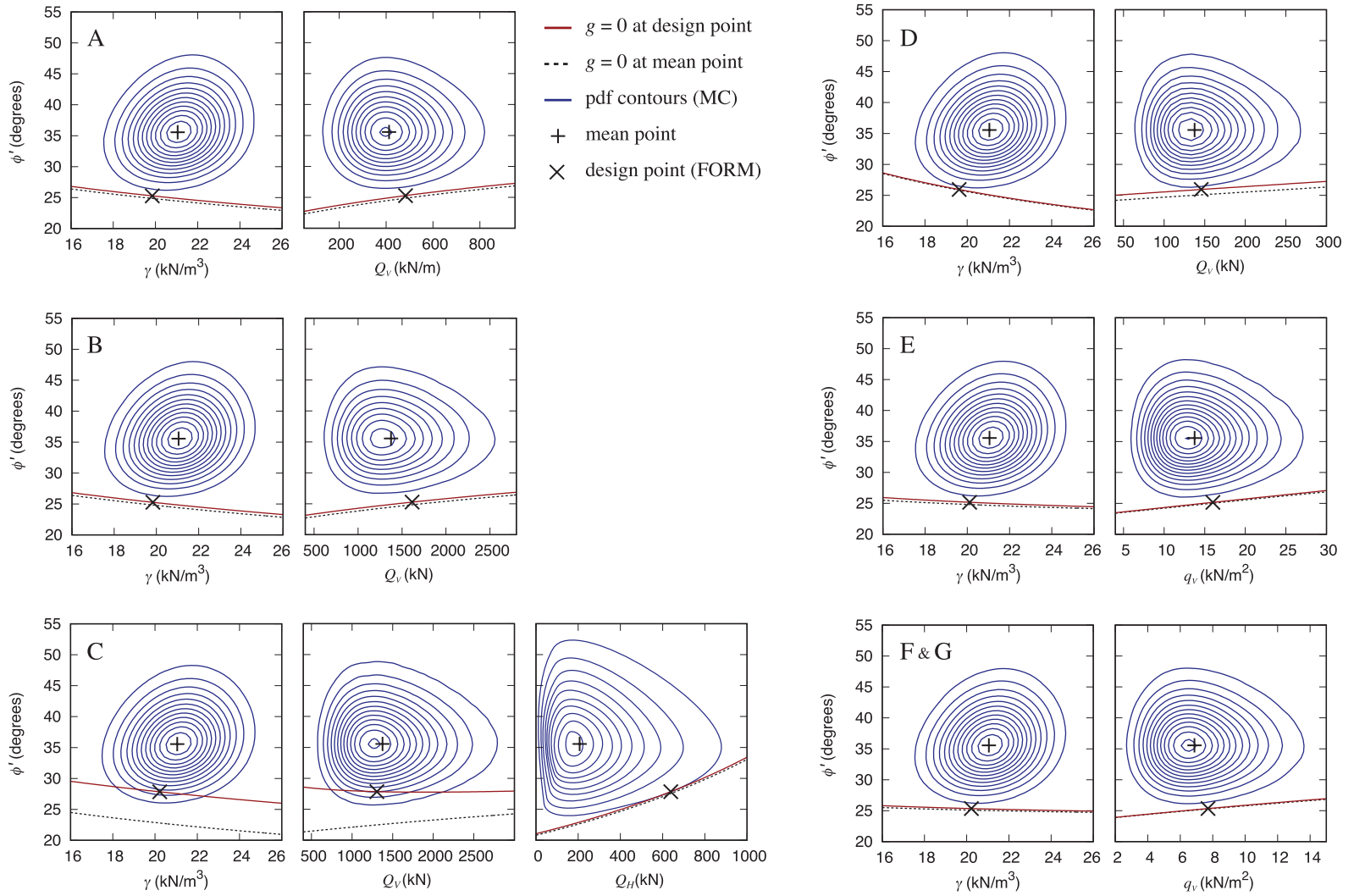
Figure 3.1: Marginal sections through parameter space to illustrate the reliability calculations. Plots for Examples F and G are almost identical, so that only F is shown.
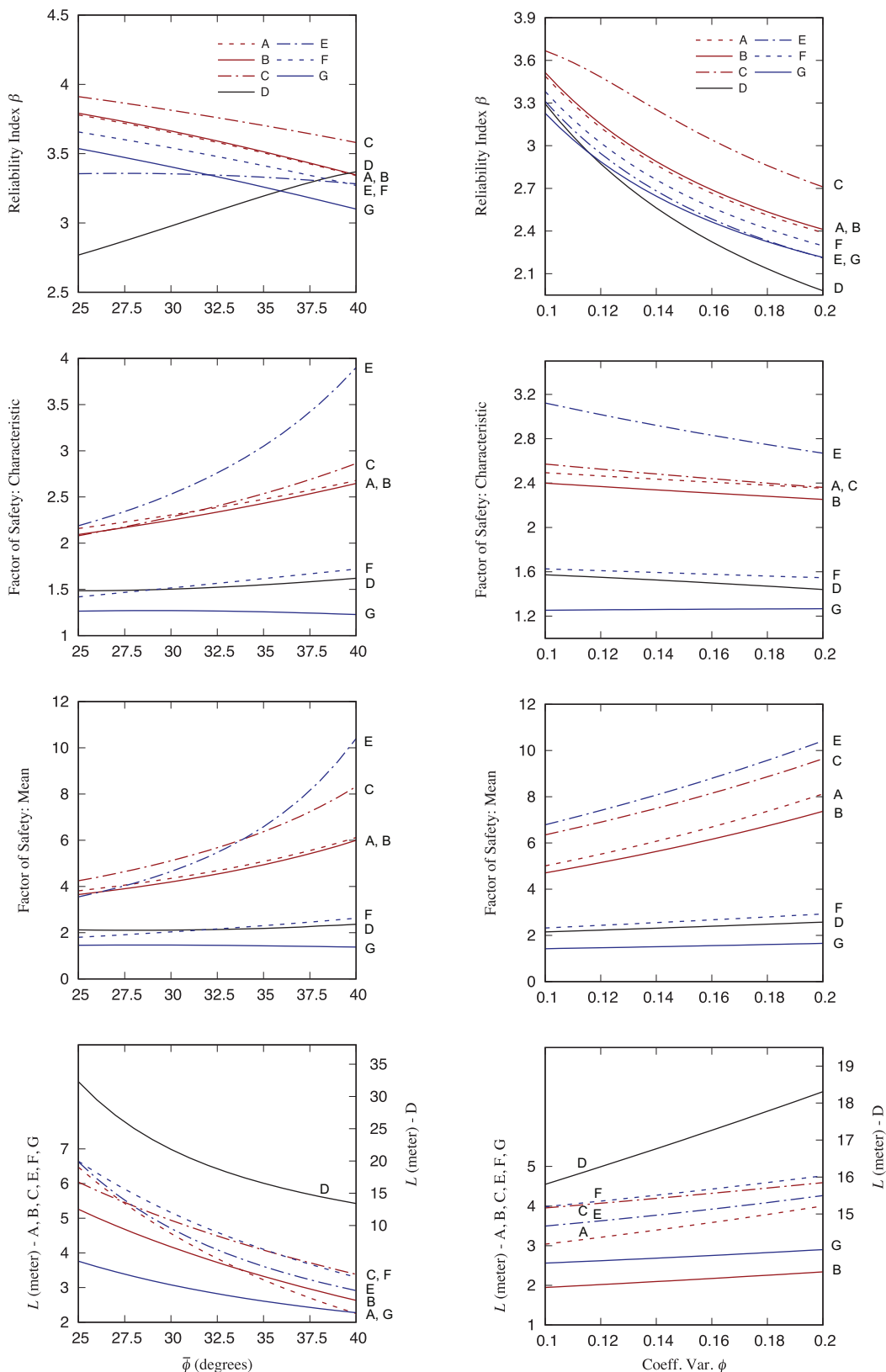
Figure 3.2: Variation of analysis results with $\overline{\phi'}$ (left) and $c_v(\phi')$ (right). All other parameter values are kept at their reference values.
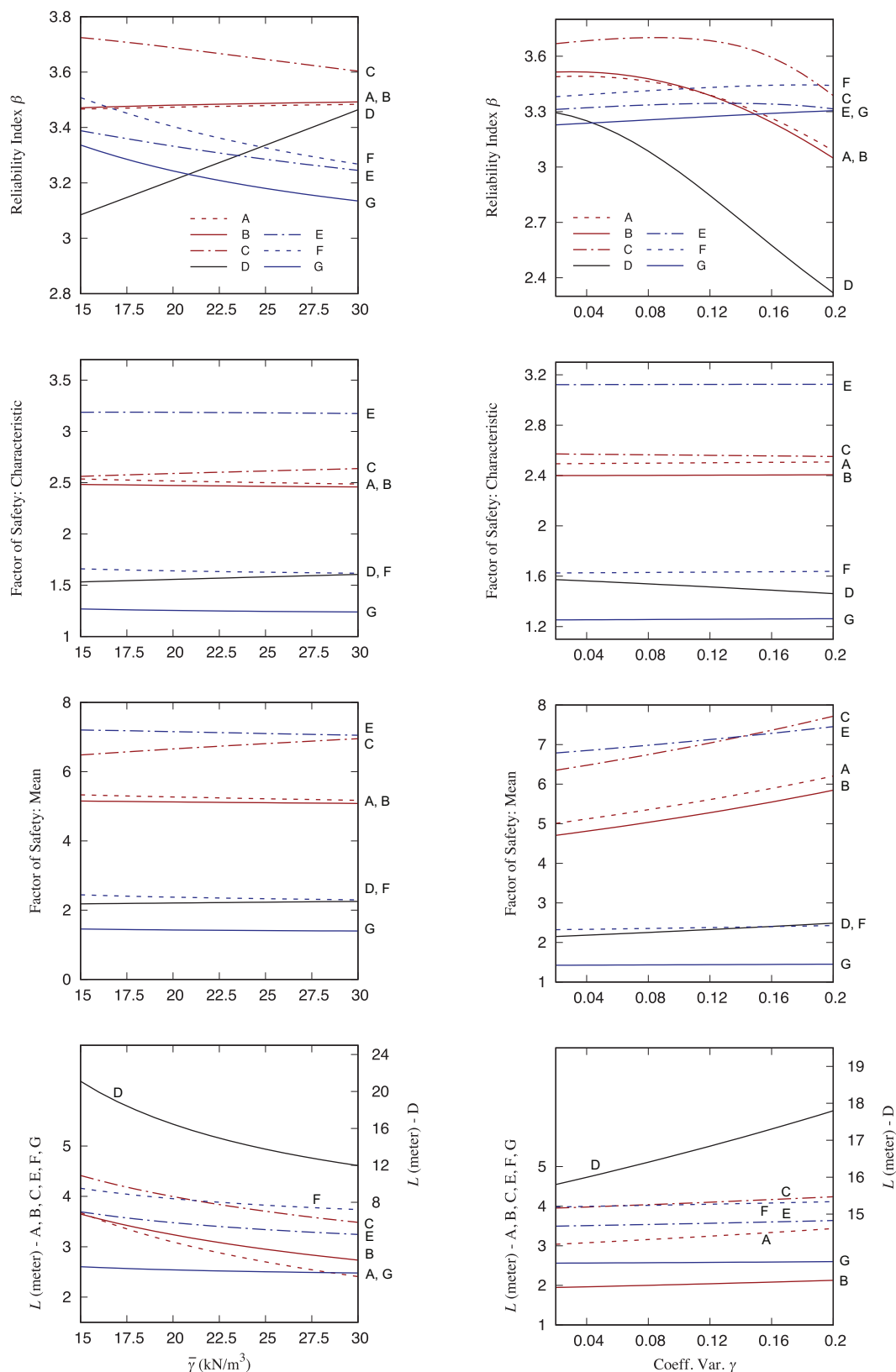
Figure 3.3: Variation of analysis results with $\overline{\gamma}$ (left) and $c_v(\gamma)$ (right). All other parameter values are kept at their reference values.
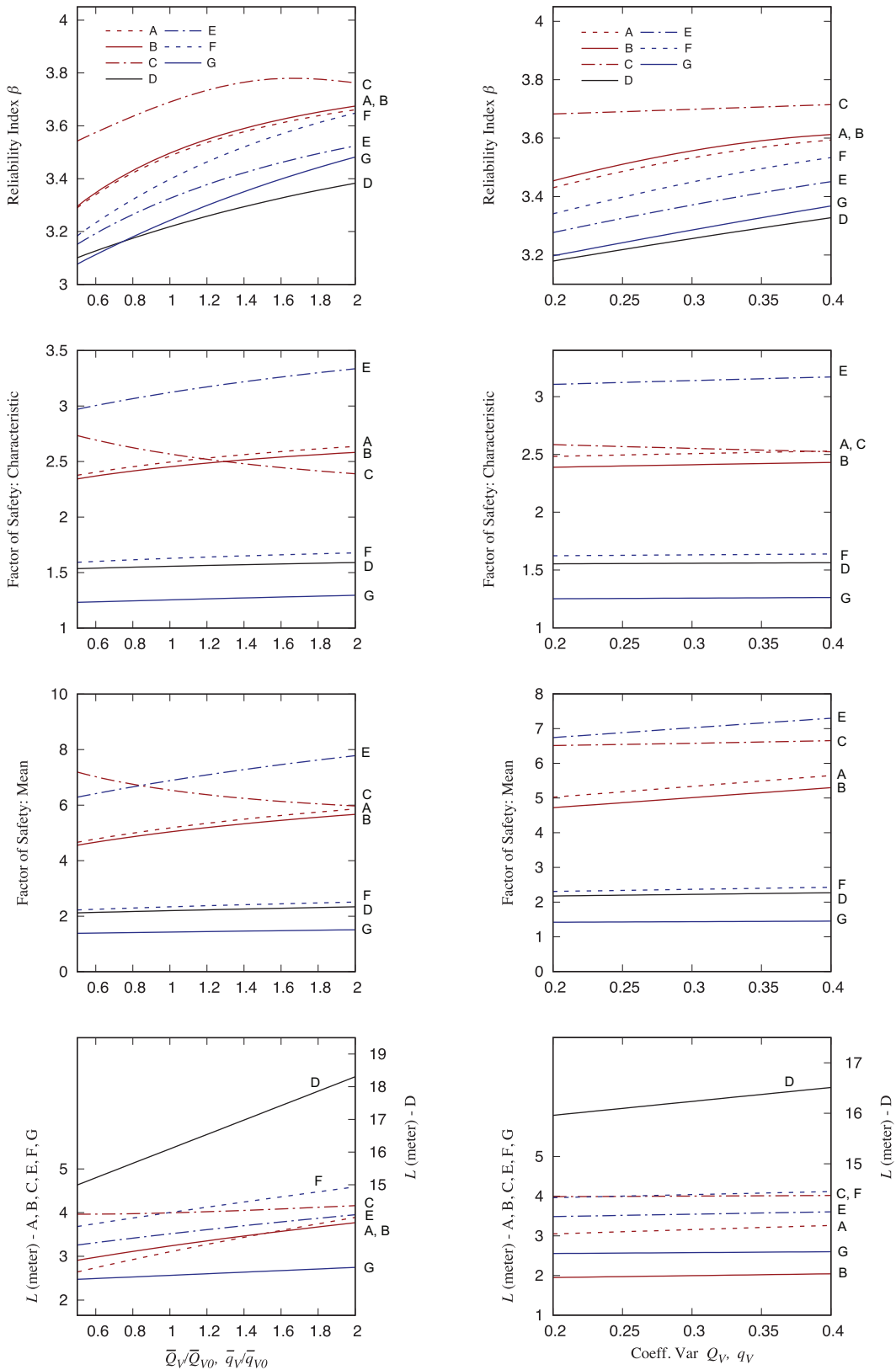
Figure 3.4: Variation of analysis results with $\overline{Q}_V$ or $\overline{q}_V$ relative the reference values (left) and $c_v(Q_V)$ or $c_v(q_V)$ (right). All other parameter values are kept at their reference values.
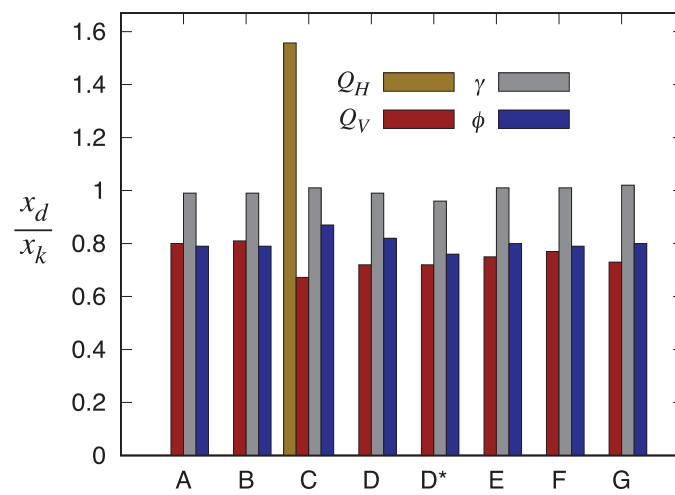
Figure 3.5: Comparison of design point values for each to the stochastic parameters x_d to the corresponding characteristic values x_k. D* refers to the x_k values for the pile shaft, for which $\eta_k = -0.05$.
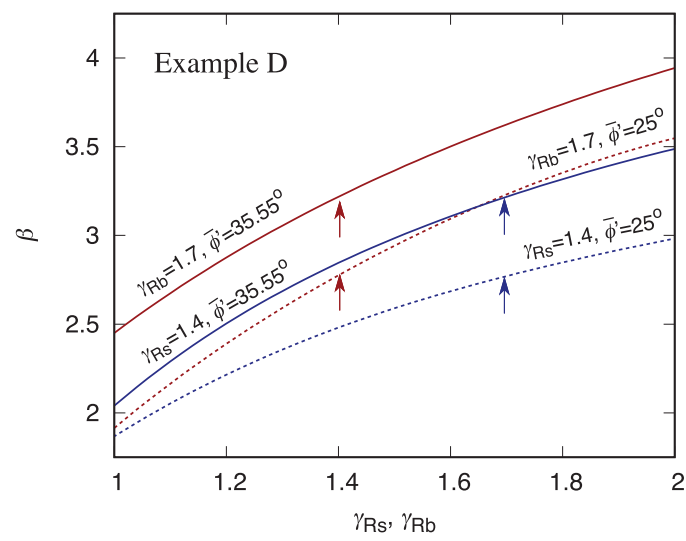
Figure 3.6: Dependence of reliability index β for piles on the partial shaft and base resistance factors (γ_{Rs} and γ_{Rb}).

Chapter 4

Reliability Analysis of EN1997 Design Approaches for Eccentrically Loaded Footings

Nico de Koker, Peter Day

Summary

EN 1997-1:2004 provides a choice of three design approaches with various combinations of partial factors applied to loads, material properties and/or resistances. A modification to design approach 2 has been suggested in which actions are combined prior to being factored. The merits of this alternative, generally referred to as DA2*, are considered in the context of spread footings subject to vertical and horizontal loads (H and V), giving rise to inclined, eccentric loading at founding level.

Evaluation of the reliability of strip and square footings designed according to design approaches DA1 to DA3, as well as DA2*, indicate that at high H/V the DA2* approach yields significantly lower reliability than the three recognised EN 1997-1:2004 options. In addition, the reliability of DA2* designs show a greater decrease with increasing H/V, as the approach does not meaningfully distinguish between favourable versus unfavourable effects of vertical loads. It is shown that the approach effectively reduces the limit states design framework to a working stress design one. The approach is therefore considered to be less suitable for limit states design of eccentrically loaded shallow footings than the recognised options.

Notation

B	dimension determined from limit states design
C	generic constant
c_v	coefficient of variation
D	depth of founding
E	applied load or action
e	eccentricity
F	cumulative distribution function
G	permanent load
g	performance function
H	horizontal load
h	height
$i_q,\ i_\gamma$	inclination factors
k	characteristic multiplier
m	shape coefficient in shape factor
$N_q,\ N_\gamma$	bearing capacity coefficients
n	number of random variables
p	probability
Q	imposed load
R	resistance capacity
$\mathbf{R}$	correlation matrix
$s_q,\ s_\gamma$	shape factors
V	vertical load
X	normalised horizontal load
x	random variable of any distribution
$\overline{x}$	sample mean for x
Y	normalised vertical load
$\mathbf{z}_\mathrm{f}$	most likely point of failure (standard normal)
β	reliability index
γ	soil density
γ_x	partial factor for property x
δ	angle of soil-concrete interface friction
ξ	statistical measure of spread
Φ	standard normal cumulative distribution function
ϕ	soil friction angle

4.1 Introduction

EN 1997-1:2004 offers a framework for limit states geotechnical design, with three design approach options (DA1, DA2, or DA3) that can be followed by EU member states as prescribed in their national annexes. For foundations subjected to vertical and horizontal loads (H and V), i.e. inclined, eccentric loading at founding level, each design approach requires the designer to consider both the favourable and unfavourable effects of actions on the structure through combinations of partial factors that reflect these scenarios.

Frank *et al.* (2004) included a modification to DA2, in which actions are combined *before* they are factored. This approach, commonly referred to as DA2*, is favoured for the German design specification by Vogt and Schuppener (2006), who consider it to yield economical designs that best fit the "tried and tested safety levels of the global safety concept". Simpson (2007) questioned the adequacy of the database for high H/V designs to support a preference for DA2* over DA2, and showed that DA2* yields strip foundation designs markedly smaller than the other design approaches. Comparison of these contrasting design approaches in the context of reliability analysis has not yet been performed, and can highlight the extent to which either option potentially over- or under designs.

This study builds on the results of Simpson (2007) by first comparing the reliability of designs for an eccentrically loaded strip footing obtained using the different EN 1997-1:2004 design approaches, including DA2*. The results are then evaluated from a limit states design perspective, in the context of the geometry of the failure boundary with increasing H/V. Finally, the findings are illustrated via a practical design example.

4.2 Theoretical Development

4.2.1 Reliability Analysis and Limit States Design

Central to both reliability and limit states analysis is the requirement that the design resistance R_d must exceed the design load E_d to avoid failure, as expressed by the performance function

$$g = R_\mathrm{d} - E_\mathrm{d} \geq 0. \tag{4.1}$$

Starting from the probability of failure p_f, the reliability of a design can be expressed via the reliability index β, which measures the minimum number of standard deviations from the mean to the failure boundary at $g = 0$. This description of β follows from its standard definition (Hasofer and Lind, 1974),

$$\beta = -\Phi^{-1}(p_\mathrm{f}), \tag{4.2}$$

where Φ is the standard normal cumulative distribution function.

The reliability index formulated in this way assumes the main parameters (loads and material properties) follow known statistical distributions even at extreme values, and that no unforeseen events or actions occur. It should therefore not be viewed as the final arbiter of safety provisions. Despite these limitations, the reliability index provides a valid measure for comparison of different design approaches based on a mutually common set of assumptions.

The reliability problem, in which n parameters have meaningful uncertainty, is analysed by determining the reliability index via the first order reliability method (FORM, Rackwitz and Fiessler, 1978; Low and Tang, 2007) as

$$\beta = \min \sqrt{\mathbf{z}_f^T \mathbf{R}^{-1} \mathbf{z}_f} \quad \text{such that} \quad g = 0. \tag{4.3}$$

Here, $\mathbf{R}$ is the correlation matrix, and $\mathbf{z}_f$ represents the most likely point of failure ("design point") expressed in standard normal units. Generally for a parameter x_i with cumulative distribution function $F(x_i)$ its equivalent standard normal parameter value is given by

$$z_i = \Phi^{-1}[F(x_i)]. \tag{4.4}$$

For x_i normally distributed, this reduces to the familiar form $z_i = (x_i - \mu_i)/\sigma_i$.

Eurocodes seek to represent the possible variation in parameters by a set of load combinations and partial factors which reflect the extent of uncertainty of each parameter. These partial factors are then applied to characteristic values x_k, which are determined as reasonable upper/lower bounds on one-sided confidence intervals about the mean $\overline{x}$,

$$x_k = \overline{x}\left(1 + kc_v\right), \tag{4.5}$$

where c_v is the coefficient of variation, and k depends on the confidence level of the interval. These values are then further adjusted via partial factors γ_x to obtain the design values x_d used to evaluate the relevant performance function (Equation 4.1).

4.2.2   Design of an Eccentrically Loaded Footing

In the context of limit states design, a strip footing (Figure 4.1) subjected to high H/V design loading is considered

$$V_d = \gamma_G V_k = \gamma_G G_{Vk}, \tag{4.6}$$

$$H_d = \gamma_{QH} H_k = \gamma_{QH} Q_{Hk}, \tag{4.7}$$

where G and Q are permanent and variable actions, respectively, G_{Vk} includes the self weight of the footing, and the γ_x terms denote the relevant limit states design partial action factors. An imposed vertical load Q_V is not included here,

because the vertical load is generally favourable for eccentrically and inclined loaded footings. As such, a partial action factor of zero would be applied causing Q_V to drop out of the equation.

If the footing is founded in cohesionless granular soil, the resistance to sliding is

$$R_d^{sl} = \tan \delta_d V_d / \gamma_R, \tag{4.8}$$

$$\delta_d / \phi_d' = \delta / \phi', \tag{4.9}$$

and bearing resistance capacity is

$$R_d^{br} = \left(\gamma' D s_q i_q N_q + \frac{1}{2} \gamma' B' s_\gamma i_\gamma N_\gamma \right) B' / \gamma_R, \tag{4.10}$$

where γ_R is the partial factor of resistance.

Equation 4.10 is the extended solution to bearing capacity (Reissner, 1924), with

$$N_q = \exp \left(\pi \tan \phi_d' \right) \tan^2 \left(\tfrac{\phi_d'}{2} + 45° \right), \tag{4.11}$$

$$N_\gamma = 2 \left(N_q - 1 \right) \tan \phi_d', \tag{4.12}$$

where the design value of the effective friction angle is

$$\tan \phi_d' = \left(\tan \phi_k' \right) / \gamma_\phi, \tag{4.13}$$

and the eccentricity and inclination of loading is accounted for by

$$B' = B - 2e_B, \tag{4.14}$$

$$e_B = \frac{\gamma_{QH}}{\gamma_G} \frac{H_k}{V_k} (h + D) \leq B/3, \tag{4.15}$$

$$i_q = i_\gamma^{m/m+1} = \left(1 - \frac{\gamma_{QH}}{\gamma_G} \frac{H_k}{V_k} \right)^m, \tag{4.16}$$

with $m = 2$ and 3 for strip and square footings respectively, and the geometry of the footing by

$$\text{strip}: \quad s_q = s_\gamma = 1, \tag{4.17}$$

$$\text{square}: \quad s_q = 1 + \sin(\phi_d'); \quad s_\gamma = 0.7. \tag{4.18}$$

In the general formulation presented above, N, i, and s are design values calculated using the value of ϕ_d' from Equation 4.13 and the appropriate partial factor from Table 4.1. Using a partial factor of 1.0 is equivalent to omitting the partial factors in Equations 4.11-4.18. The resistance factor γ_R is either 1.0 or 1.4 as given in Table 4.1.

For DA2* all partial material factors in the generalised form used for Equations 4.6-4.18 are set to 1.0, and a resistance factor of 1.4 is applied to the

calculated resistance. The component loads H and V are combined prior to factoring, and the resultant load vector is then factored by the appropriate partial action factor. This is equivalent to factoring both H and V by the same factor prior to combining the loads, which is the formulation shown in Table 4.1.

At high H/V values, H has an unfavourable effect on bearing capacity and V has a favourable effect. However, in DA2* H and V are not factored independently, so both must be regarded as either favourable or unfavourable. DA2* would typically apply a partial action factor of 1.35 applicable to unfavourable permanent actions, but for completeness sake the effect of a partial action factor of 1.0 for favourable permanent actions is also considered. Factoring H and V together results in less conservative eccentricity effects, and reduces the original limit states design framework to a working stress design problem using characteristic values, with a single safety factor of $\gamma_G \times \gamma_R = 1.0 \times 1.4 = 1.4$ for G_V favourable and $\gamma_G \times \gamma_R = 1.35 \times 1.4 = 1.89$ for G_V unfavourable.

4.3   Analysis of a Strip Footing

4.3.1   Reliability Analysis of Limit States Design

To illustrate the contrast between designs obtained via approaches DA1, DA2, and DA3 and the design resulting from DA2*, first the analysis of Simpson (2007) is repeated for a strip footing subject to eccentric and inclined loading (Vogt and Schuppener, 2006) (Figure 4.1). The smallest allowable width B of the footing required for sufficient bearing capacity is determined for a given ratio of vertical to horizontal characteristic loads H_k/V_k. This calculation is repeated for each design approach.

With the determination of minimum base widths B for each design approach completed, the corresponding reliability values β are then determined. To do this, Q_H, ϕ', and γ are taken as random variables, with statistical parameters chosen to yield the same characteristic values used by Simpson (2007) (Table 4.2; De Koker and Day, 2017; Phoon and Kulhawy, 1999).

β is calculated using the first order reliability method, which was previously shown to provide comparable results for spread footings when compared to Monte-Carlo calculations (De Koker and Day, 2017).

The results of the analysis are summarised in Figure 4.2. As already noted by Simpson (2007), it is seen that the minimum widths required by DA1, DA2, and DA3 are similar, with DA3 giving the most conservative design. This trend is reflected in the reliability indices, which lie between 2.8 and 3.2 at the higher H_k/V_k values considered.

By contrast, DA2* requires a notably smaller footing size. This "economical" result (e.g. Vogt and Schuppener, 2006), corresponds to reliability values

that are markedly lower, reaching $\beta = 2.2$ for $H_k/V_k = 0.4$.

While it is tempting to compare the resulting reliability indices with the target values given in ISO 2394:2015 and EN 1990:2002, it should be realised that the value of the reliability index is dependent on the assumptions made regarding the statistical distributions of parameters as given in Table 4.2. Nevertheless, as the same assumptions are made for all design approaches, it can be concluded that the design obtained using DA2* is significantly less reliable than the other EN 1997-1:2004 design approaches.

The importance of a limit states design approach in which both unfavourable and favourable vertical loading are considered is reflected in the contrast between reliability indices for DA2 and DA2* (Figure 4.3). DA2 designs are governed by G_V unfavourable at $H_k/V_k < 0.06$, while G_V favourable governs at higher H_k/V_k values. As a result, reliability does not vary strongly, with $2.8 < \beta < 3.3$ over the H_k/V_k range. By contrast, DA2* designs are governed by G_V unfavourable throughout, with reliability plummeting from 3.2 to 2.2 – more than an order of magnitude increase in failure probability.

Differences in DA2* designs for G_V unfavourable versus G_V favourable (Figure 4.3) result only because of the different equivalent working stress design factors of safety the approach implies (1.4 and 1.89, see above). The problem of low DA2* reliability at high H/V can therefore not be rectified by simply using larger partial factor values (Marques, 2017), as the unfavourable vertical load case remains dominant for the full H/V range, resulting in large β values towards $H/V = 0$. Figure 4.3 illustrates the case where $\gamma_G = 1.75$, corresponding to a working stress design safety factor of $1.75 \times 1.4 = 2.45$.

4.3.2 Design Point Analysis

Taking a different view of the design problem, we consider the failure envelope for a strip footing of constant width $B = 4$ m in *V*-*H* space, normalised to the maximum allowable vertical load capacity V_{d0} (i.e. at $H = 0$). It can be shown from Equation 4.10 that the failure envelope takes the implicit form

$$Y = \frac{[C_D - X/Y]\left[C_q\left(1 - X/Y\right)^2 + C_\gamma\left(1 - X/Y\right)^3\left(C_D - X/Y\right)\right]}{C_D\left[C_q + C_\gamma C_D\right]}, \quad (4.19)$$

where

$$X = H_d/V_{d0}, \quad Y = V_d/V_{d0}, \quad (4.20)$$

$$C_q = \gamma'Ds_qN_q, \;\; C_\gamma = \frac{1}{2}\gamma's_\gamma N_\gamma, \;\; C_D = \frac{B}{2(h+D)}. \quad (4.21)$$

The interaction curve (Figure 4.4) is a generalisation of the parabolic relation found by Butterfield and Gottardi (1994), mapping the loci of failure points corresponding to a range of H/V values similar to that considered in Section 3, and has its turning point at $H/V = 0.13$.

In a similar way, the failure envelope for sliding can be shown to be simply

$$X = Y \tan(\phi'_{\mathrm{d}} \delta/\phi)/\gamma_R. \tag{4.22}$$

For an optimised design, V_{d} and H_{d} lie on the failure envelope. Characteristic values V_{k} and H_{k}, that would give this condition can be derived by dividing optimised design values by the partial load factors γ_{G} and γ_{Q}. This process is shown in Figure 5 for DA2 and DA2*, and for $H_{\mathrm{k}}/V_{\mathrm{k}} = 0.05$ and 0.25.

For DA2 (Figure 4.5(a) and (b)) there are two candidate points on the failure envelope that map to characteristic values on a particular $H_{\mathrm{k}}/V_{\mathrm{k}}$ trend, corresponding to G_{V} favourable and unfavourable, respectively. The more conservative member of the pair then dominates the design: G_{V} unfavourable for $H_{\mathrm{k}}/V_{\mathrm{k}} = 0.05$, and G_{V} favourable for $H_{\mathrm{k}}/V_{\mathrm{k}} = 0.25$. In the case of DA2* (Figure 4.5(c) and (d)), $H_{\mathrm{d}}/V_{\mathrm{d}} = H_{\mathrm{k}}/V_{\mathrm{k}}$ so that there is only one candidate point on the failure envelope, and a distinction between favourable and unfavourable load cases is not meaningful.

At high H/V (Figure 4.5(b) and (d)), a design to DA2 can withstand an increase of 50% in H/V (V held constant). By contrast, DA2* is more is more sensitive to uncertainty in H/V: the characteristic point for DA2 is located only 10% of H_{k} below the failure line. Because the failure and characteristic points fall on the same $H_{\mathrm{k}}/V_{\mathrm{k}}$ trend line, its characteristic points are always closer to the failure line than those for DA2.

A similar effect would result if V_{k} is overestimated, though a more striking contrast in the case of the vertical loads is that of the normalised V_{k} values implied by DA2 versus DA2*. Because V favourable is critical for DA2, but not even considered in DA2*, the latter permits a characteristic strength nearly 3 times larger than the maximum allowed by DA2.

4.4   Design Example

4.4.1   Conveyor Support Structure on Square Footings

The differences between the design approaches are illustrated using a more practical design example. Consider a square footing foundations of a conveyor structure (Figure 4.6) at an ore processing plant. The conveyor is supported on columns every 10 m, and clad with corrugated sheeting along its top and sides.

Bearing capacity and sliding resistance for the footing is respectively determined using Equations 4.8 and 4.10. For simplicity, the same soil parameters used in Table 4.2 are assumed here.

Loading on the structure is summarised in Figure 4.6. Self-weight and imposed load are estimated according to the members in the structure and the

density of the conveyed material. Wind load on the structure is determined as specified in EN 1991-1-4:2005.

Two load combinations are considered, with partial factors and combination factors as stipulated in EN 1990:2002 for storage areas. Letting DL represent the self-weight, LL the imposed load, and WL the load due to wind,

LC1: γ_GDL $+ \gamma_{QV}$LL $+ \gamma_{QH}$WL,

LC2: γ_GDL $+ \gamma_{QH}$WL.

The design of the square footing is repeated for each design approach. The reliability index of the governing failure mode for each of these is then calculated.

Results of the analysis are summarised in Table 4.3. In all cases bearing failure under LC2 governs, with eccentricity exceeding $B/3$, so that a tolerance of 0.1 m is included in the design footing size.

LC1 and LC2 provide an explicit framework for considering vertical loads as unfavourable versus favourable. However, even within this framework, DA2* finds unfavourable vertical loads to dominate at a high H/V ratio (Table 4.3).

All three accepted EN 1997-1:2004 design approaches give very similar results, with reliability indices for bearing between $\beta =2.9$ and 3.1. These values are therefore comparable to the results obtained in Section 3.1.

In contrast, the DA2* designed footing is markedly smaller, with associated reliabilities of $\beta = 2.2$ for bearing failure.

4.5   Conclusion

An acceptable codified design approach should yield designs that are both safe and economical over the full range of expected scenarios. The partial factors recommended for use in EN 1997-1:2004 are calibrated to satisfy this criterion, but assume that the designer considers a sensible selection of load cases.

The reliability indices determined for high H/V footings illustrate that, while these criteria hold for design approaches 1, 2, and 3, design approach 2* yields significantly lower reliabilities at high H/V values.

Our analysis illustrates two significant shortcomings of the DA2* option. Firstly, it does not differentiate favourable and unfavourable loads, reducing the limit states design framework to a working stress design problem. Secondly, the reliability values corresponding to DA2* designs are not robust with variations in H/V, and are significantly lower than those achieved by DA1-DA3.

Table 4.1: EN 1997-1:2004 partial factors relevant to bearing of a strip footing, for the three design approaches explored.

			γ_G	γ_{QH}	$\gamma_{\phi'}$	γ_R
DA1-1	V	fav.	1.0	1.5	1.0	1.0
	V	unfav.	1.35	1.5	1.0	1.0
DA1-2			1.0	1.3	1.25	1.0
DA2	V	fav.	1.0	1.5	1.0	1.4
	V	unfav.	1.35	1.5	1.0	1.4
DA2*	V	fav.	1.0	1.0	1.0	1.4
	V	unfav.	1.35	1.35	1.0	1.4
DA3	V	fav.	1.0	1.5	1.25	1.0
	V	unfav.	1.35	1.5	1.25	1.0

Table 4.2: Statistical parameters used for variable action and material properties, from which characteristic values are determined via Equation 4.5, with confidence intervals as suggested by EN 1997-1:2004.

	Distribution	Mean	c_v	k	p_k
Actions					
Q_H	Gumbel	via H/V	0.50[†]	1.866	95.0%
Material Parameters					
ϕ'	Log-Normal	36.11°	0.1[‡]	-1.0	14.8%
γ	Normal	20 kN/m³	0.05[‡]	-1.0	15.8%

† – Harris and Bond (2010); ‡ – Phoon and Kulhawy (1999)

Table 4.3: Summary of limit states design and reliability analysis for conveyor support footing in Section 4.1. Values for non-critical load cases are italicised; H/V and β refer to critical load case.

| | LC1 | | LC2 | | |
| | Bearing | Sliding | Bearing | | |
	B (m)	B (m)	B (m)	H_k/V_k	β
DA1	*2.07*	*2.44*	$3.31^{\dagger}$	0.16	2.92
DA2	*2.18*	*3.04*	$3.35^{\dagger}$	0.16	3.00
DA3	*2.33*	*2.79*	$3.40^{\dagger}$	0.16	3.11
DA2*	*2.14*	*2.33*	$2.98^{\dagger}$	$0.21^{\ddagger}$	2.24

$\dagger$ – $e > B/3$, footing size adjusted by 0.1 m according to clause 6.5.4 of EN 1997-1:2004

$\ddagger$ – higher value results from lower self-weight of the smaller footing accepted by DA2*
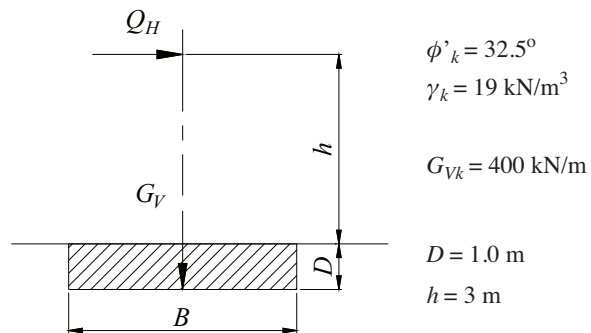
Figure 4.1: Loading and geometrical parameters for the strip footing subjected to eccentric and inclined loading.
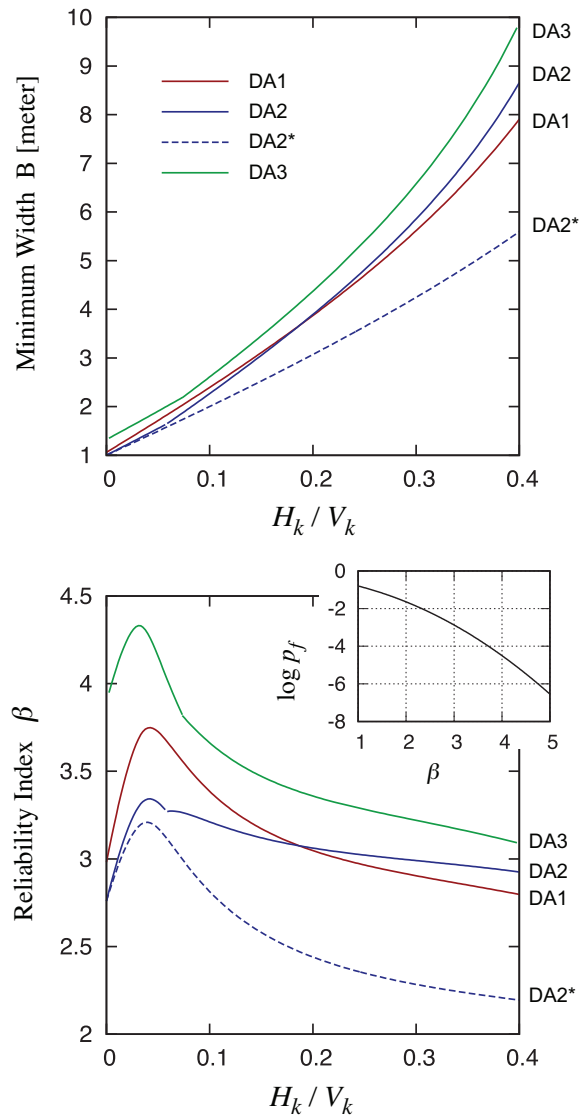
Figure 4.2: Strip footing designs determined using the different design approaches, and their corresponding reliability levels.
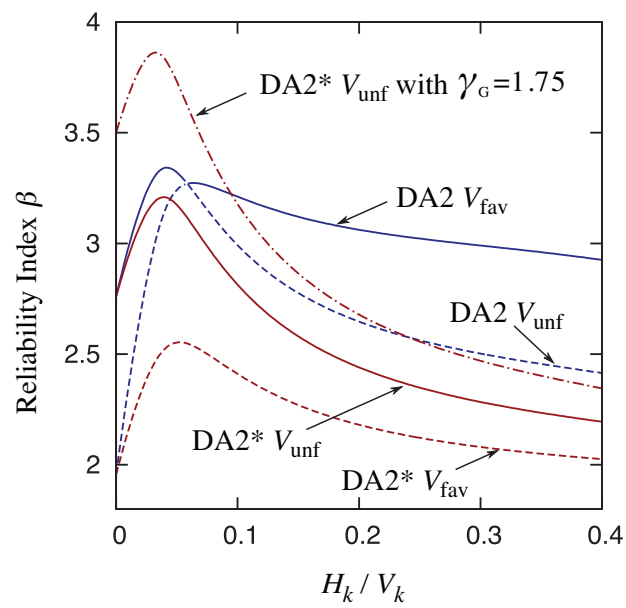
Figure 4.3: Reliability of DA2 and DA2* designs for load cases where G_V is favourable and unfavourable.
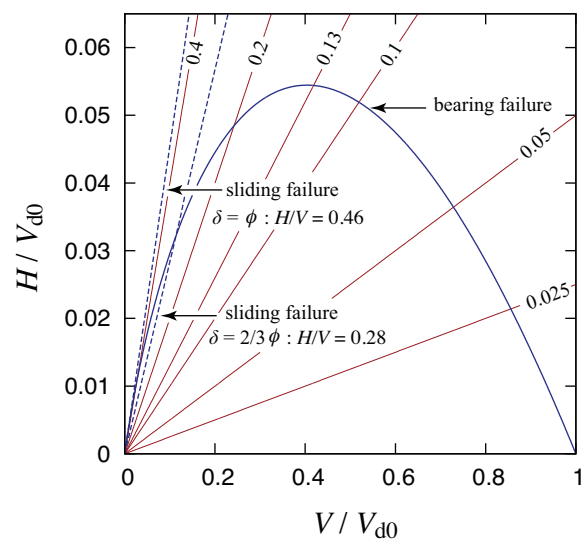
Figure 4.4: Failure envelope for a strip footing of width $B = 4$m. Solid diagonal lines indicate constant H/V ratios. Values are normalised to V_{d0}, the maximum allowable design vertical load capacity when $H = 0$.
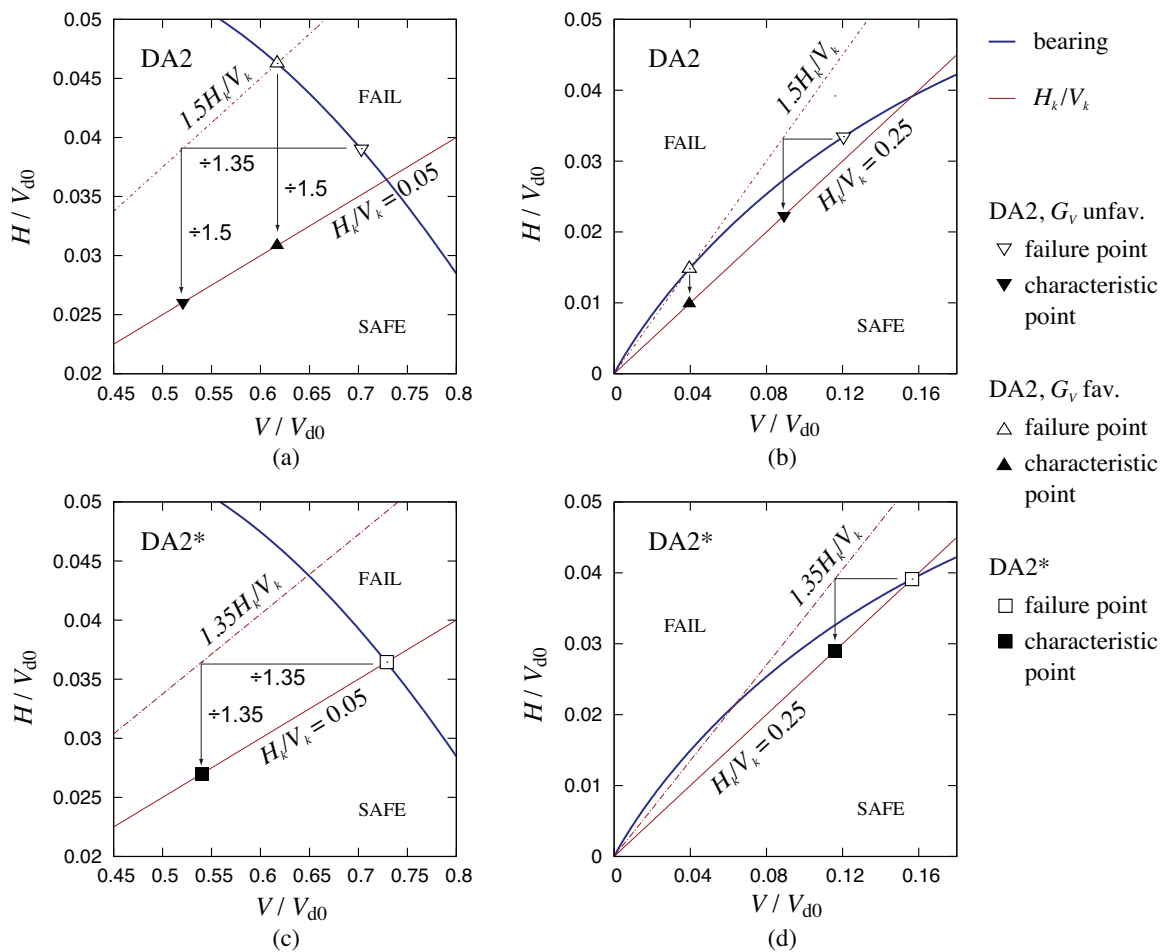
Figure 4.5: Characteristic points (closed symbols) corresponding to designs obtained using DA2 vs. DA2*, such that the optimal design values (open symbols) fall on the failure line. (a) and (c) consider the bearing failure line (Figure 4.4) where V is unfavourable; (b) and (d) consider the bearing failure line where V is favourable.
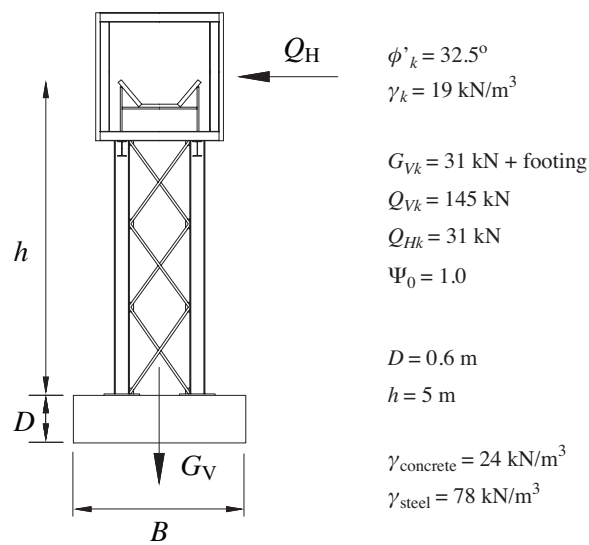
Figure 4.6: Loading and geometrical parameters for the example problem of a conveyor support structure anchored to a square footing considered in Section 4.1.

Chapter 5

Assessment of Reliability Based Design of Stable Slopes

Nico de Koker, Peter Day, Andrew Zwiers

Summary

The viability of applying reliability based design in the limit equilibrium evaluation of slope stability is assessed. Two model slopes are designed according to the limit states specification of EN 1997:2004 and reliability assessed using full Monte Carlo calculation with 10^6 trials. Comparison of these results with reliability estimates obtained via a spectrum of different analysis techniques, broadly grouped into first order reliability methods (FORM) and performance function moment estimation methods, indicate that FORM-based techniques are superior, with a first order response surface method found to provide the best combination of accuracy, stability, and speed of convergence. In this way, accurate reliability indices for non-closed form problems of the nature considered here can be obtained within 20-30 function calls, depending on the number of free parameters and required precision.

Notation

B	dimension determined from limit states design
c	cohesion
D	depth of phreatic surface
E	expected value
F	load
$\mathcal{F}$	factor of safety
g	performance function
$g*$	surrogate performance function
N	number of Monte Carlo trials
n	number of random variables
p	probability
$\mathbf{R}$	correlation matrix
S	resultant load on a slice
$\mathbf{T}$	Cholesky decomposition of $\mathbf{R}$
u	uncorrelated standard normal variable
$\mathbf{u}$	uncorrelated standard normal vector
$\mathbf{u}_{\mathrm{d}}$	design point in $\mathbf{u}$ space
V	variance
w	pore water pressure
W	weight of a slice
x	random variable of any distribution
$\mathbf{x}$	correlated vector of components x
$\mathbf{z}$	correlated standard normal vector
α	slice base inclination
β	reliability index
γ	soil density
γ_x	partial factor for property x
δ	coefficient of variation
λ	resultant load angle
μ	mean
σ	standard deviation
η	characteristic multiplier
ξ	statistical measure of spread
ζ	response surface sampling factor
Φ	standard normal cumulative distribution function
ϕ	soil friction angle

Subscripts

T	total
V	vertical
d	design value
f	failure
k	characteristic value

5.1 Introduction

Reliability based geotechnical and structural design allows the practitioner to target the relevant level of risk directly. The approach differs from the more traditional design frameworks by considering the probability of failure directly, rather than via proxy indicators such as partial factors of safety. However, it requires notable additional computational effort, as well as more stringent requirements for data quality (e.g. Phoon, 2016*a*). As a result its design office use has remained mostly limited to supplementary inquiry into unusual problems.

Advances in computational power and data analysis techniques now permit its application as a primary means of design (e.g. Phoon, 2008*a*; Jonkman and Schweckendiek, 2015). While this is especially the case for problems that are examinable via closed-form design equations (De Koker and Day, 2017), its true utility to advanced practitioners would lie in the analysis of more complex structural and geotechnical problems, which require rigorous iterative numerical solution techniques. Computation times for such calculations would typically be of a scale that the modeller can observe, i.e. a couple of seconds at the very least. Very large numbers of computations are therefore not routinely practicable, so that the method chosen to perform the reliability analysis should preferably provide accurate results from a relatively small number of capacity evaluations.

An efficient structural design should reflect the tradeoff between the cost of construction and maintenance, and the risk associated with its possible failure (consequences $\times$ failure probability). By considering this tradeoff JCSS (2008*b*) and ISO 2394:2015 have compiled guidelines for the range of reliability levels that designs should aim to achieve (Retief *et al.*, 2016). Indeed, most modern design codes are calibrated in some form with these target levels in mind (Ellingwood *et al.*, 1980; Gulvanessian, 2010; Retief and Dunaiski, 2010; Fenton *et al.*, 2016). The nominal failure probabilities associated with these target reliabilities imply at least $10^5 - 10^6$ Monte Carlo trials to obtain reliability estimates with reasonable precision.

Determining the stability of slopes is a common problem in geotechnical design. Analyses are generally carried out via limit-equilibrium methods, such as those of Bishop, Spencer, or Morgenstern-Price (e.g. Duncan and Wright, 2005). Execution times for these calculations are small enough for full Monte Carlo calculations to be accessible, even if not practical on a routine basis.

Previous studies that considered the reliability of slope design (Kirsten, 1983; Wong, 1985; Christian *et al.*, 1994; Low *et al.*, 1998; Duncan, 2000; Husein Malkawi *et al.*, 2000; Low, 2008; Gibson, 2011; Li *et al.*, 2016) either consider slope failure probabilistically in the context of the relatively simple moment-based reliability estimates, or focus on the technical details of implementing some variation on the more advanced first order reliability method. Some of these methods are complex and lack the benefits of intuitive under-

standing and transparency needed for routine design office use while others are simplified to the extent that they yield inaccurate results.

The various methods for estimating reliability of a model structure all seek to reduce the computational burden of a brute force Monte Carlo calculation by making more direct use of the underlying statistics of the problem (Ang and Tang, 1984; Harr, 1987; Baecher and Christian, 2003). As a result, these methods range significantly in both the severity of simplifying assumptions and computational cost.

The primary objective of this paper is to assess the extent to which the various reliability methods can be practically and routinely used in a geotechnical design office for the design of slopes. This is done by comparing reliability estimates from a spectrum of methods to accurate values determined via full Monte Carlo calculations, in terms of computational effort and stability. Such an analysis is not currently available, and is necessary if a reliability-based geotechnical design standard is to be compiled.

An overview of the theoretical basis for reliability analysis and limit equilibrium analysis of slope stability is presented in Section 2, after which reliability analysis of two model slope problems is examined using a variety of reliability analysis techniques (Section 3 and 4). Insights gained from these analyses are discussed in Section 5 in the context of both limit states and reliability based design.

5.2   Theoretical Development

Any design framework aiming to balance cost and risk seeks to place an optimally sufficient margin between the realised design and the most likely conditions that would bring about failure. A first requirement for this process is to locate the boundary of the set of failure conditions. A common means of defining this boundary is via the performance function g, for which negative values are taken to denote failure. The boundary of the failure region is then given by the condition

$$g(\mathbf{x}) = 0, \tag{5.1}$$

where $\mathbf{x} = [x_1, x_2, \ldots, x_n]$ is a coordinate vector of physical parameters treated as random variables with specified distributions. Specifically, x_i is characterised by mean μ_i and variance σ_i^2, and has a distribution that is generally not normal.

5.2.1   Performance Function for Slope Stability

Limit equilibrium slope analysis methods express stability via the factor of safety $\mathcal{F}$. From the condition for stability $\mathcal{F} \geq 1$, the performance function can then be expressed as

$$g = \mathcal{F} - 1. \tag{5.2}$$

The approach aims to determine a lower bound on the factor of safety by finding the critical slip surface, i.e. the surface that yields the smallest factor of safety $\mathcal{F}$. The mobilised portion of the slope is discretised into a set of vertical slices that terminate at a continuous slip surface which, for the purpose of this manuscript, is assumed to be of circular geometry (Figure 5.1), and then evaluates conditions for equilibrium.

The nature of this equilibrium characterisation constrains the choice of formulation. For example, EN 1997:2004 requires the method to satisfy vertical, horizontal, and moment equilibrium of slices (clause 11.5.1). This requirement disqualifies the simpler formulations, including that of Bishop. With this condition in mind, we will use the method of Spencer (Spencer, 1967) in this manuscript.

Spencer's formulation introduces the angle λ as an unknown parameter in addition to $\mathcal{F}$ (Figure 5.1). These two unknowns are determined by solving the equations for resultant force and moment equilibrium (Duncan and Wright, 2005),

$$\sum S = 0, \tag{5.3}$$

$$\sum S \left(\Delta x \sin \lambda - \Delta y \cos \lambda \right) = 0, \tag{5.4}$$

with

$$S = \frac{F_T \sin \alpha - c' \Delta \ell / \mathcal{F} - [F_T \cos \alpha - w \Delta \ell] \tan \phi' / \mathcal{F}}{\cos(\alpha - \lambda) + \sin(\alpha - \lambda) \tan \phi' / \mathcal{F}}, \tag{5.5}$$

where $F_T = W + F_V$, Δx and Δy are the horizontal and vertical moment arms at the base of the slice, and w is the pore water pressure. The soil is characterised by the effective friction angle ϕ', cohesion c', and density γ.

5.2.2 Statistical Framework to Quantify Reliability

Treatment of the reliability problem is most convenient after transforming the parameter space coordinate vector $\mathbf{x}$ into uncorrelated standard normal space $\mathbf{u}$. This is done by first determining the univariate standard normal value z_i corresponding to each component x_i using the Rosenblatt transformation equations (Table 5.A) yielding the vector $\mathbf{z}$, and then accounting for correlation via

$$\mathbf{u} = \mathbf{T}^{-1}\mathbf{z}(\mathbf{x}), \tag{5.6}$$

where $\mathbf{T}$ is the upper triangular Cholesky decomposition of the correlation matrix $\mathbf{R} = \mathbf{T}^T\mathbf{T}$.

After this transformation the contours of the multi-variate probability density function in $\mathbf{x}$-space become a set of concentric hyper-spheres centred about the origin in $\mathbf{u}$-space (Figure 5.2 illustrates this in two dimensions). The failure condition $g(\mathbf{u}) = 0$ forms a hyper-surface that will be tangent and orthogonal to a hypersphere at its point of closest approach to the origin. This tangent

point represents the most likely point of failure (the "design point" $\mathbf{u}_d$), and its distance from the origin is given by (Rackwitz and Fiessler, 1978)

$$\beta_{\text{FORM}} = \min\sqrt{\mathbf{u}^T\mathbf{u}}, \quad \text{such that } g(\mathbf{u}) = 0. \tag{5.7}$$

The primary objective of the reliability problem is to obtain this probability of failure. Integration of the n-dimensional probability density function over the volume where the failure condition $g < 0$ is met represents this probability of failure. It is convenient to express reliability via the reliability index (Hasofer and Lind, 1974),

$$\beta = \Phi[p_{\text{f}}], \tag{5.8}$$

where Φ is the standard normal cumulative distribution function.

To the extent that the performance function boundary $g = 0$ is a linear hyperplane, we have $\beta = \beta_{\text{FORM}}$, which is the basic assumption of the first order reliability method (FORM) discussed below.

5.2.3   Partial Factor Based Limit States Design

The partial factor framework speeds the design process by representing the design point approximately instead of attempting to find it explicitly. First, characteristic values are determined as conservative bounds on the mean parameter values,

$$x_{\text{k}} = \overline{x}\left(1 + \eta\delta\right), \tag{5.9}$$

where δ is the coefficient of variation, and η depends on the confidence level p_{k} of the interval on the mean for which x_{k} represents the bounding value. (Table 5.A includes equations by which η can be determined for the various distributions used in this manuscript).

Next, design values are obtained by scaling the characteristic values by the partial factors specified in the relevant design code (Table 5.1). These partial factors are typically calibrated to provide designs that broadly satisfy the target reliability values of JCSS (2008b) and ISO 2394:2015.

5.2.4   Methods for Reliability Determination

In principle, the probability of failure can be most accurately evaluated by means of a Monte Carlo counting procedure in which instances of $\mathbf{x}$ are randomly sampled from its multivariate distribution a large number of times N and the number of failure instances N_{f} counted. The probability p_{f} failure then simply follows as

$$p_{\text{f}} = N_{\text{f}}/N. \tag{5.10}$$

As each iteration involves a simple Bernoulli trial, the failure probability has variance

$$V[p_{\text{f}}] = \frac{p_{\text{f}}(1 - p_{\text{f}})}{N}. \tag{5.11}$$

A consequence of this relation is that for small values of p_f, large N values are required to obtain acceptable accuracy. For example for $p_f = 1/10^4$, obtaining $V[p_f] \approx p_f/10$ requires 10^6 trials.

A number of methods attempt to circumvent the large number of function evaluations required by the Monte Carlo method. These methods draw on two primary sets of assumptions. The first idealises the shape of the failure region boundary ($g = 0$) to be linear, while the second idealises the shape of the probability density function of the performance function and/or assumes the underlying variables to be normal.

The linear failure boundary used in the first assumption reduces the problem to a one dimensional description in terms of the separation between the most likely overall conditions and the most likely failure conditions, represented via a one-dimensional marginal probability distribution. The effect of this assumption is generally small, because the approximation takes effect away from the most likely point of failure, so that parts of the failure boundary where deviations from linearity become large are at small probability densities.

Because the performance function is not generally normally distributed, the second assumption can only provide reasonable results at low reliability ($\beta \lesssim 1.5$), where the probability integral is dominated by the area of failure closest to the mean and the shape of the bounding function is of secondary importance. However, its effect becomes increasingly severe as p_f decreases and the failure region retracts into the distribution tail, where the shape of the probability density function becomes critical. FORM does not require any assumptions regarding the nature of parameter distributions. The method only assumes the failure boundary to be linear in the region of the design point, an assumption which is generally robust at high reliability levels, as deviations from linearity are limited to regions of extremely low probability density.

FORM evaluates β directly using Equation 5.7. By contrast, Monte Carlo finds p_f first, with β following via Equation 5.8. To find the design point, FORM approaches implement a variety of constrained optimisation schemes. One common approach, to which we will refer as NR-FORM, uses a multidimensional Newton-Raphson formulation consisting of a series of root-finding and gradient evaluation iterations (Figure 5.3; Hasofer and Lind, 1974; Rackwitz and Fiessler, 1978). An alternative approach, collectively known as response-surface methods (e.g. Wong, 1985), replaces the performance function with a surrogate, analytical parameterisation of g (the "response surface"). The design point is then found by using the iteratively refined response surface. We will refer to these methods as RS-FORM.

The NR-FORM algorithm is very efficient for problems where the local root and gradient evaluation can be analytically expressed, rather than numerically evaluated. The RS-FORM approaches seek to harness this strength for problems where the performance function is expensive to compute, by substituting it with a "surrogate" closed form parameterisation $g*$. In this manuscript we consider the case of first and second order polynomial surrogate functions (RS1

and RS2), that is

$$g_1* = a_0 + \sum_i^n a_i x_i \tag{5.12}$$

$$g_2* = b_0 + \sum_i^n b_{i1} x_i + b_{i2} x_i^2. \tag{5.13}$$

where the $n+1$ coefficients a_j and b_j are evaluated by determining g at $n+1$ points on a constellation about an iteratively refined best estimate of the design point $\mathbf{u}_d^{[k]}$ (Bucher and Bourgund, 1990, see Figure 5.3)

$$\mathbf{u}_j^{[k+1]} = \left[u_{d1}^{[k]} \pm \zeta, u_{d2}^{[k]} \pm \zeta, \ldots, u_{dn}^{[k]} \pm \zeta \right], \tag{5.14}$$

where ζ is a pre-selected sampling factor with values around $1.0 - 2.0$. The value of ζ should be carefully chosen, especially in the case of second (or higher) order surrogate functions. If the candidate updated estimate to the design point $\mathbf{u}_d^{[k+1]}$ does not fall within the domain covered by the constellation $\mathbf{u}^{[k+1]}$, spurious extrapolation outside the region can result in divergence; too large a constellation could be associated with parameter values for which the performance function itself is poorly defined, such as high friction angle or negative cohesion values.

Points where g are evaluated are therefore chosen using an intuitive scheme that can be readily implemented in a design office. While this method is sufficient for many engineering problems, more efficient ways of determining the sampling points have been developed, and would be useful when evaluation of g becomes extremely expensive to compute (e.g. Sudret, 2015).

In contrast to the FORM class of methods, which require several iterations of performance function evaluations to reach converged estimates of the design point, the more approximate moment-based methods seek to estimate reliability directly. This is done by simplifying the problem description to a single variable ($\mathcal{F}$) which depends on the underlying stochastic parameters via a model relation (eg. Equation 5.5), and assigning a new distribution for $\mathcal{F}$ (or g). Of course, characterising the distribution still requires several evaluations of g, depending on the approach taken, which include the first order second moment equation (FOSM) and the point estimate method (PEM) (Ang and Tang, 1984; Baecher and Christian, 2003).

A common choice in these moment based methods is to simply assume $\mathcal{F}$ to be normally distributed, resulting in the expression (e.g. Christian *et al.*, 1994)

$$\beta_{\mathrm{N}} = \frac{E(\mathcal{F}) - 1}{\sqrt{V(\mathcal{F})}} = \frac{E(g)}{\sqrt{V(g)}}, \tag{5.15}$$

where $E()$ is denotes the mean and $V()$ the variance of the argument. Equation 5.15 is only valid for g normally distributed, and is not suitable as a general definition of β.

5.3   Investigation Methodology

5.3.1   Problems Considered

To compare the various reliability analysis methods discussed in Section 2.4, we will analyse two slope problems. The first is the model problem discussed by Länsivaara and Poutanen (2013), with a drained homogeneous soil. The second is a variation of this model slope, with a phreatic surface at depth D below the plateau, seeping to the slope toe.

Parameters for the problem are summarised in Figure 5.1 and Table 5.1. Statistical distributions and variation coefficients for soil parameters and the surcharge load are assigned based on the work of Phoon and Kulhawy (1999) and Retief and Dunaiski (2010).

5.3.2   Procedure of Analysis

The starting point for each analysis is a limit states design using the partial factors prescribed by NA to BS EN 1997:2004, obtained by determining the slope width B for which $\mathcal{F} = 1$. This optimal design is then analysed using full Monte Carlo, NR-FORM, RS-FORM, FOSM, and PEM. All analyses are performed using Spencer's formulation with 50 slices.

The reliability response to changes in the value of a single parameter or variation coefficient is then explored by repeating the limit states design optimisation and subsequent RS-FORM analyses over a representative range of mean parameter values and coefficients of variation. Values of the remaining parameters are kept at their mean/reference values (Figure 5.1, Table 5.1), while only the parameter of interest is varied.

5.3.3   Method of Analysis

The limit equilibrium slope analysis method for calculation of g has two nested layers of numerical analysis (Equations 5.3-5.5). The inner involves an iterative root-finding algorithm to solve for $\mathcal{F}$ and λ on a given slip surface geometry. A a non-linear Newton method (Press *et al.*, 2007) is used for this. The outer requires minimisation of $\mathcal{F}$ over candidate slip surfaces to find the critical surface. This is done using a conjugate gradient algorithm (Press *et al.*, 2007). An example of such a failure surface optimisation search is shown in Figure 5.4.

The resulting performance function is then used in the various reliability analyses to determine β and p_f values. For the Monte Carlo analyses, N uncorrelated sets of standard normal variables $\mathbf{u}$ are generated by means of the default random engine of the C++11 standard library (ISO/IEC CD 14882:2013). These variables are then transformed to correlated parameter

space **x** via the Rosenblatt equations in Table 5.A and the inverse of Equation 5.6.

To find the design point, NR-FORM analyses use Brent's root finding algorithm, and numerical derivatives obtained either by simple finite differencing or by Ridder's method (Press *et al.*, 2007), depending on the level of refinement reached by the algorithm. The surrogate performance function (Equation 5.12) implemented in RS-FORM is parameterised from performance function evaluations on the parameter constellation by means of Gaussian elimination. This parameterisation allows analytical solution for the design point on the surrogate function $g*$.

5.4   Results

Limit states design and reliability analysis results for four different slope combinations are summarised in Table 5.2. Reliability results are broadly similar for the optimised drained versus seeping slopes. Very close agreement is found between the β values determined using Monte Carlo and FORM methods, while the moment based methods yield β values that are 20-30% lower than the Monte Carlo equivalents. Monte Carlo and FORM results further indicate the negative correlation between c' and ϕ' has a strong impact on reliability values.

This influence of correlation is further seen in Figure 5.5, which illustrates the reliability solutions for the seeping slope through marginal projections of the four dimensional density function, together with the FORM-located design point, and the failure boundary line through it. The boundary of the failure region shows very little curvature. Design values used in the limit states slope design calculation are also shown on the figure, and are further compared to the respective design points in Table 5.3.

Figure 5.6 compares the variation of FORM-determined β, and factor of safety $\mathcal{F}$, over reasonable ranges of parameter values and their coefficients of variation, respectively. Note that the slope angle is optimised for each parameter value, as previously done using limit states design. Of particular note is the contrast between $\mathcal{F}$ and β: $\mathcal{F}$ remains mostly constant around 1.3, while β varies strongly over the ranges considered. A similar trend is seen with variations in the parameter coefficients of variation.

5.5   Discussion

5.5.1   Reliability Analysis

The good agreement between Monte Carlo and FORM can be understood in terms of the lack of strong curvature of the failure boundary (Figure 5.5). The assumption of a linear boundary plane (the basis of FORM) is therefore

reasonable. As such, the reliability techniques that rely on this assumption can be expected to provide accurate reliability estimates for slope problems.

Comparison of the number of performance function evaluations required to locate the design point (Figure 5.7) indicate that the first and second order polynomial response surface approaches (RS-FORM) are superior to the Newton-Raphson approach (NR-FORM). The latter requires a much higher number of function evaluations – a result of the root finding step in which it aims to return to the failure boundary. In addition, the first order response surface approach (RS1) is found to be more robust than the second order option, as the optimisation algorithm is less susceptible to divergence and instability resulting from spurious extrapolation.

A broader comparison of the number of function evaluations required by the various methods (Figure 5.8) indicates that there is no significant advantage to performing moment-based reliability estimation calculations. The number of function evaluations required by these methods is comparable to those associated with the RS-FORM approaches, which provide superior reliability estimates when compared to the Monte Carlo results.

This underestimation of β by the moment based methods can be understood by considering the frequency distribution of safety factor values obtained during the full Monte Carlo calculations for the seeping slope (Figure 5.9, with correlation included). The distribution is clearly skewed, with the mode located towards lower $\mathcal{F}$ relative to the mean. By assuming $\mathcal{F}$ to be normally distributed, these methods can only be expected to be accurate in cases where the reliability is low and the tail of the distribution has little effect on the probability of failure. However, at target reliability values for civil structures, the probability of failure is represented entirely by an area in the tail of the distribution, and the assumption of normality will have a significant influence.

To illustrate this difference, consider the contrast between Normal and Log-Normal distribution functions, both computed using the mean and standard deviation of the Monte Carlo values (Figure 5.9). Although both distributions follow the cumulative distribution values close to the mean, the Log-Normal distribution provides a notably superior representation of the distribution, especially in the tail, where the values associated with failure are located. $\mathcal{F}$ is located well into the tail, so that the actual p_f value is almost $10\times$ smaller than that implied by a normal distribution.

This comparison suggests that $\mathcal{F}$ would be better represented as Log-Normally distributed, in which case β follows as

$$\beta_{LN} = \frac{\ln(\mu)}{\xi} - \frac{1}{2}\xi, \ \ \text{with} \ \ \xi = \sqrt{\ln(1 + (\sigma/\mu)^2)}. \tag{5.16}$$

Moment-based β estimates derived in this way compare somewhat more favourably with the Monte Carlo and FORM results (Figure 5.8), though the improvement is not sufficient to justify their use.

A full Monte Carlo calculation, in which the critical slip surface is found for every trial parameter combination, can require a significant amount of time to execute. At around 0.5 seconds per trial, a single 10^6 step calculation needs around six days to complete if run in series. As a result, some slope analysis packages perform Monte Carlo "probabilistic" calculations which keep the critical failure surface fixed at that found for the mean parameters (speeding the calculation by a factor of order 10^4). In principle this approach would result in a distribution located at somewhat higher $\mathcal{F}$ values than that of a full Monte Carlo run, so that the reliability would be over-estimated.

Comparison of the frequency distributions of full versus single-slip surface Monte Carlo runs confirms this prediction, though only with a small margin. β determined with a single-slip Monte Carlo run of $N = 10^6$ steps is 3.82, somewhat above the 95% interval on the full Monte Carlo value ($3.69^{+0.05}_{-0.04}$, based on the binomial standard deviation). A similar result was reported by Low (2008). A fixed surface probabilistic run can therefore provide a relatively good estimate of the reliability that a full Monte Carlo run would yield, though such a result will always overestimate β to some extent, and can only be considered as an upper bound.

5.5.2   Implications for Limit States Design

The contrast between the extent to which reliability β and factor of safety $\mathcal{F}$ vary with changes in parameter mean and coefficient of variation values is concerning (Figure 5.6). The reliability for a limit states designed slope geometry changes by as much as 35% over the range of parameter values considered, falling to values as low as $\beta = 2.2$ in the case of high cohesion. By contrast, the factor of safety computed using the characteristic parameter values remains virtually unchanged over the same range of parameter values. This implies that designing to a target factor of safety will yield conservative designs for some soil conditions, and insufficient levels of reliability for others.

Limit states slope design may therefore treat a problem less reliably than desired in some cases. This is further illustrated in Table 5.3. Comparison between the design point and its limit states representation (design value determined from partial factors) indicates that failure occurs at a much lower surcharge load than that assumed in the limit states design, due to the lower design point cohesion value.

The range of β values obtained over the spectrum of parameter values considered lies mostly below the target value of $\beta = 3.8$ suggested by EN 1997:2004, a contrast which is enhanced if the negative correlation between c' and ϕ' is excluded. Back-analysis of failed slopes (e.g. Kirsten, 1983; Santamarina *et al.*, 1992) suggest that the nominal probability of failure associated with slopes tend to be considerably higher than the generic target levels provided by JCSS (2008*b*) and ISO 2394:2015. However, comparison of the failure probability of a structure to these target values must be done in the context

of the use of the structure. Slopes associated with mining-operations have relatively short design lifetimes and are often monitored; slopes associated with public infrastructure have long lifetimes and cannot be expected to be regularly monitored. The low slope reliabilities found by these studies can therefore not be used to justify obtaining reliabilities below the JCSS (2008b) and ISO 2394:2015 target values.

5.5.3   Reliability Based Design

To enable reliability based design to be meaningfully performed, the formulation used in the design should not overestimate the reliability and thus result in a relatively unsafe structure. However, the technique should also not underestimate reliability to such an extent that designs are unnecessarily conservative and uneconomical.

While comparison to the Monte Carlo results indicates all the methods considered to result in safe designs, the moment-based methods (FOSM, PEM) will yield overly conservative and uneconomical designs, as the corresponding "true" β value (Monte Carlo) will be quite a bit higher than the target value used in the design. The FORM-based approaches are therefore preferable from an accuracy perspective.

Two practical considerations concerning the numerical implementation of non-closed form reliability calculation should be pointed out. Firstly, because any non-closed form analysis will involve an iterative numerical convergence, a number of nested layers result when combined with the FORM-type reliability methods. To ensure numerical compatibility, tolerances must narrow towards inner layers, so that achieving satisfactory precision on reliability can require very high precision on these layers, implying an increase in execution time.

Secondly, some optimisation algorithms used in slope analysis programs evaluate the objective function over a discrete grid, and simply return the point yielding the lowest value without refining it. This approach results in a piecewise variation of $\mathcal{F}$ with changes in material parameters, which can destabilise outer level algorithms used to locate the design point. The response-surface methodology (RS-FORM) circumvents this difficulty for the most part, by choosing a continuous surrogate performance function parameterised using values at discrete points.

Taking accuracy, stability, speed of convergence, and adaptability into account, the RS-FORM methodology stands out as the most suitable to reliability analysis of non-closed form and iterative problem types of the nature considered in this manuscript.

5.6   Conclusion

A detailed assessment of the viability of routinely applying reliability analysis as a design tool for slope stability was carried out. Two model slopes were analysed using Spencer's formulation of the limit equilibrium method, with slope dimensions designed to satisfy the limit states specification of EN 1997:2004. Benchmark reliability values were then determined using a full Monte Carlo calculation with 10^6 trials.

A spectrum of reliability analysis techniques was then applied to the same slope structures. These techniques can be broadly grouped into first order reliability methods (FORM) and performance function moment estimation methods (PEM and FOSM). Comparison to the Monte Carlo benchmarks indicates FORM-based techniques to be superior, with a first order response surface method found to provide the best combination of accuracy, stability, and speed of convergence.

These results suggest that accurate reliability indices for non-closed form problems of the nature considered here can be obtained within 20-30 function calls, depending on the number of free parameters and required precision, indicating that the routine use of reliability analysis in slope design is practical. However, a similar study for geotechnical design using finite element analysis is required to evaluate the utility of reliability analysis over a more representative range of non-closed form problems. Such a study would also be able to account for the extent to which spatial variability in soil properties should be explicitly included in geotechnical reliability analysis problems.

Table 5.1: Statistical parameters used for the surcharge load and soil properties.

	Distribution	δ	η	γ_x
Surcharge				
q_V	Log-Normal	0.25	1.818	1.3
Material parameters				
γ	Normal	0.05	-0.5	1.0
c'	Log-Normal	0.40	-0.5	1.25
ϕ'	Log-Normal	0.10	-0.5	1.25
	Correlation: $\rho_{c\phi} = $ -0.3			

Table 5.2: Summary of analysis results at the reference mean parameter values noted in Figure 5.1 and Table 5.1

	Limit States Design		Reliability Index β					
	Slope Geometry	Factor of Safety	Monte		FORM		Moment-Based	
		(characteristic)	Carlo	NR	RS1	RS2	FOSM	PEM
Drained								
$\rho_{c\phi} = 0$	$B = 19.92$ m	1.29	3.11	3.02	3.01	3.02	2.14	2.36
$\rho_{c\phi} = -0.3$	(inclined at 26.7°)		3.63	3.59	3.58	3.59	2.54	2.80
Seeping								
$\rho_{c\phi} = 0$	$B = 27.97$ m	1.27	3.14	3.11	3.11	3.11	2.23	2.48
$\rho_{c\phi} = -0.3$	(inclined at 19.7°)		3.69	3.64	3.65	3.64	2.64	2.94

Table 5.3: Comparison of FORM-derived design points with the characteristic and design values used in limit states design of the two model slopes.

		q_v (kN/m^2)	γ (kN/m^3)	c (kPa)	ϕ' (deg)
Limit States Design					
Characteristic values		50.0	17.6	6.40	24.7
Design values		65.0	17.6	5.12	20.2
Reliability Analysis					
Design point					
Drained	$\rho_{c\phi} = 0$	38.1	18.1	3.60	20.6
	$\rho_{c\phi} = -0.3$	39.9	18.3	3.52	20.9
Seeping	$\rho_{c\phi} = 0$	37.6	17.6	3.76	20.2
	$\rho_{c\phi} = -0.3$	39.5	17.4	4.16	20.0
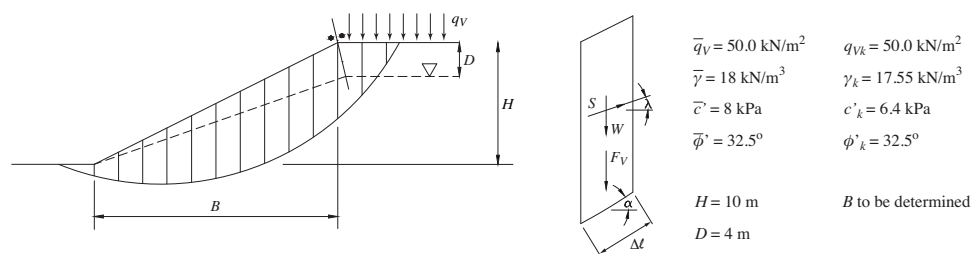
Figure 5.1: Slope geometry, loading and soil parameters for the model slope problem considered.
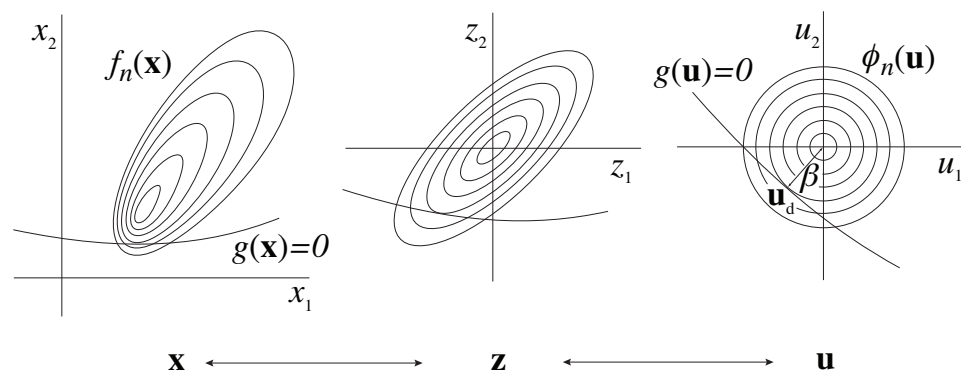
Figure 5.2: Geometrical relationship between parameter space **x** and uncorrelated standard normal space **u**. Contours of the multi-variate probability density function become spherical, with the most likely failure vector normal to the boundary of the failure region.
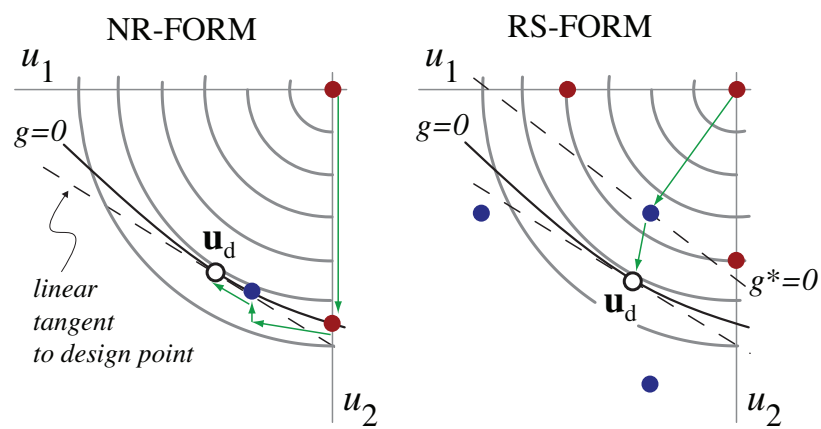
Figure 5.3: Schematic illustration of the iterative path used to find the design point using Newton-Raphson vs response surface FORM. Point colours group iterations of each technique.
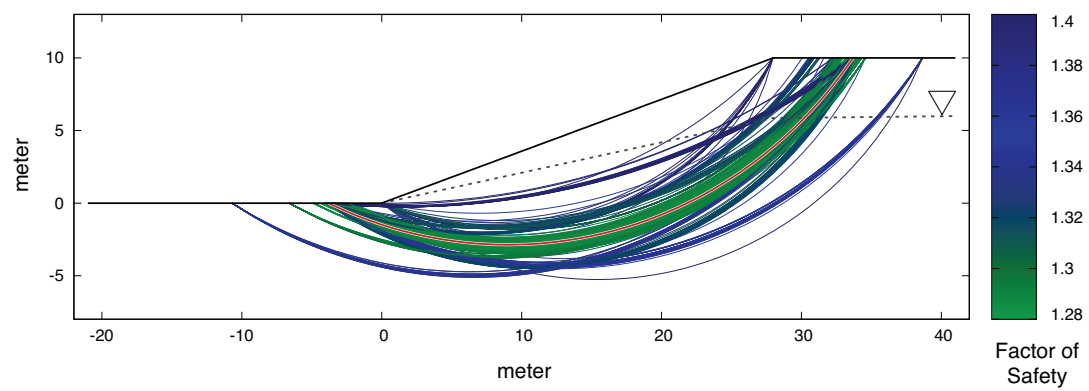
Figure 5.4: Surfaces probed by the factor of safety minimisation algorithm to locate the critical failure surface (drawn in red).
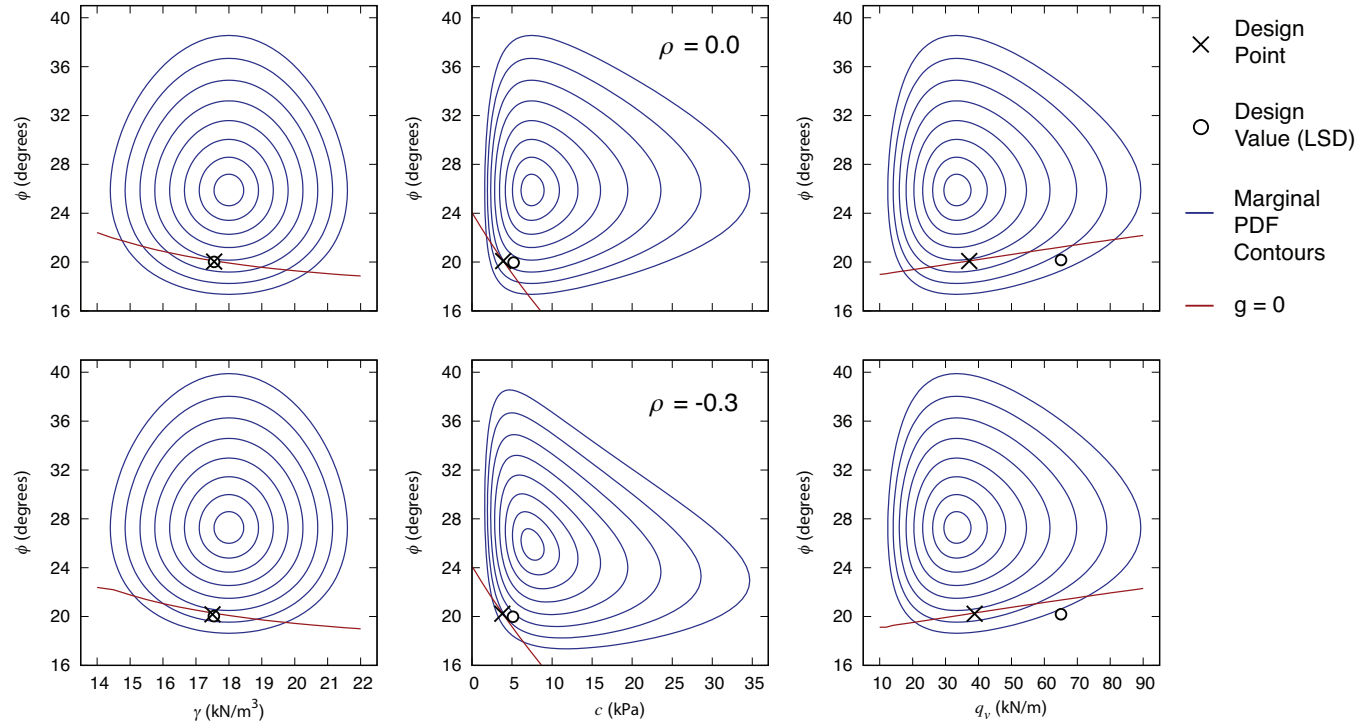
Figure 5.5: Marginal projections of the four dimensional density function (pdf) with the FORM-determined design point and projected failure boundary line of the seeping slope. LSD indicates limit states design. Note the effect of negative correlation on the volume in the failure region.
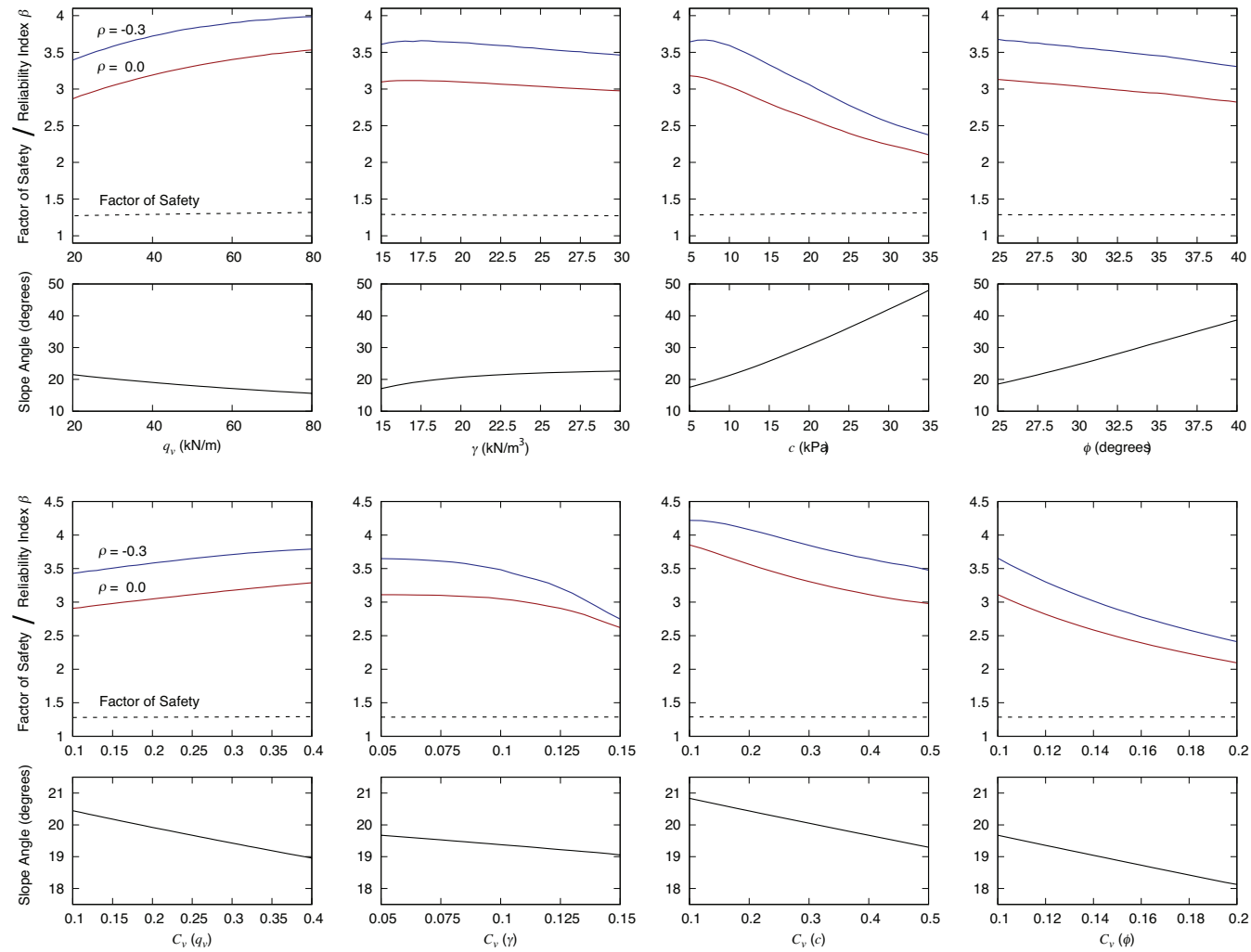
Figure 5.6: Variation of FORM-determined β and characteristic value factor of safety with variations in parameter mean and coefficient of variation values, determined for the seeping slope.
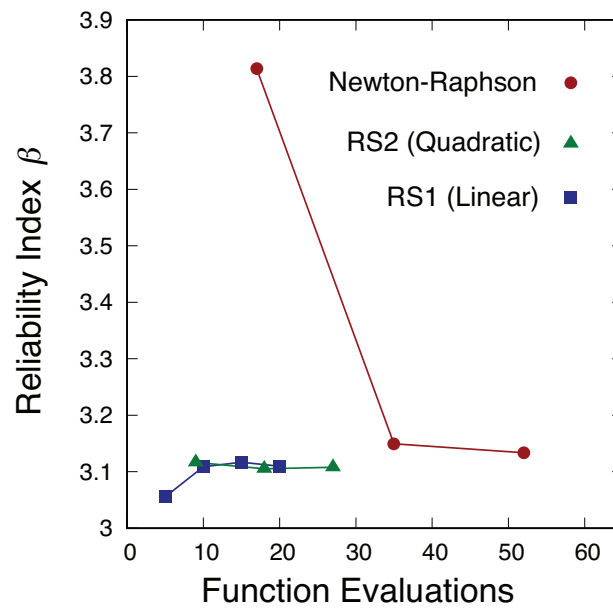
Figure 5.7: Comparison of function evaluations required by the different FORM methodologies to locate the design point and determine the reliability index (seeping slope).
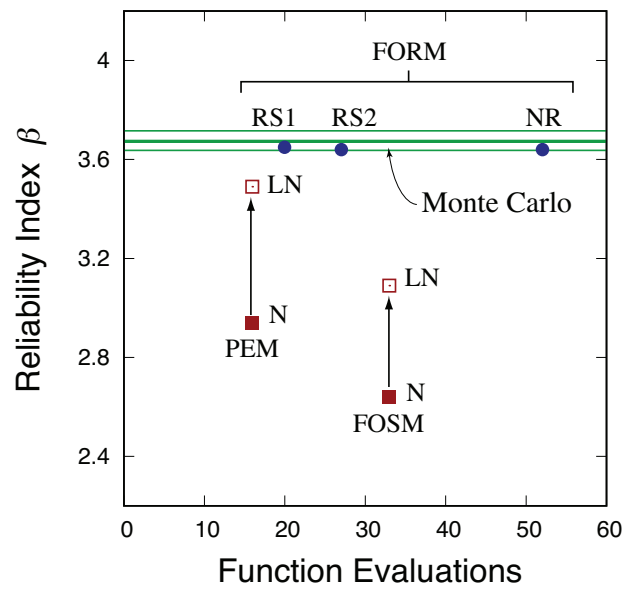
Figure 5.8: Function evaluations required by the various methods to determine the reliability index (seeping slope). Green line indicates Monte Carlo value (10^6 trails) together with the 95% confidence interval based on Binomial standard deviation.
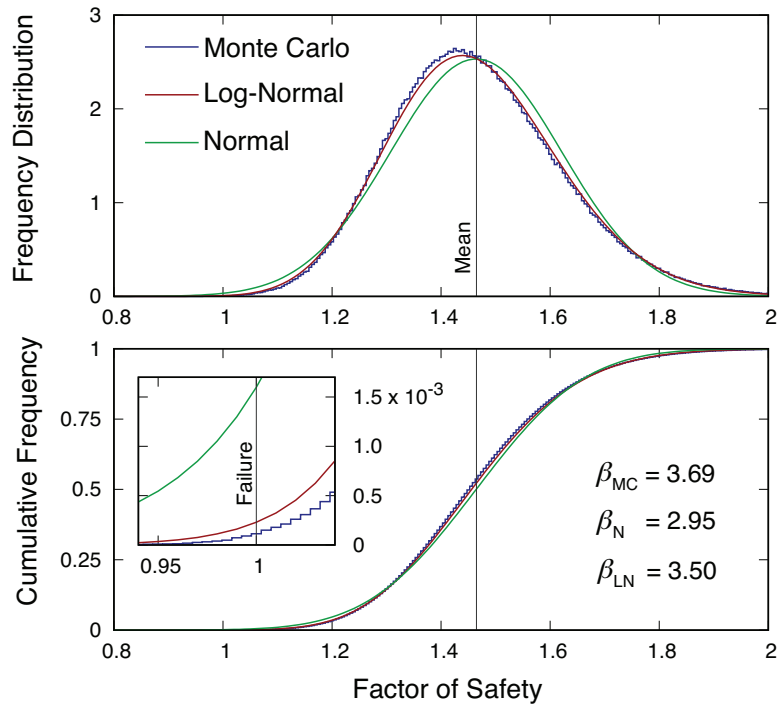
Figure 5.9: Frequency distribution of a 10^6 trial full Monte Carlo computation (seeping slope with correlation), compared to normal (N) and log-normal (LN) distributions determined from its mean and standard deviation.

Appendix

Table 5.A: Rosenblatt equations for transforming random variables between parameter space x and standard normal space z, and for relating the characteristic multiplier η to the appropriate confidence interval p_k value. After Ang and Tang (1984). $\gamma_e = 0.577216\dots$ is the Euler-Mascheroni constant.

$x \sim \mathrm{N}(\mu, \sigma)$	$z = \frac{x - \mu}{\sigma}$
	$x = \mu + z\sigma$
	$\eta = \Phi^{-1}(p_k)$
	$p_k = \Phi(\eta)$
$x \sim \mathrm{LN}(\mu, \sigma)$	$z = \frac{\ln x - \lambda}{\xi}$
	$x = \exp(\lambda + \xi z)$
	$\lambda = \ln\left(\mu / \sqrt{1 + \delta^2}\right)$
	$\xi = \sqrt{\ln(1 + \delta^2)}$
	$\eta = \frac{\exp\left[\xi^2\left(\Phi^{-1}(p_k) - 1/2\right)\right] - 1}{\delta}$
	$p_k = \Phi\left(\frac{\ln(1 + \eta\delta)}{\xi^2} + \frac{1}{2}\right)$
	$\delta = \frac{\sigma}{\mu}$
$x \sim \mathrm{Gumbel}(\mu, \sigma)$	$z = \Phi^{-1}\left(\exp\left(-\exp\left(\frac{\lambda - x}{\xi}\right)\right)\right)$
	$x = \lambda - \xi \ln\left(-\ln\left(\Phi(z)\right)\right)$
	$\lambda = \mu - \xi\gamma_e$
	$\xi = \frac{\sqrt{6}}{\pi}\sigma.$
	$\eta = -\frac{\sqrt{6}}{\pi}\left[\gamma_e + \ln\left(-\ln p_k\right)\right]$
	$p_k = \exp\left[-\exp\left(-\left(\frac{\pi\eta}{\sqrt{6}} + \gamma_e\right)\right)\right]$

Chapter 6

Assembling Meaningful Input Parameters: Bayesian Updating and Parameter Constraints

Summary

Robust parameter estimation represents a key component for successful standardisation of reliability based design, especially in geotechnical applications, where material parameters are a primary source of uncertainty. Yet characterising this variation is difficult, as geotechnical site investigations typically rely on very small sample sizes. We explore the use of Bayesian updating to supplement and combine sample measurements with other information regarding the site, notably soil classification and *in situ* measurements.

Based on these results, and supported by theory, it is recommended that Bayesian updating of sample values be done only for the mean, and then only if there is sufficient overlap between the prior and likelihood functions. Sample variance can only be meaningfully updated in cases where very large samples are available, with recognised estimates of inherent variability from the literature used in routine analyses.

The conjugate updating equations by which sample statistics and prior hyper-parameters are combined can provide standardised, robust updating methods, with use of the normal distribution sufficient. However it is important that the same distribution be used for a given parameter in both code calibration as well as design.

Bayesian updating can provide valuable additional information to supplement sample measurements, but cannot act as a substitute for good quality data. The small sample sizes that are routinely used in geotechnical design represent a major obstacle to accurate reliability analysis.

Notation

c	normalisation constant
$E()$	expected value operator
$f()$	probability density function
$L()$	likelihood function
M	random variable for mean
n	sample size
P	random variable for precision (inverse variance)
T	random variable for θ
s_x^2	sample variance
S	random variable for standard deviation
$V()$	variance operator
x	instance of a random variable
$\overline{x}$	sample mean
X, Y	generic random variables
δ	coefficient of variation
ζ	scale parameter of the Γ distribution
θ	generic distribution parameter
κ	shape parameter of the Γ distribution
μ	mean
σ^2	variance
σ_I^2, σ_E^2	inherent variance, measurement variance
τ	pseudo-observations in the Γ-Normal distribution
ϕ_p'	effective peak friction angle
$\overline{\phi'}_p$	sample mean ϕ_p' value
ω	ratio of measurement and inherent variances

6.1   Introduction

Studies of reliability based design techniques (including those presented in the previous chapters) invariably use assumed values for the parameter mean and variance as a starting point. However, the results of a reliability analysis can only be as good as the input data used to describe the distributions of the respective stochastic variables. For the distribution types used in reliability analysis, characterisation of the stochastic variation of a given model parameter predominantly requires two statistical parameters to be specified for each model parameter: the mean, and the variance.

In contrast to the parameters required for reliability of structures, the material properties that describe the resistance capacity of the soil that supports a foundation or slope structure are very variable (e.g. Phoon *et al.*, 1995; Phoon and Kulhawy, 1999). In addition, geotechnical site investigations tend to be limited to very small sample sizes, hampering accurate characterisation of the variability of these material properties. Bond and Harris (2008) notes that for triaxial test determinations of the friction angle, between one and four tests are sufficient per soil stratum, depending on the amount of experience with the soil stratum in question (four samples corresponding to the case where no previous experience is available).

Accepted best practice for geotechnical site investigation, sampling, and laboratory testing is well documented and standardised – see for example Clayton *et al.* (1995), Mayne *et al.* (2001), EN 1997-2:2007, and SAICE (2010). In addition to guidelines on the types of testing required to determine a given material property directly, EN 1997-2:2007 also allows for correlation models to be used to estimate material parameters from *in situ* measurements taken on site.

EN 1997:2004 is a load and material factor design code that is partially calibrated using a reliability basis (Gulvanessian, 2010). These calibrations rely on detailed analyses of catalogued soil strength properties, which determine the inherent variability to be expected for a typical soil of a given type (Phoon *et al.*, 1995; Phoon and Kulhawy, 1999). In addition to identifying typical value ranges of different strength and index properties for each common soil type, these studies have also yielded estimates of the magnitude of inherent variability associated with each.

The use of small sample sizes is usually justified by arguing that measurements are supplemented with other information from the site through qualitative engineering judgement (Christian, 2004; Peck, 1969). This process of updating and combining diverse sources of information into a final result is formalised quantitatively in Bayesian updating (e.g. Straub and Papaioannou, 2015). A number of studies have considered its application in a geotechnical context (Straub and Papaioannou, 2015; Ching *et al.*, 2012; Cao *et al.*, 2016; Wang *et al.*, 2016) focussing either on how the Bayes equation can be applied to geotechnical problems, or applying it to calibrate empirical transformation

models.

This study considers Bayesian parameter updating in the context of standardisation and the requirements of reliability based design. Four update strategies to a sample are explored, and the results evaluated and discussed in terms of the difficulties and pitfalls a reliability standard would have to recognise. In performing this study, our focus will be the peak friction angle of cohesionless sand, ϕ'_p.

6.2 Statistical Foundation

6.2.1 Bayesian Updating

In contrast to the frequentist view of sampling, the Bayesian description of uncertainty starts from the known sample, and treats the associated population parameters as random variables. Bayesian updating refines the parameters estimates as more information is gained, for example from sample measurements. This updating process is expressed via Bayes' rule in terms of prior and posterior parameter distributions. The principle is widely used in data science and decision theory, and a number of specialised texts are available, notably O'Hagan (1994) and DeGroot (1970). The following summary is based on these sources.

Let X be a continuous random variable of known distribution characterised by parameter(s) θ, and let T be the random variable(s) associated with θ in the Bayesian framework. A sample consisting of n observations, $x_1, \ldots, x_n$ is taken. Bayes' rule combines this dataset with prior knowledge as

$$f(T|x_1, \ldots, x_n) = cL(x_1, \ldots, x_n|T)f(T), \tag{6.1}$$

where $f(T)$ is the prior distribution, $L(x_1, \ldots, x_n|T)$ is the likelihood function, and $f(T|x_1, \ldots, x_n)$ is the posterior distribution. The updating process can be repeated, with the posterior serving as the prior of the following update. We will generally drop the conditional parenthesis and use the notation f_{prior}, and f_{post} for brevity.

The normalisation constant c ensures that the axioms of probability are satisfied, and is given by

$$1/c = \int_{-\infty}^{\infty} L(x_1, \ldots, x_n|T)f(T)dT. \tag{6.2}$$

L reflects the information in the current sample. In the case of point observations, it is expressed as a product of probability density values L_i for each sample value, from the appropriate distribution of X

$$L = \prod_{i=1}^{n} L_i. \tag{6.3}$$

In principle f_{prior} can have any functional form reflecting the prior knowledge, including a probability density function to reflect the distribution of values, or a cumulative density function to reflect lower/upper bounds on values. However, for special cases, notably where the form of prior corresponds to that of the distribution of X, the functional forms of f_{prior} and f_{post} correspond to form "conjugate priors". In such a case, the parameters (other than θ) that describe these functional forms, can be analytically related with the prior, and updated using the statistics of the sample.

6.2.2   Bayesian Updating of Parameters for Normal Random Variables

The following overview of the equations for Bayesian updating focusses on normally distributed random variables. Log-normally distributed variables can be updated using the same framework, by applying it to the logarithms of the original variables. The summary is based on explanations in Hald (1952); DeGroot (1970); Box and Tiao (1973); O'Hagan (1994); Murphy (2007); Straub and Papaioannou (2015). Note that the parameters of the Γ distribution are customarily denoted as α and β. To avoid confusion with these symbols in their reliability context, these parameters are denoted using symbols κ and ζ instead.

Let $X \sim \mathrm{N}(\mu, \sigma)$. Within the Bayesian view we define random variates for the mean M, precision P and standard deviation $S = \sqrt{1/P}$, such that

$$E(M) = \mu, \qquad E(P) = 1/\sigma^2, \tag{6.4}$$

are unbiased estimators for the distribution parameters μ and σ^2.

It is generally more convenient from an engineering perspective to consider the standard deviation S. From transformation of variables follows that

$$f(M, S) = \frac{2f(M, P)}{S^3}. \tag{6.5}$$

In the case where X is log-normally distributed, the equations above are applied to $Y = \ln X$, and M, S, and P are defined in terms of Y. Hyperparameters are also determined and updated using mean and variance values for $\ln X$. Transformation of variables then gives

$$f(M_X, P_X) = \frac{S_X}{S_Y M_X^3} f(M_Y, P_Y) \tag{6.6}$$

$$f(M_X) = \frac{1}{M_X} f(M_Y) \tag{6.7}$$

$$f(P_X) = \frac{P_Y^2}{2P_X + M_X^2} f(P_Y). \tag{6.8}$$

6.2.3   Updating with both μ and σ unknown: The Γ-Normal distribution

For M and S uncorrelated (i.e. the coefficient of variation is not fixed) the joint distribution of M and P follows a Γ-normal distribution. The prior can be written as

$$f(M, P) = f_\Gamma(P|\kappa_0, \zeta_0) f_N(M|\mu_0, 1/\tau_0 P) \tag{6.9}$$

in which κ_0, ζ_0, μ_0, and τ_0 are the prior hyper-parameters of the Γ and normal distributions,

$$f_\Gamma(P|\kappa, \zeta) = \frac{P^{\kappa-1} \exp(-P/\zeta)}{\Gamma(\kappa)\zeta^\kappa}, \tag{6.10}$$

$$f_N(M|\mu, 1/\tau P) = \left(\frac{P\tau}{2\pi}\right)^{\frac{1}{2}} \exp\left(\frac{-P\tau}{2}(M-\mu)^2\right). \tag{6.11}$$

τ reflects a number of pseudo-observations, and is intended to decouple the precision of M from P, the precision of X.

Using the sum of squares identity, the likelihood function for a sample of size n can be written as

$$L(x_1, \ldots, x_n|M, P) \propto P^{n/2} \exp\left(-\frac{Pns_x^2}{2}\right) \exp\left(-\frac{Pn}{2}(\overline{x}-M)^2\right) \tag{6.12}$$

Combination of the prior and likelihood functions via Equation 6.1 gives the posterior distribution

$$f(M, P|x_1, \ldots, x_n) = f_\Gamma(P|\kappa_1, \zeta_1) f_N(M|\mu_1, 1/\tau_1 P), \tag{6.13}$$

in which

$$\kappa_1 = \kappa_0 + n/2 \tag{6.14}$$

$$\frac{1}{\zeta_1} = \frac{1}{\zeta_0} + \frac{ns_x^2}{2} + \frac{n\tau_0}{2}\frac{(\overline{x}-\mu_0)^2}{(\tau_0+n)} \tag{6.15}$$

$$\mu_1 = \frac{\tau_0\mu_0 + n\overline{x}}{\tau_0 + n} \tag{6.16}$$

$$\tau_1 = \tau_0 + n. \tag{6.17}$$

The posterior mean and variance for X then follow as

$$E(X) = \mu_1 \tag{6.18}$$

$$V(X) = 1/\kappa_1\zeta_1. \tag{6.19}$$

The hyper-parameters of the prior distribution can be determined based on a dataset of n_d values, with mean $\overline{x}_d$ and variance s_d^2, as

$$\kappa_0 = (n_d - 1)/2 \tag{6.20}$$

$$\zeta_0 = 1/s_d^2 \kappa_0 \tag{6.21}$$

$$\mu_0 = \overline{x}_d \tag{6.22}$$

$$\tau_0 = 1/V(M)\kappa_0\zeta_0. \tag{6.23}$$

Note that $\tau_0 = 1$ if $V(M) = s_d^2$.

6.2.4   Updating only μ: Normal Distribution

If only the mean is treated as a random variable, the Γ-normal distribution reduces to its conditional density function for a given variance, so that the conjugate prior is

$$f(M) = f_{\mathrm{N}}(M|\mu_0, \sigma_0) \tag{6.24}$$

where μ_0, and σ_0 are the hyper-parameters of the prior. The likelihood function becomes

$$L(x_1, \ldots, x_n | M) \propto \exp\left(-\frac{n}{2s^2}(\overline{x} - M)^2\right) \tag{6.25}$$

and the posterior

$$f(M|x_1, \ldots, x_n) = f_{\mathrm{N}}(M|\mu_1, \sigma_1) \tag{6.26}$$

in which

$$\mu_1 = \sigma_1^2 \left(\frac{\mu_0}{\sigma_0^2} + \frac{n\overline{x}}{s_x^2}\right), \tag{6.27}$$

$$\sigma_1^2 = \frac{\sigma_0^2 s_x^2}{n\sigma_0^2 + s_x^2}. \tag{6.28}$$

As before, the hyper-parameters of the prior distribution can be determined based on a dataset of n_d values, with

$$\mu_0 = \overline{x}_d, \tag{6.29}$$

$$\sigma_0^2 = s_d^2. \tag{6.30}$$

The posterior mean of X then follows as

$$E(X) = \mu_1 = \frac{s_d^2 s_x^2/n}{s_d^2 + s_x^2/n} \left(\frac{\overline{x}_d}{s_d^2} + \frac{\overline{x}}{s_x^2/n}\right). \tag{6.31}$$

6.2.5 Updating only σ^2: Γ Distribution

If only the precision is treated as a random variable, the Γ-normal distribution reduces to its conditional density function for a given mean, so that the conjugate prior is

$$f(P) = f_\Gamma(P|\kappa_0, \zeta_0). \tag{6.32}$$

with κ_0, and ζ_0 the hyper-parameters of the prior. The likelihood function becomes

$$L(x_1, \ldots, x_n|P) \propto P^{n/2} \exp\left(-\frac{Pns_x^2}{2}\right) \exp\left(-\frac{Pn}{2}(\overline{x} - \mu)^2\right) \tag{6.33}$$

and the posterior

$$f(P|x_1, \ldots, x_n) = f_\Gamma(P|\kappa_1, \zeta_1). \tag{6.34}$$

in which

$$\kappa_1 = \kappa_0 + n/2, \tag{6.35}$$

$$\frac{1}{\zeta_1} = \frac{1}{\zeta_0} + \frac{ns_x^2}{2} + \frac{n}{2}(\overline{x} - \mu)^2. \tag{6.36}$$

As before, the hyper-parameters of the prior distribution can be determined based on a dataset of n_d values, with

$$\kappa_0 = (n_d - 1)/2, \tag{6.37}$$

$$\zeta_0 = 1/s_d^2 \kappa_0. \tag{6.38}$$

The posterior variance of X then follows as

$$V(X) = 1/\kappa_1\zeta_1 = \frac{(n_d - 1)s_d^2 + n(s_x^2 + (\overline{x} - \overline{x}_d)^2)}{n_d + n - 1}. \tag{6.39}$$

6.2.6 Separating Sources of Uncertainty

Structural and geotechnical uncertainty is often divided into aleatory and epistemic variability (e.g. Ang and Tang, 1984; Der Kiureghian and Ditlevsen, 2008). To perform reliability analysis we require the variance of a given model parameter to reflect only its inherent variability (i.e. the aleatory component); contributions to dispersion from measurement error and transformation model uncertainty should ideally not be included. As a general principle, the total observed variance can be decomposed as

$$\sigma^2 = \sigma_I^2 + \sigma_E^2, \tag{6.40}$$

where σ_I reflects inherent dispersion, and σ_E reflects other sources including measurement error.

If the analytical equations for the updated hyper-parameters of a conjugate prior are to be used, these errors should preferably be removed from the sample measurements before the updates are performed. Including Equation 6.40 directly in the update equations breaks the symmetry upon which conjugate forms are based, a problem which is compounded when the value of σ_E is different between the prior and likelihood (if it is known at all).

6.3 Application to Shear Strength: ϕ'_p in Sand

We will consider a cohesionless sand sample, characterised by five peak friction angle ϕ'_p values, $\phi'_p = [27°, 34°, 39°, 35°, 40°]$, with $\overline{x} = 35°$ and $s_x = 5.15°$ ($\delta = 0.147$). Although the values are based on an original set of triaxial measurements, some values were adjusted to increase the dispersion for the analysis to follow.

Updates of the mean and/or variance will be considered in the context of three different sources of prior information and the type of information each of these can provide.

In the analyses that follow, we will assume σ_E to be absent in the prior – either because we know it is, or because we don't know its value and make this choice as a conservative bound. The variance in the likelihood function is then reduced by correcting the sample variance via

$$s^2_{cor} = s^2/(1+\omega), \tag{6.41}$$

where

$$\omega = \sigma^2_E/\sigma^2_I. \tag{6.42}$$

As σ^2_E is not known, we consider a range of ω values between 0 and 4.0.

6.3.1 Update of μ_ϕ using SPT values.

We first illustrate the use of a transformation model to update the value of ϕ'_p measured for samples from the same stratum using *in situ* SPT blow counts, $(N_1)_{60}$. This example therefore combines two separate sets of information, together with the soil classification, for the site in question to obtain the updated estimate of the mean ϕ' for the site.

A number of transformation models between $(N_1)_{60}$ and ϕ' for coarse grained soils exist (see Ching *et al.*, 2017, for a summary). We will use the model of Chen (2004) and it's further analysis by Ching *et al.* (2017),

$$\phi'_N = 9.2 \log(N_1)_{60} + 27.5 \tag{6.43}$$

$$s_{\phi'_N} = 0.095\phi'_N \tag{6.44}$$

From this transformation model, the prior distribution is given by Equation 6.24 with $\mu_0 = \phi'_N$ and $\sigma_0 = s_{\phi'_N}$, from which the posterior for the sample is found via Equations 6.26-6.27.

Using $(N_1)_{60} = 15$ as an example, the parameters for the prior distribution are included in Tables 6.1 and 6.2, along with the updated parameters and moments of the posterior distribution. Figure 6.1 shows the corresponding distributions for cases where ϕ' is normal and log-normal, along with the changes in the posterior mean and variance when different magnitudes of measurement error are assumed. Figure 6.2 shows the variation of the mean values of the prior, likelihood, and posterior distributions as a function of $(N_1)_{60}$ (taking $\phi' \sim \mathrm{LN}$).

6.3.2   Update of μ_ϕ using a database.

Consider a case with the same sample, where no other site information than the soil type is available.

The SAND/7/2794 database (Ching *et al.*, 2017) includes a set of peak friction angle ϕ'_p values, $n_d = 239$ of which are for natural sands from a number of different sites. The relative distribution of this set of values is shown in Figure 6.3. Note that this distribution simply reflects all the ϕ'_p values for natural samples in the database – sites with more measurements therefore contribute more values to the distribution.

The prior for μ_ϕ implied by this dataset is parameterised via Equation 6.24. The parameters for the prior distribution are included in Tables 6.1 and 6.2, along with the updated parameters and moments of the posterior distribution. Figure 6.4 shows the respective distributions for cases where ϕ' is normal and log-normal.

6.3.3   Update of both μ_ϕ and σ_ϕ^2 using a database.

The variance of the SAND/7/2794 natural ϕ'_p values includes contributions from inherent variability, measurement error (including that associated with the Mohr-Coulomb failure model), as well as from differences in the range of values across different sites. The variance of this prior dataset can therefore be expected to be larger than the average inherent variability σ_I^2, and can thus be viewed as a rather lenient upper bound on the possible inherent variability. In this context, we consider the extent to which the natural ϕ'_p database can be used to update both μ_ϕ and σ_ϕ via the Γ-normal conjugate prior.

The prior hyper-parameters are determined via Equations 6.20; note that the value of $V(M)$ is purposely taken to reflect the spread in ϕ'_p values, not that of the mean itself, so that $\tau_0 = 1$. The prior and posterior distribution parameters and moments are presented in Tables 6.1 and 6.2. Figure 6.5 illustrates the cases where ϕ' normal and log-normal.

6.3.4   Update of σ_ϕ^2 using a database of δ values.

Phoon *et al.* (1995) performed a careful review of data in the literature at the time to compile a dataset of sample parameters in which all external sources of variation have been removed, leaving only the inherent variation. This dataset consists of the sample size n, mean $\overline{\phi'_p}$, and coefficient of variation δ for 7 samples reported in terms of ϕ'_p and 13 samples reported in terms of $\tan \phi'_p$. Figure 6.6 maps the scatter of values in the dataset. $\overline{\phi'}$ and s_ϕ values for the $\tan \phi'$ component of the Phoon *et al.* (1995) dataset are obtained as follows.

$$\overline{\phi'} = \tan^{-1}(\tan \phi'), \tag{6.45}$$

$$s_\phi = \tfrac{1}{2}\left(\tan^{-1}((1+\delta)\tan\phi) - \tan^{-1}((1-\delta)\tan\phi)\right). \tag{6.46}$$

The Γ prior hyper-parameters are determined by applying the conjugate update Equations 6.35 recursively to each of the sample sets in the Phoon *et al.* (1995) data. That is, $7 + 13$ successive updates are preformed using the s^2 and n values of each sample (the conjugate update equations are invariant to the order in which updates are performed). The parameters for the prior distribution are included in Tables 6.1 and 6.2, along with updated parameters and moments for the posterior distribution. Figure 6.7 illustrates illustrates cases assuming ϕ' normal and log-normal.

6.4   Discussion

6.4.1   Analysis

The simple forms of the conjugate hyper-parameter update equations, especially when ϕ' is normally distributed, make them ideal for use in a standardisation sense, allowing time consuming and error prone numerical integrations to be avoided. The equations for both the mean and the variance are effectively weighted averages of the parameters of the prior distribution and that of the sample, with the weights depending on the relative amounts of information and dispersion.

The relative weights for the conjugate posterior mean (Equation 6.31) depend primarily on the relative variances of the prior and the sample, values which tend to be relatively similar. By contrast, the weights for the conjugate posterior variance (Equation 6.39) depend on the sizes of the prior database and of the sample, values which will usually differ by one or two orders of magnitude. This contrast can be understood in terms of the sampling distribution of the mean, versus that of the variance ($V(\overline{x}) = \sigma^2/n$ vs. $V(s^2) \propto \sigma^4/n$, Hald, 1952), which shows that much larger samples are needed to decrease the variation of the sample variance (balance of 2nd vs. 4th powers). As a result, the posterior μ_ϕ value lies more or less in between the prior and sample estimates

(example Figure 6.2), yet the posterior σ_ϕ values remain essentially unchanged compared to the prior (Figure 6.7).

Prior and posterior σ_ϕ values associated with the Phoon *et al.* (1995) dataset fall at the upper end of the range of coefficient of variation values (Figure 6.6), as a result of the large sample sizes associated with high σ_ϕ values in the dataset. The posterior estimate for σ_ϕ is consistent with the general assumption of $\delta = 0.1$ for ϕ' (Phoon and Kulhawy, 1999). Interestingly, this apparent correlation between variance and sample size suggests that smaller samples are likely to underestimate the dispersion. Alternatively, the smaller samples may be the result of the engineering judgement, with practitioners taking smaller samples where strata are observed to be more uniform. Regardless, the sample sizes in the Phoon *et al.* (1995) dataset are unusual for geotechnical practice, where 2 to 5 specimens per sample are the norm (Bond and Harris, 2008).

6.4.2 Standardisation

As Bayesian updating of the variance requires large sample sizes, its routine use in geotechnical practice is not worthwhile, be it in combination with the mean or as the sole updated parameter. The focus of sample measurements should rather be the mean, with a value for δ assumed based on estimates from the literature (e.g. Phoon and Kulhawy, 1999).

The Bayesian updating method implies a number of assumptions that are important to consider if it is to form part of the design process. It is implicitly assumed that the information in the prior and the likelihood function pertain to the same type of material, i.e. the values upon which the prior is based are drawn from the same population as the sample values. When updating site data with a prior based on a broad dataset, this assumption is only partially correct, as it can be reasonably expected that individual sites with soil of the same classification will have somewhat different mean parameter values. Using such a database as prior further assumes that the total variance of each site in the database is comparable, even though it can be reasonably expected that some sites will have greater inherent variability and some laboratories will have smaller measurement error values. If sample values fall predominantly outside the primary range of the prior distribution, it is possible that the prior is not relevant to the sample.

Although the distribution type used for the material parameter of interest (in this case ϕ') in the Bayesian analysis can be viewed as prior information in itself, it is seldom unique. Inspection of the SAND/7/2794 database values in Figure 6.3 does not provide support for the choice of normal in preference to log-normal. The log-normal distribution is used for material properties such as ϕ'_p mostly as a matter of convention, with the argument that negative values are automatically absent.

In contrast, the choice of distribution is critically important in reliability analysis, where the tail of the distribution is of primary concern. Repeating the analyses presented in Chapters 3 to 5 with normally distributed ϕ'_p values results in markedly lower β values (around 1.8-2.2, instead of 3.2-3.6).

This strong dependence of reliability analysis on the chosen parameter distribution types appears troubling in the context of the observation that the 'correct' distribution cannot be determined. However, the discrepancy only poses a problem if the parameter distribution applied in a design problem differs from that used in calibrating the relevant partial factors or establishing the target β value. This problem can be avoided by explicitly standardising which distribution type is appropriate for each parameter of interest to reliability analysis, including loading-related variables (Ditlevsen, 1994).

The lack of a clear preference for either normal or log-normal distributions seen in the prior is further reflected in the similarity of posterior moments (Tables 6.1 and 6.2). This close correspondence can be understood in the context of the central limit theorem, and suggests that there is very little advantage to updating parameters via the more intricate formulation associated with the log-normal distribution. With moments about the mean as the focus of Bayesian updating, use of the hyper-parameter update equations assuming a normally distributed random variable is therefore preferable for standardisation purposes, where simplicity and robustness is desirable.

6.4.3   Pitfalls

The Bayesian update framework allows one to combine multiple priors. While such an approach can be an efficient use of all the information available, multiple priors are prone to be correlated. Unless the correlation is explicitly accounted for (e.g. Straub and Papaioannou, 2015), bias in the prior will be amplified in the derived posterior distribution. For example, the SPT transformation model of Chen (2004) (Equation 6.43) is calibrated using data also included in the SAND/7/2794 database. If there is overlap between the SPT prior and that derived using the natural samples in the database, correlation will be introduced when both the dataset and the SPT transformation model are used as priors in a single Bayesian update process.

By providing a seemingly larger support basis for obtaining *some* value to represent the mean, the approach can inadvertently encourage practitioners to take fewer samples, or even opt to rely solely on the prior information. Practitioners might also inadvertently select the prior information to suit the result they believe should be reflected by the posterior distribution, diminishing the value of the approach.

Engineering judgement applies experience to perform a similar averaging of information to that which Bayesian updating provides quantitatively. However Bayesian updating cannot substitute experience: care is required on the part of the practitioner to ensure that the prior information is relevant and unbiased.

As nothing in the method prevents the combination of incompatible prior and sample information, care must be exercised.

6.5   Conclusion

Robust parameter estimation represents a key component for successful standardisation of reliability based design. This is especially the case in geotechnical applications, where the variability of the material parameters play a major role. Best practice procedures for geotechnical sampling and investigation is well documented and standardised. Ideally, code specifications with reliability based design in mind should build on these specifications with only minimal changes and additions.

In promoting sensible robust analyses, a reliability based design standard should encourage practitioners to use prior information that is unbiased and representative of the sample information. It is recommended that Bayesian updating of sample values be done only for the mean, and then only if there is sufficient overlap between the prior and likelihood functions. In addition, sample variance can only be meaningfully updated in cases where very large samples are available. For regular strata the recognised estimates for the inherent variability can be used, while values smaller than these estimates should be avoided.

The conjugate updating equations by which prior hyper-parameters are supplemented to obtain the posterior distribution can provide standardised, robust updating methods. As these updates focus on the central moments of the parameter in question, the normal distribution can be assumed even if the log-normal distribution is used for the parameter in the rest of the design process. However it is important that the same distributions be used for a given parameter in both code calibration as well as design.
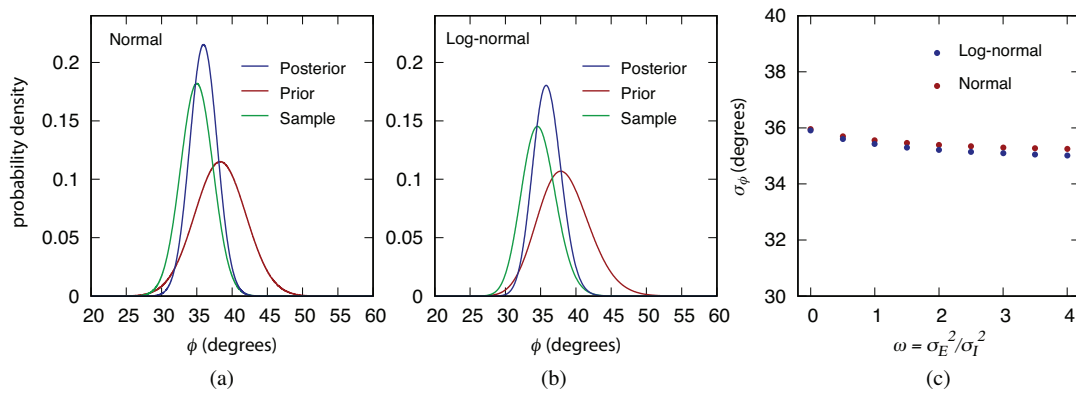
Although Bayesian updating can provide valuable additional information to supplement sample measurements, it cannot act as a substitute for good quality data. The small sample sizes that are routinely used in geotechnical design represent a major obstacle to accurate reliability analysis. The following chapter will consider the optimal sample size in greater detail.

Table 6.1: Conjugate prior and posterior hyper-parameters for the four updating strategies considered, when ϕ'_p is normally distributed.

Sample							
$\overline{\phi'_p}$	35.0°						
$s_{\phi'_p}$	5.15°						
n	5						
SPT: $(N_1)_{60} = 15$		SAND/7/2794		SAND/7/2794		Phoon *et al.* (1995)	
μ		μ		μ, σ		σ	
Theory in section							
6.2.4		6.2.4		6.2.3		6.2.5	
Prior							
μ_0	38.3°	μ_0	41.6°	κ_0	119	κ_0	518
σ_0	3.64°	σ_0	4.06°	ζ_0	5.10×10^{-4}	ζ_0	1.18×10^{-4}
				μ_0	41.6°		
				τ_0	1.0		
Posterior							
μ_1	35.9°	μ_1	36.6°	κ_1	121.5	κ_1	520.5
σ_1	1.95°	σ_1	2.00°	ζ_1	4.92×10^{-4}	ζ_1	1.17×10^{-4}
				μ_1	36.1°		
				τ_1	6.0		
μ_ϕ	35.9°		36.6°		36.1°		
σ_ϕ					4.09°		4.05°
δ_ϕ					0.11		0.11

Table 6.2: Conjugate prior and posterior hyper-parameters for the four updating strategies considered, when ϕ'_p is log-normally distributed.

Sample							
$\overline{\ln \phi'_p}$	3.55°						
$s_{\ln \phi'_p}$	0.156°						
n	5						
SPT: $(N_1)_{60} = 15$		SAND/7/2794		SAND/7/2794		Phoon *et al.* (1995)	
μ		μ		μ, σ		σ	
Theory in section							
6.2.4		6.2.4		6.2.3		6.2.5	
Prior							
μ_0	3.64	μ_0	3.72	κ_0	119	κ_0	518
σ_0	0.0947	σ_0	0.0975	ζ_0	0.885	ζ_0	0.170
				μ_0	3.72		
				τ_0	1.0		
Posterior							
μ_1	3.58	μ_1	3.61	κ_1	121.5	κ_1	520.5
σ_1	0.0562	σ_1	0.0567	ζ_1	0.839	ζ_1	0.168
				μ_1	3.58		
				τ_1	6.0		
μ_ϕ	35.9°		36.9°		35.9°		
σ_ϕ					3.57°		3.95°
δ_ϕ					0.11		0.11

Figure 6.1: Prior, likelihood, and posterior distributions updating the test sample with the SPT transformation model of Chen (2004), assuming $(N_1)_{60} = 15$, and (a) $\phi'_p \sim \mathrm{N}$, (b) $\phi'_p \sim \mathrm{LN}$. The posterior mean tends to that of the sample as the total fraction of the variance attributed to measurement error is increased (c).
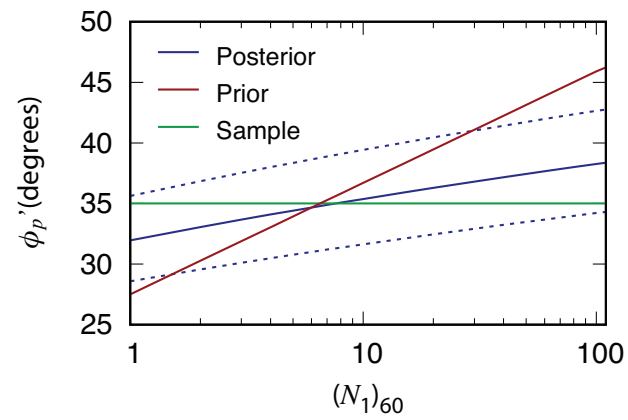
Figure 6.2: Mean values of the prior and posterior distribution functions as a function of $(N_1)_{60}$, assuming $\phi'_p \sim$ LN. Dotted lines denote 95% confidence bounds from the posterior distribution.
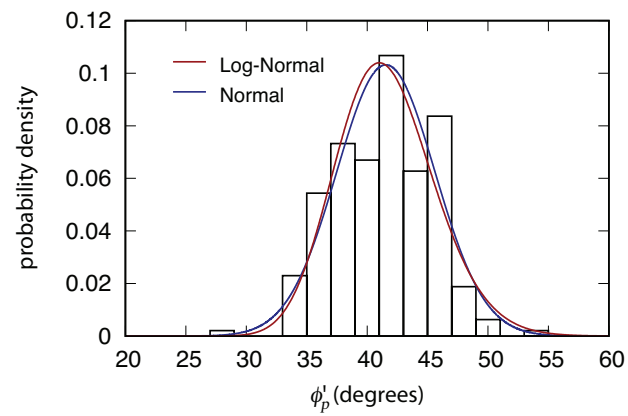
Figure 6.3: Distribution of peak friction angle values determined by triaxial testing for natural samples in the SAND/7/2794 database (Ching *et al.*, 2017)

.
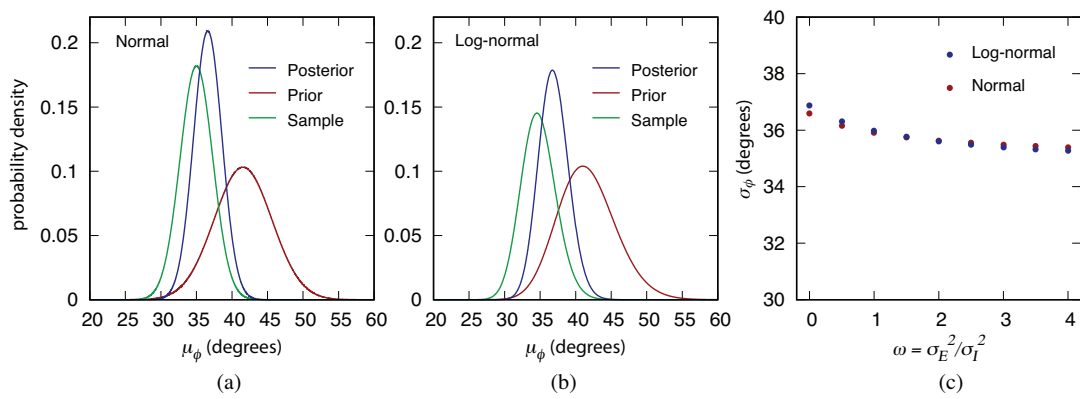
Figure 6.4: Prior, likelihood, and posterior distributions updating the test sample with ϕ'_p values for natural samples in the SAND/7/2794 database (Ching *et al.*, 2017), assuming (a) $\phi'_p \sim N$ and (b) $\phi'_p \sim LN$. The posterior mean tends to that of the sample as the total fraction of the variance attributed to measurement error is increased (c).
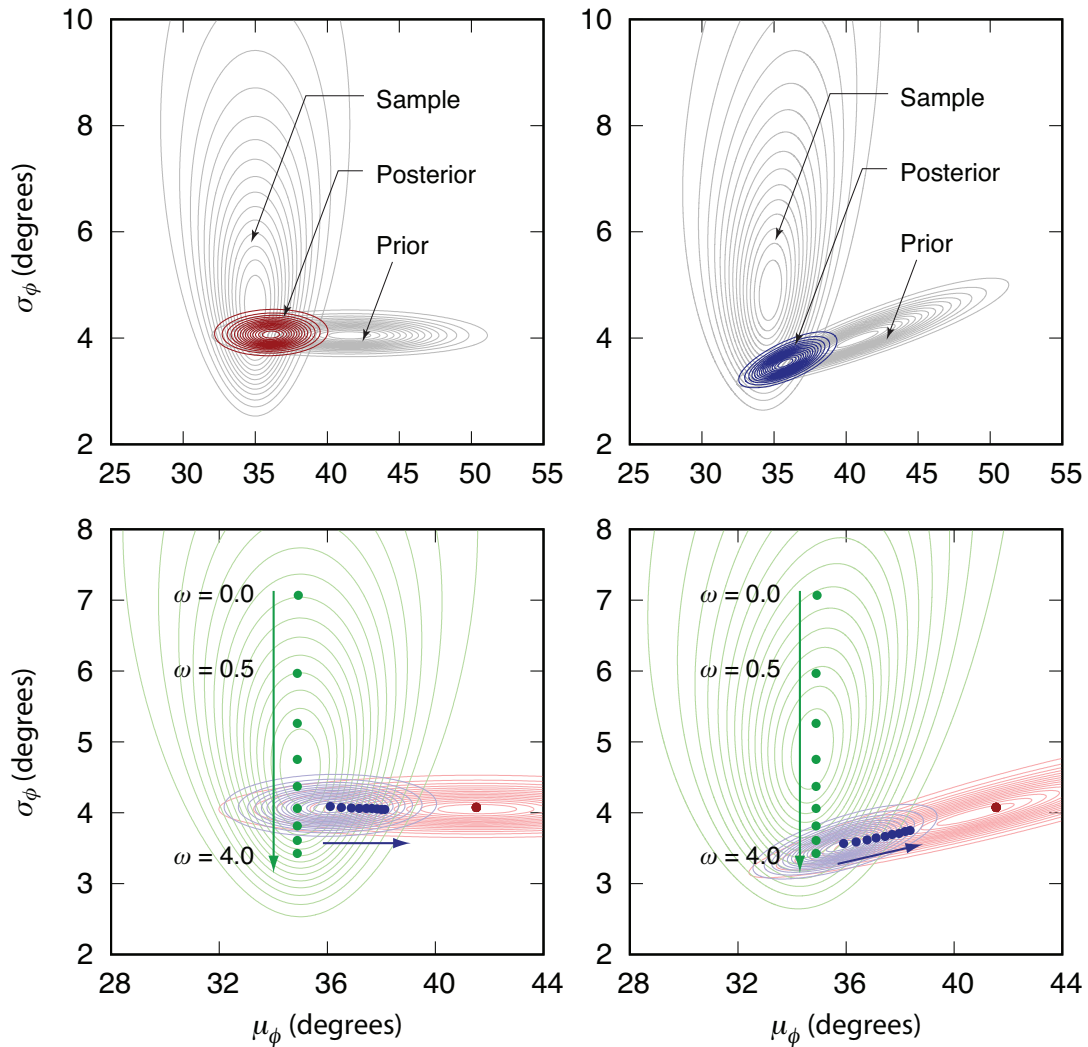
Figure 6.5: Prior, likelihood, and posterior distributions updating both μ_ϕ and σ_ϕ for the test sample with ϕ'_p values for natural samples in the SAND/7/2794 database (Ching *et al.*, 2017). (a,c) $\phi'_p \sim$ N; (b,d) $\phi'_p \sim$ LN. The posterior mean tends to that of the prior as the total fraction of the variance attributed to measurement error is increased (c,d), due to decreasing overlap between the prior and likelihood distributions.
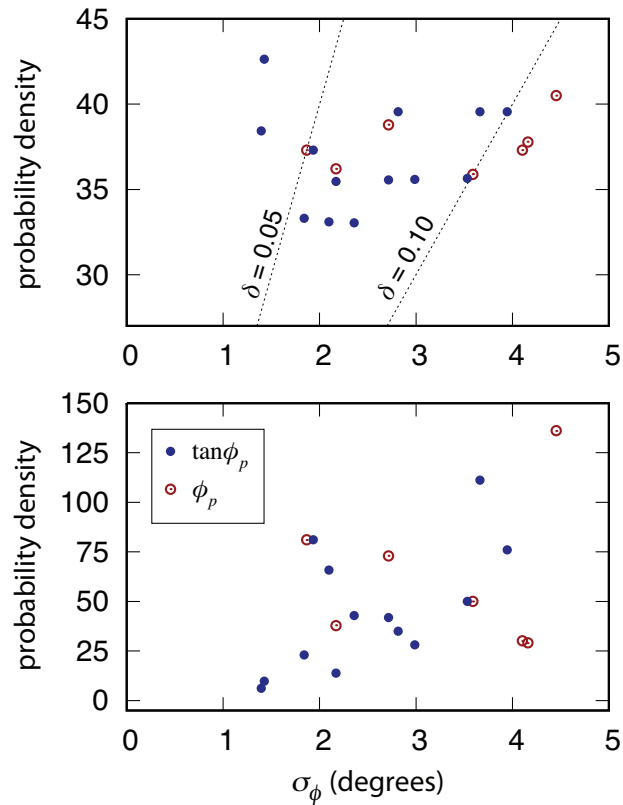
Figure 6.6: Mean and standard deviation values determined from the compiled dataset of Phoon *et al.* (1995). Note the apparent correlation between dispersion and sample size.
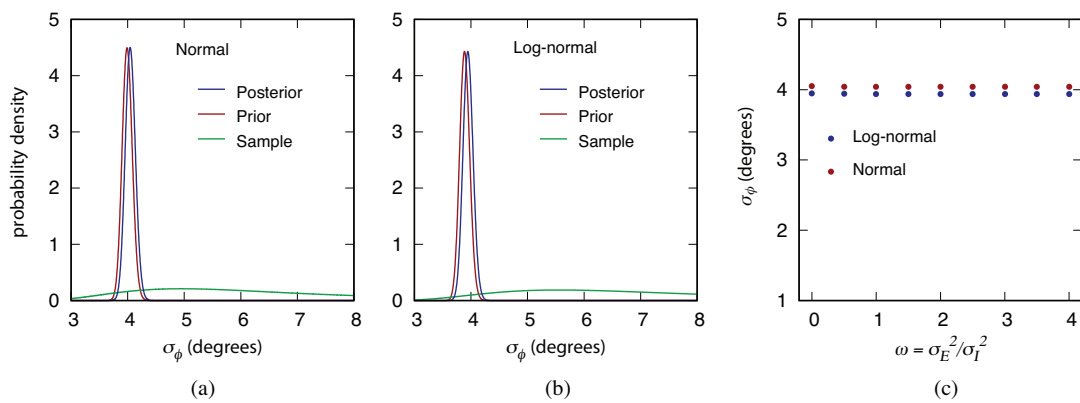
Figure 6.7: Prior, likelihood, and posterior distributions updating the test sample with sample variances from the dataset of (Phoon *et al.*, 1995), assuming (a) $\phi'_p \sim \text{N}$ and (b) $\phi'_p \sim \text{LN}$. The prior and posterior variance coincide to the extent that accounting for measurement error in the sample has no effect (c).

Chapter 7

Optimal Sampling for Reliability Based Design

Summary

Routine reliance on small sample sizes in soil strength determinations for geotechnical design is often cited as a primary culprit in failures and delays during and after construction. This deficiency is especially relevant when design is to be performed directly to a target reliability value. However, it is not entirely clear how much larger sample sizes should be.

A decision analysis framework is developed using the predictive reliability index, which accounts for both the uncertainty in model variables as well as the uncertainty in their statistical parameters. The result is a relation between the optimal sample size, the conditional reliability used as target value in design, and the expected damages associated with failure. This relation is used to derive a set of reference charts that can be directly used to determine the optimal sample size for a given problem. While these charts apply principally to a normally distributed limit state function, the relative uncertainty in forecasts of liability suggest that it can be applied more generally. A correction factor can nonetheless be determined, should a more accurate optimisation be required.

Consideration of the design charts for a target reliability of $\beta_0 = 3.0$ suggests that typical optimal sample sizes should fall between 5 and 15. The results confirm previous work in showing that greater initial investment in obtaining good quality information on the subsurface conditions can save developers significant expenses later on in the project and after commissioning.

Notation

B	footing width
c	unit cost of testing a single sample
c_u	cohesion of an undrained clay
D	footing depth of founding
d	liability and damages associated with failure
(d/c)	liability ratio
E	total load effect
$E()$	expected value operator
$f()$	probability density function
$\tilde{f}()$	predictive probability density function
g	performance function
$\tilde{g}$	auxiliary performance function
$\mathcal{I}$	marginal value of information
$\mathcal{L}$	total expected loss
N_c, N_q, N_γ	bearing capacity coefficients
n	sample size
n_{opt}	optimal sample size
p_{f0}	conditional probability of failure
$\tilde{p}_f$	predictive probability of failure
R	total resistance capacity
s_q, s_γ	shape factors
$V()$	variance operator
X	generic random variable
x	instance of a random variable
$\overline{x}$	sample mean
β_0	conditional reliability index
$\tilde{\beta}$	predictive reliability index
γ'	effective density
δ	coefficient of variation
μ	mean
σ^2	variance
Φ	standard normal cumulative density function
ϕ'	effective friction angle

7.1   Introduction

Estimates of soil strength characteristics based on samples comprising a minimal number of specimens are very common in geotechnical design. Best practice site characterisation is documented in a number of standards and guidelines (including EN 1997-2:2007, and Clayton *et al.*, 1995; Mayne *et al.*, 2001; Bond and Harris, 2008; SAICE, 2010). These guides tend to rely heavily on the expertise of the practitioner, and are relatively lenient with respect to small sample sizes (e.g. Bond and Harris, 2008). An unfortunate effect of this is that engineers often find it difficult to convince clients and developers to pay for more tests than the minimum requirement, despite numerous accounts of difficulties arising later during construction or commissioning due to insufficient initial geotechnical information (e.g. Phoon and Ching, 2013*a*; Phoon, 2016*b*; Day, 2017*b*).

As noted in Chapter 6 such small samples can only provide estimates of the mean parameter value, and are not sufficient to derive information on its variation. Consideration in the context of Bayesian updating suggests it is best to simply assume the values from the literature for inherent variability (Phoon *et al.*, 1995; Phoon and Kulhawy, 1999).

The effect of small sample sizes in partial factor limit states design (pfLSD) can be illustrated by repeating the analysis of the vertically loaded square footing in Example 2 of Chapter 3, considering the contrasting designs that would be obtained using two opposing sample outcomes from a target stratum (Figure 7.1). The 'true' stratum distribution for ϕ', which is not known to the engineer, is sampled according to the central limit theorem. Apparent reliability indices β_{apparent} for the designs, determined using the sample mean $\overline{\phi}$, are then compared to the actual reliability index β_{actual}, the index determined using the true stratum mean μ_ϕ.

In the under-designed case ($\overline{\phi'} > \mu$) the actual β is 75% of the apparent value, corresponding to failure being 20 times more likely than believed by the designers. In the over-designed case ($\overline{\phi'} < \mu$) the actual β of the design is 125% of the apparent value, and failure is 65 times less likely than believed by the designers.

Neither case is ideal: In the one case the structure is significantly less safe than believed, while in the other case the client could have been saved a significant sum of money. It is debatable whether the margin of safety built into the design via the partial factors is intended to account for this effect.

Although the difficulties associated with small sample sizes are evident, there is very little guidance on how much larger sample sizes need to be. It is also not realistic to expect routine studies to take a large number of specimens. This study aims to determine the optimal sample size from the perspective of balancing risk with the cost of information, in the framework of decision theory.

7.2   Theoretical Development

Routine reliability analysis, as applied during code calibration and reliability based design, uses specified values for statistical parameters. For example, the example problems in Chapter 3, each assumed a fixed value for the mean and standard deviation (via coefficient of variation) of variables such as the friction angle ϕ', density γ', and imposed loads Q_V. Yet the values of these parameters are based on sampling, and therefore have a degree of uncertainty that can be expected to decrease reliability.

As described by Der Kiureghian (2008), Ditlevsen showed that a rational decision maker should be indifferent between two design alternatives with the same predictive failure probabilities but different degrees of uncertainty. However, this indifference does not extend to the choice of data to use in the design. If the same decision maker is to choose between two sets of parameters upon which to base their analysis, they would choose the parameter set with the smaller likelihood of being incorrect, as now their decision is about the parameter set itself, rather than about the outcome of the structural analysis.

7.2.1   Reliability with Uncertain Parameters

The theory of reliability when uncertainty of parameters is taken into account is derived in detail by Der Kiureghian (1998) and Der Kiureghian (2008). The following summary simplifies this theory for a single random variable with known variance and uncertain mean, which will be used in the decision analysis framework developed in the next section.

Consider a geostructural design problem characterised by performance function $g(x)$, where x represents realisations of the stochastic variable X, with probability distribution function $f(x)$ and mean μ. The failure condition is then $g(x) < 0$.

In practice the value of μ would be based on a sample mean or on prior data. If μ has a fixed value, the probability of failure is given by

$$p_{f0} = \int_{g<0} f(x|\mu)dx, \tag{7.1}$$

from which the reliability follows as (Hasofer and Lind, 1974)

$$\beta_0 = \Phi^{-1}(1 - p_{f0}). \tag{7.2}$$

As this 'conditional' reliability is the standard definition used in reliability analysis, it is denoted using the subscript 0.

The predictive distribution of X takes the uncertainty in μ into account (e.g. Ang and Tang, 1984; Hald, 1952). It is given by

$$\tilde{f}(x) = \int_{-\infty}^{\infty} f(x|\mu)f(\mu)d\mu, \tag{7.3}$$

and represents the expected distribution function of X in the context of the parameter distribution function $f(\mu)$.

Ignoring all sources of error other than the inherent variability, the predictive probability of failure is then

$$\tilde{p}_f = \int_{g<0} \tilde{f}(x)dx, \tag{7.4}$$

and the associated predictive reliability

$$\tilde{\beta} = \Phi^{-1}(1 - \tilde{p}_f). \tag{7.5}$$

It can be shown (Wen and Chen, 1987; Der Kiureghian, 2008) that $\tilde{\beta}$ is equivalent to the reliability associated with the auxiliary performance function

$$\tilde{g} = u + \beta_0 \tag{7.6}$$

where u is a standard normal variable, i.e. $\mu_u = 0$ and $\sigma_u = 1$. From linearity follows that

$$\mu_{\tilde{g}} = \mu_{\beta_0}, \qquad \sigma_{\tilde{g}}^2 = 1 + \sigma_{\beta_0}^2. \tag{7.7}$$

If it is assumed that β_0 is normally distributed, then $\tilde{g} \sim \mathrm{N}(\mu_{\tilde{g}}, \sigma_{\tilde{g}})$, and

$$\tilde{\beta} = \mu_{\tilde{g}}/\sigma_{\tilde{g}}. \tag{7.8}$$

For the case where σ is known, this assumption can be expected to hold approximately via the central limit theorem.

Consider the case where $X \sim \mathrm{N}(\mu, \sigma)$. A n-sized sample is taken to estimate μ via $\overline{x}$, so that $\sigma_\mu = \sigma/\sqrt{n}$. If $g(x)$ is linear in x,

$$\beta_0 = \overline{x}/\sigma, \tag{7.9}$$

and

$$\mu_{\beta_0} = \overline{x}/\sigma, \qquad \sigma_{\beta_0}^2 = \sigma_\mu^2/\sigma^2 = 1/n, \tag{7.10}$$

which is substituted into Equations 7.7 and 7.8 to obtain

$$\tilde{\beta}_{\mathrm{N}} = \beta_0 \Big/ \sqrt{1 + 1/n}. \tag{7.11}$$

Equation 7.9 no longer holds when X is not normally distributed and/or $g(x)$ is nonlinear. In such an instance, μ_{β_0} and σ_{β_0} can be determined numerically, to give $\tilde{\beta}$ via Equation 7.8.

7.2.2 Optimal Risk

Consider a scenario where the unit cost of testing a soil sample (denoted c) is constant and independent of the number of tests. Taking the usual definition of risk as the product of the probability of failure and the value of the resultant liabilities and damages (denoted d), the expected loss is

$$\mathcal{L} = n + (d/c)\, \tilde{p}_f = n + (d/c)\, \Phi\left(-\tilde{\beta}\right),\qquad(7.12)$$

where (d/c) is the liable damages payable in the event of failure. Note that $\mathcal{L}$ has measures monetary value in units of c, the cost of a single test. Note further that we're using the predictive failure probability, as we're specifically interested in the effect of parameter uncertainty.

The marginal value of information $\mathcal{I}$, which indicates the true value of doing one additional test, is then given by

$$\mathcal{I} = -\left.\frac{\partial \mathcal{L}}{\partial n}\right|_{(d/c)} = \frac{(d/c)}{\sqrt{8\pi}} \exp\left(-\tilde{\beta}^2/2\right) \frac{d\tilde{\beta}}{dn} - 1.\qquad(7.13)$$

The optimal sample size n_{opt} corresponds to $\mathcal{I}$ reaching zero, such that

$$(d/c) = \sqrt{2\pi} \exp\left(\tilde{\beta}_{n_{\mathrm{opt}}}^2/2\right) \bigg/ \left.\frac{d\tilde{\beta}}{dn}\right|_{n_{\mathrm{opt}}}.\qquad(7.14)$$

In general n_{opt} must be found numerically. However, for the case when g itself is normally distributed, substituting Equation 7.11 for $\tilde{\beta}$ then gives

$$(d/c)_{\mathrm{N}} = \frac{\sqrt{8\pi}}{\beta_0} n_{\mathrm{opt}}^2 (1 + 1/n_{\mathrm{opt}})^{3/2} \exp\left(\frac{\beta_0^2/2}{1 + 1/n_{\mathrm{opt}}}\right),\qquad(7.15)$$

from which the optimal sample size n_{opt} for a given (d/c) follows implicitly.

Finally, taking the ratio of Equation 7.14 and 7.15 gives a correction factor by which (d/c) can be found from $(d/c)_{\mathrm{N}}$, as

$$\frac{(d/c)}{(d/c)_{\mathrm{N}}} = \frac{\beta_0/2}{n_{\mathrm{opt}}^2 (1 + 1/n_{\mathrm{opt}})^{3/2}} \exp\left(\tilde{\beta}_{n_{\mathrm{opt}}}^2/2\right) \exp\left(\frac{-\beta_0^2/2}{1 + 1/n_{\mathrm{opt}}}\right) \bigg/ \left.\frac{d\tilde{\beta}}{dn}\right|_{n_{\mathrm{opt}}},$$
$$(7.16)$$

with $\tilde{\beta}$ and $d\tilde{\beta}/dn$ evaluated numerically at n_{opt} via Equation 7.8.

7.3   Implementation

To illustrate the utility of the theory developed in Section 7.2, we will consider the vertically loaded square footing in Figure 7.2 in the context of reliability analysis with uncertain input parameters determined from a sample of size n.

In both cases, the performance function is represented as

$$g = R - E, \tag{7.17}$$

where R is the bearing capacity determined for the relevant soil type, and E is the total vertical load to be resisted. For the purposes of illustration, the value of E is kept at its mean value, and only one of the model parameters for R is treated as a stochastic variable.

7.3.1   Normal Cohesion in Undrained Clay

In the first case, the soil is represented as an undrained clay ($\phi' = 0$), with only the undrained cohesion c_u treated as a stochastic variable, which is assumed to be normally distributed here. For this problem the bearing capacity is given by

$$R = B^2 \left(c_u N_c + \gamma' D \right), \tag{7.18}$$

with N_c Skempton's bearing capacity coefficient (Skempton, 1951).

The model variables and distribution parameters for this example are given in Figure 7.2. For consistency, we will use the footing size $B = 3.24\,\text{m}$ determined previously in Example 2 of Chapter 3. This value is very close to that from a fresh design according to EN 1997:2004, which gives $B = 3.20\,\text{m}$. With $c_u \sim \text{N}$ the corresponding conditional reliability is $\beta_0 = 1.97$; for comparison, $\beta_0 = 3.82$ if $c_u \sim \text{LN}$.

Because R and therefore g are linear with c_u, $\tilde{\beta}$ can be determined using Equation 7.11 (Figure 7.3a). The resulting risk analysis is illustrated is Figures 7.3b&c for $(d/c) = 400$. This construct allows the optimal n to be determined numerically as a function of (d/c) – discrete numerical results are compared to the theoretical prediction determined using Equation 7.15 in Figure 7.3d.

7.3.2   Log-Normal Friction Angle in Cohesionless Sand

In the second case, the soil is taken to be a cohesionless sand, with the friction angle ϕ' treated as a log-normally distributed stochastic variable. For this problem the bearing capacity is given by

$$R = B^2 \left(\gamma' D s_q N_q + \tfrac{1}{2} \gamma' B s_\gamma N_\gamma \right), \tag{7.19}$$

where

$$N_q = \exp(\pi \tan \phi') \tan^2(\phi'/2 + 45°), \tag{7.20}$$

$$N_\gamma = 2(N_q - 1) \tan \phi', \tag{7.21}$$

$$s_q = 1 + \sin \phi', \quad s_\gamma = 0.7. \tag{7.22}$$

The model variables and distribution parameters for this example are again given in Figure 7.2. As in the previous case, the design from Chapter 3 is adopted, with $B = 3.24$ m, which corresponds to $\beta_0 = 3.84$ for $\phi' \sim$ LN. Note that this value is somewhat higher than the result in Chapter 3, as only a single random variable is used in the current analysis.

In this instance R is not a linear function of the stochastic variable, and therefore will not have a simple functional form for $f(g)$. $\tilde{\beta}$ is determined numerically by finding $E(\tilde{g})$ and $V(\tilde{g})$, assuming μ_g to be normally distributed with variance σ/n, based on the central limit theorem (Figures 7.4a). The resulting risk analysis is illustrated in Figures 7.4b&c for $(d/c) = 7000$. This construct allows the optimal n to be determined numerically as a function of (d/c). The discrete numerical results are compared to the theoretical prediction determined using Equation 7.15 and 7.16 in Figure 7.4d.

7.4   Discussion

For small samples, the predictive reliability $\tilde{\beta}$ is notably lower than the conditional reliability β_0, which it approaches from below relatively rapidly as n increases. As a result the risk and upfront investigation cost balance at an optimal sample size, the value of which depends on the magnitude of β_0, and the liable damages (d/c) payable upon failure.

The marginal value of a single test $\mathcal{I}$ increases proportionally with the liability ratio (d/c), and decreases for larger samples. If the value of a single additional test is greater than the cost of that test – as is the case for small sample sizes – it would be more profitable in the long run for the practitioners to do an additional test than to take a chance on a design based only on the information already at their disposal.

These trends are visible for both the idealised case where g is normally distributed (Figure 7.3), as well as the case when its distribution is not simple (Figure 7.4). In the latter, optimal sample size can be determined via the correction in Equation 7.16, though this additional calculation may not be justified in the light of relative uncertainty associated with the likely liability ratio (d/c). In the case for cohesionless sand considered above, the liability associated with an optimal sample size of around 10 is about 3 times lower than the value in the normally distributed case. A simplified correction of this nature should be sufficient in almost all cases.

Equation 7.15 provides guidance for the optimal sample size required in a given risk scenario. If an estimate of the potential damages and liabilities and the value of a single test is known, the target reliability to which a given design is performed can be used to determine the associated optimal sample size. Figures 7.5a&b provide reference charts determined from this equation.

As an example, consider a geostructural design based on a set of measurements with a unit cost of R2000 per test. If the design is found to be insufficient during later stages of construction, it is estimated that the cost of modification, repair, and the associated delays would be around R10-20 million, implying $(d/c) = 5 - 10 \times 10^3$. For a target reliability $\beta_0 = 3.0$, the optimal sample size is $n_{\mathrm{opt}} \approx 10$.

Note that the charts in Figure 7.5 are independent of the type of structure under design, although they do assume g to be normally distributed. As the form of g generally depends on the form of the resistance equation (Equations 7.18 vs 7.19, for example), separate charts would in principle have to be calculated for a given geotechnical parameter in a given geostructural setting.

However, given the rather arbitrary nature of current sample size choices, and the uncertainty in liability forecasts, the charts in Figure 7.5 provide sufficient initial guidance. These charts principally show that the minimal sampling practice currently accepted is seldom optimal, with sample sizes of around 5-15 a better choice. A sample size of $n = 10$ in the example discussed in the introduction to this Chapter, would result in the difference between the two characteristic values reducing from 21% to within 10% of each other, so that the two designs would more closely correspond to that which would be obtained from the actual stratum parameters.

7.5 Conclusion

A number of reliability engineers and researchers have pointed out that routine reliance on small sample sizes in soil strength determinations for geotechnical design is one of the primary culprits in geotechnical failures and subsequent delays during and after construction.

A decision analysis framework using predictive reliability indices has been developed, providing a relation between the optimal sample size, the conditional reliability (used as target β value), and the expected damages in case of failure. This relation is used to derive a set of reference charts that can be directly used to determine the optimal sample size for a given problem. Although these charts apply principally to a normally distributed limit state function, the relative uncertainty in forecasts of liability suggest that the charts can be applied more generally. A correction factor can nonetheless be determined, should a more accurate optimisation be required.

Consideration of the design charts for a target reliability of $\beta_0 = 3.0$ suggests that typical optimal sample sizes should fall between 5 and 15. While these values are notably higher than the minimal sizes characteristic of current practice, they are not impractical or unrealistic.

The analysis therefore suggests that greater initial investment in obtaining good quality information on the subsurface can save developers significant expenses later on in the project. However, although these results should be approximately relevant to realistic cases where multiple variables have meaningful uncertainty, a multivariate study including the effects of correlation, and of tests in which multiple properties are determined from a single sample, would clarify the relevance in a multivariate context.
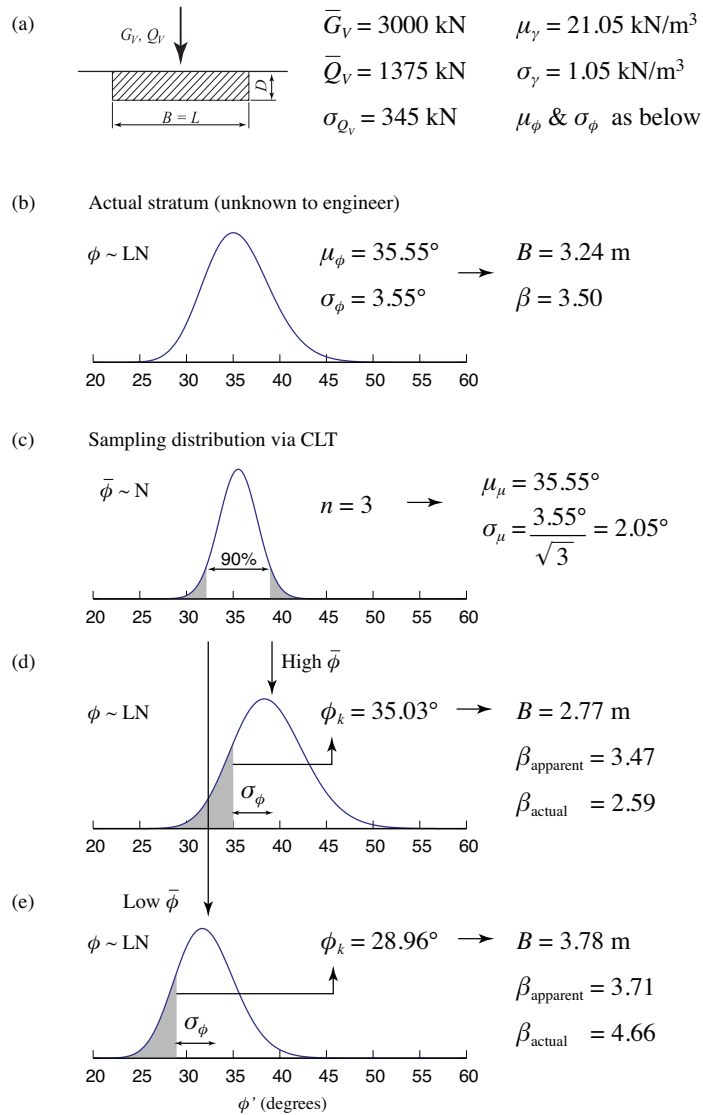
Figure 7.1: The effect of small samples on the range of characteristic values results in a notable range of designed footing width values and associated reliabilities.
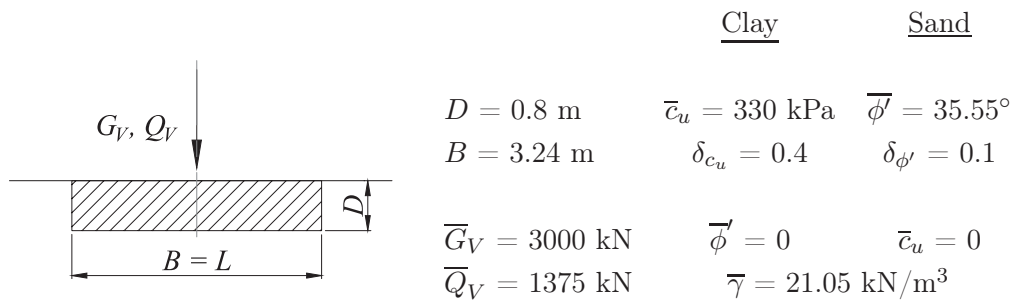
Figure 7.2: Loading and geometrical parameters for the square footing subjected to vertical loading, together with parameters for case when soil is an undrained clay and when it is a cohesionless sand.
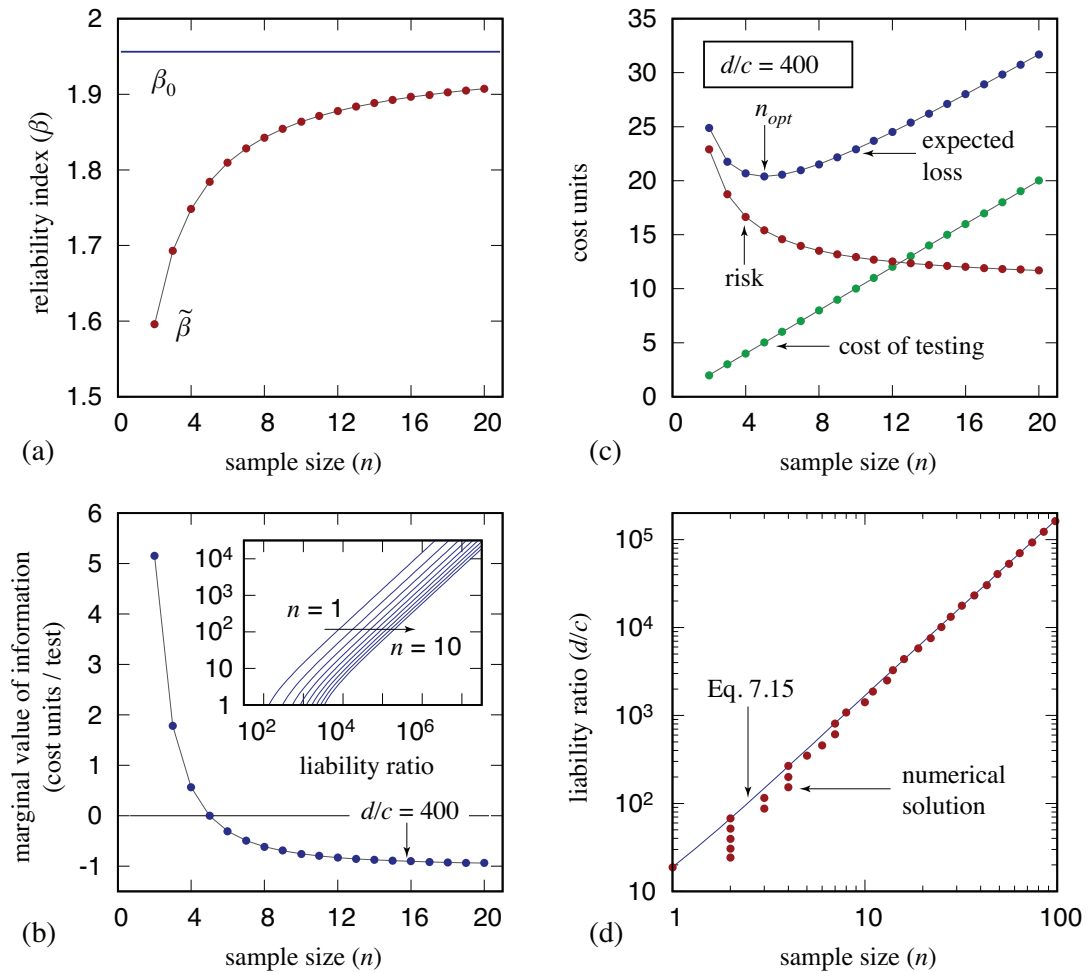
Figure 7.3: Risk analysis for vertically loaded square footing bearing on an undrained clay.
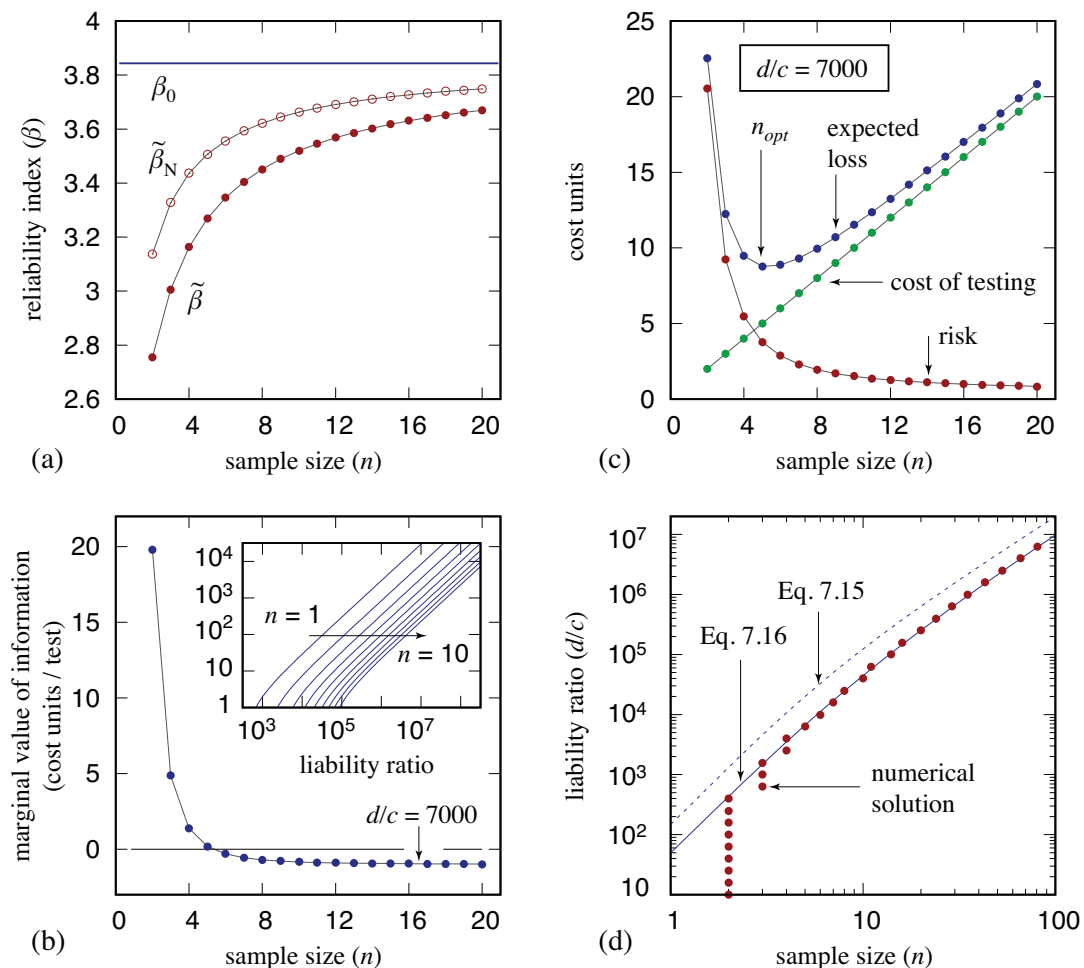
Figure 7.4: Risk analysis for vertically loaded square footing bearing on a cohesionless sand.
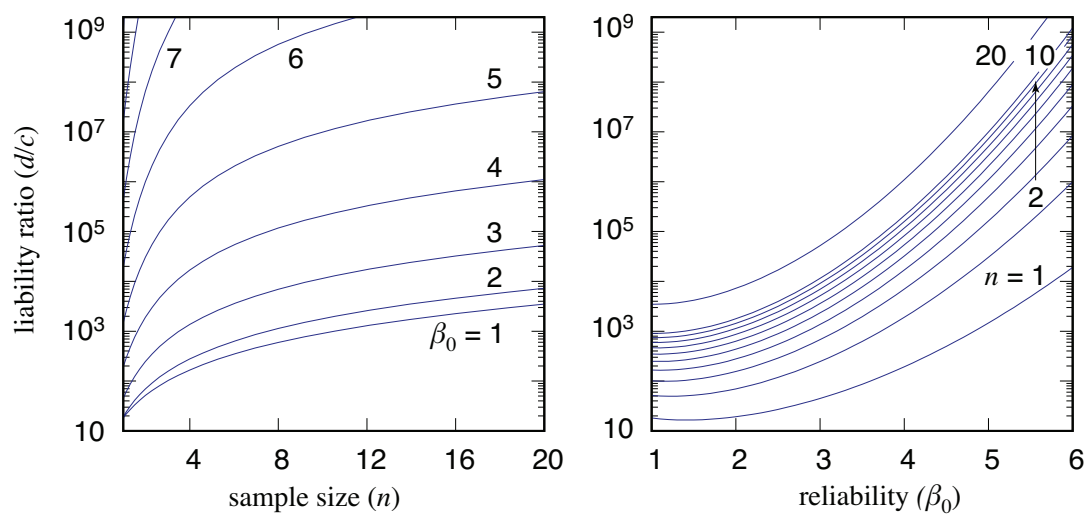
Figure 7.5: Reference charts for determining optimal sample size for a normally distributed random variate.

Chapter 8

Guidelines for Standardised Reliability Based Geostructural Design

8.1 Reliability Analysis in Geostructural Design

Design to a target reliability is possible in geostructural engineering, provided that the resistance model and the statistics describing its parameters, are accurate and unbiased. These requirements are not unique to probabilistic reliability based design (pRBD), and are certainly not a new idea – partial factor limit states design (pfLSD) requires knowledge of parameter distributions and typical mean and variation values to calibrate partial factors, and then requires a characteristic value to be determined for the site under consideration. The quality of sampling and measurement will affect pRBD just as severely as pfLSD. It is therefore of paramount importance that good quality site investigation and sample characterisation be performed for any geotechnical design with a reliability basis.

One might argue that rather than increasing upfront expenses on more thorough site investigation, a more economical means of dealing with the high uncertainty associated with small samples is to simply be more conservative in the design. Of course, it is seldom clear how much more conservative to be, while it is sometimes not even apparent how to be conservative in the first place (as the case considered in Chapter 4 illustrates). Yet more fundamentally, given the choice between a few more geotechnical tests and directly implementing a more conservative design *at the same cost*, opting for greater insight can potentially save the client money by either identifying unforeseen difficulties, or by showing that subsurface conditions are less adverse than originally anticipated (Phoon and Ching, 2013b). Combining more thorough investigation with reliability based design should therefore provide the most

cost-effective solution in the long run.

For reliability based design to be a useful tool for practicing engineers, the analysis technique needs to be robust and transparent, giving accurate reliability values with reasonable computational effort. As seen in the preceding chapters, a number of formulations are available to evaluate reliability. Our analysis indicates that, of the range of techniques available, the variants of the first order reliability method (FORM), in combination with an analytical surrogate performance function (response surface) where required, provides the best balance of transparency, economy, and accuracy.

8.2   Recommendations for a Geostructural Design Code

8.2.1   Reliability analysis techniques

As shown in Chapter 5, the elementary moment based analysis methods such as the point estimate method (PEM) and first-order second moment method (FOSM), are not sufficiently accurate to apply in a geotechnical context. While these methods are reasonably simple to implement, a comparable amount of computational effort can be used with the FORM variants to obtain far more accurate reliability estimates.

Three variations on the implementation of FORM can be considered, all based on Equation 2.67. The first is the Newton-like optimisation algorithm (NR-FORM in Chapter 5, also sometimes referred to as the HLRF algorithm). This option is especially suitable for closed-form performance functions, in which the gradient can be expressed analytically, and which includes an applied load as a free-standing stochastic variable. These requirements allow the numerical evaluation of the gradient and numerical root finding, respectively, to be replaced with closed-form analytical expressions.

The second option also involves finding the design point by optimisation, but uses a generic minimisation algorithm (see for example, Press *et al.*, 2007). This approach would be used when analysing a closed-form performance function in a generic numerical environment, as is done in the spreadsheet implementation of Low and Tang (2007). This option often involves a far greater number of performance function evaluations, but the difference has no practical significance for closed form formulations.

The third option applies either approach in the preceding two options to an analytical surrogate representation of the performance function (response surface), iteratively parameterised from the real one. This approach (RS-FORM) was shown to provide reliability estimates within a number of evaluations of the performance function comparable to those required by the PEM and FOSM methods. The geometrical implementation used in Chapter 5 is not the most optimal approach (for this, see the polynomial chaos expansion approach, e.g.

Sudret, 2015), but it is straightforward to implement in spreadsheet form, providing a good balance of robustness, transparency, accuracy, and economy.

The first or second approaches to FORM are therefore recommended for closed-form geostructural design problems, while the third is recommended for non-closed form problems requiring specialised software for the evaluation of the performance function. However, when applying FORM, the assumption of a linear limit state function, which forms its basis should not be lost from view, especially when multiple limit states are comparably critical.

8.2.2   Description of limit state function

Regardless of the technique used to determine reliability, an accurate, unbiased criterion for failure is required. Standardised empirical relationships used in working stress design or even limit states design codes are often parameterised to err towards being conservative (i.e. have mean model factor values larger than one). Unless the model factor is explicitly included in the analysis, reliability analyses using such relationships as performance functions will result in reliability values that are lower than the true value of the structure.

While descriptions of resistance capacity that are derived using the principles of statics and of limit equilibrium (such as the relationships used in Chapters 3 to 5) would usually not include biased parameters, model uncertainty may nonetheless be of interest in a precision context. Care is required on the part of the practitioner when setting up a reliability problem to ensure that the limit state function gives an accurate estimate of the balance between loading and resisting effects.

Analyses where only a subset of parameters can be treated stochastically are often still useful, for example cases where the relative dependence of reliability on parameter values is considered, or analyses comparing different designs using the same model parameters. For example, the analyses in Chapters 3-5 compare β values for designs obtained using the partial factors of EN 1997:2004. With the exception of piles, where resistance factors are used (Table 3.2), calibration of these partial factors does not account for model uncertainty. Comparison of the β values determined for the designs to target values used in calibrating EN 1997:2004 is therefore sensible, though interpreting failure probability values in an actuarial context is not.

While evaluation of the performance function via finite element analysis (FEA) is possible (Liu and Der Kiureghian, 1991; Haukaas and Der Kiureghian, 2005), further study of its use in geostructural reliability analysis is needed. Previous studies have identified two pitfalls. The first is that the performance function, and therefore the limit state function, is not always smooth or continuous when mapped using FEA. As a result, optimisation algorithms tend to struggle. The smoothing effect of the parameterised surrogate function used in RS-FORM should relieve this difficulty, but challenges with convergence can still occur. The second problem arises in defining or reaching the fail-

ure condition (e.g. Potgieter and Jacobsz, 2018). Different criteria for failure
will produce different reliability values for the same structure, and may not
correspond to physically reasonable conditions.

8.2.3   Reliability analysis tools

Calculations performed in this thesis used programs and scripts written by the
candidate using standard numerical libraries (Press *et al.*, 2007; MATLAB,
2018). In general, practitioners should not be required to go to such lengths,
not only for lack of time, but also to minimise undetected programming errors
from affecting analyses.

A number of existing programs and libraries are available specifically for
reliability analysis (PyRe in Python, UQLab in Matlab), while Low and Tang
(2007) have prepared a Microsoft Excel spreadsheet implementing FORM
through the built-in optimisation algorithms. This spreadsheet can be eas-
ily adapted to perform RS-FORM analyses. The set of example problems
used in Chapter 3 can serve as benchmark problems for practitioners to test
their chosen analysis tools.

However, the assumptions underlying FORM must always be kept in mind.
For example, they are no longer valid in systems reliability problems, such
as complex structures with a large number of failure modes of comparable
criticality.

8.2.4   Quality and Statistical Description of Parameters

Four factors determine the stochastic behaviour of a set of random variables,
each of which need to be accurately specified for successful reliability analysis.
These are (i) the type of distribution, (ii) the mean, (iii) the standard deviation
(or coefficient of variation), and (iv) the multivariate correlation coefficients.

The available databases (e.g. SAND/7/2794, Ching *et al.*, 2017) do not
allow a clear determination of the distribution of a given property (e.g. Figure
6.3), so that practitioners have to assume distributions that are compatible
with the data and other information regarding the random variable (Ditlevsen,
1994). As noted in Chapters 5, 6, and 7, reliability values determined for the
same structure assuming different probability distributions differ markedly. It
is therefore recommended that the appropriate distribution for each model
parameter used in geostructural analysis be standardised. For example, see
the distributions used for the density, cohesion, and friction angle in Chapter 5
(Table 5.1).

A poor estimate of the mean of a given parameter can also be detrimen-
tal to the reliability of a given design (see Figure 7.1). While the mean can
be supplemented using additional information from the site, such as in-situ
measurements coupled with transformation models, caution should be applied

to ensure that the prior information is applicable to the stratum under consideration. Ultimately, there is no substitute for taking more samples and performing good quality, dependable measurements on them. The charts derived using Equation 7.15, presented in Figure 7.5 are intended to guide the risk-optimal sample sizes for a given liability exposure, and suggest that 5 to 15 specimens per sample would be most appropriate for reliability based design.

In contrast to the mean, the sampling distribution of the variance (Section 6.4.1) implies that even these somewhat larger sample sizes are not sufficient to allow the standard deviation for a specific stratum to be determined. This problem is compounded by the fact that multiple factors contribute to the measured dispersion, in addition to the inherent variation of the stratum itself. However, Phoon *et al.* (1995) and Phoon and Kulhawy (1999) performed extensive analyses of large datasets of a variety of soil properties and soil types, and provide value ranges of the inherent coefficient of variation. The choice of value from these ranges can be left to the practitioner, based on engineering judgment from site observation. The reliance on prior information for the constraint of the coefficient of variation suggests that applying reliability analysis to unusual types of granular materials (such as virgin tailings or industrial waste materials), cannot be included in the scope of a reliability standard.

The analyses in Chapter 3 and 5 contrast reliability values determined with and without relatively weak correlation between friction angle and density (+ve), and friction angle and cohesion (−ve), respectively. In the latter case, correlation results in somewhat higher reliabilities, with a very weak decrease in the former case. Neglecting negative correlation between material parameters would therefore generally result in more conservative reliability based designs. While the qualitative effect of a given correlation should be understood, the poor constraints on correlation values and the notable complexity it introduces to the multivariate reliability problem suggests it can potentially be left out of a standardised formulation.

8.3   Further Work Required

The work performed during the course of compiling this thesis suggest a number of further studies to be performed, and remaining problems to be addressed. In short these include (i) derivation of partial factors for the South African context taking the above recommendations into account, (ii) simultaneous consideration of multiple failure modes in a systems reliability context, (iii) optimal sample size in the context of multivariate sampling, (iv) improving understanding of the geostructural model uncertainties, and (v) the use of finite element analysis in geostructural reliability analysis.

The above recommendations for the statistical treatment of model parameters also apply to the determination of characteristic values for pfLSD, as well as for the partial factor calibration process. A calibration study for South

African requirements, taking these recommendations into account is needed to determine what partitioning of load cases is needed (similar to the STR vs. STR-P limit states in SANS 10160-1:2010, and the distinction suggested by Equations 6.10a and 6.10b in EN 1990:2002). Such a study would also reveal the extent to which actual reliabilities obtained using pfLSD differ from the target value used in the calibration.

All the reliability analyses performed in this thesis assumed the presence of a single critical limit state. In principle, a single reliability determination should take the performance functions of all the possible limit states into account. However, one limit state generally dominates to the extent that the other states have a negligible effect on the probability of failure. This assumption breaks down when the critical limit state changes, as for example at high eccentricity values in Chapter 4. The resulting geometry of the limit state function can be non-differentiable and multi-planar, so that the approximations made by FORM no longer apply.

The guidelines in Chapter 7 for the number of specimens that should ideally be used to characterise stratum characteristics were derived assuming that only one property is obtained from a given specimen. It is often possible to obtain values for multiple parameters from a single specimen (density, friction angle, and cohesion, for example). Repeating the analysis in Chapter 7 in a multivariate context, taking multiple measurements into account could reveal to what extent the results in Chapter 7 can be used in the multivariate case.

By the nature and scale of geostructural problems, model uncertainties are not straightforward to to constrain (Dithinde *et al.*, 2016; Lesny *et al.*, 2018; Goh *et al.*, 2009). Field measurements that are deficient due to the inherent complexity of the problem being characterised could give the impression that tried and tested geostructural models have large and/or biased model factors, yet oversimplified models will typically only be accurate for a narrow range of parameters. The interplay of these factors is illustrated by the large range in model factors for piles (e.g. Dithinde *et al.*, 2016).

As noted above, deeper consideration of how best to combine the finite element method with reliability analysis for geostructural problems is required. A number of studies have considered the effect of spatial variability in the context of reliability in a relative sense; the suggested focus here is finite element analysis for design, in the context of the overall parameter uncertainty. Representing soil behaviour requires the use of plasticity models, whose constitutive relations are not readily related to the strength properties measured in the laboratory (e.g. Borja, 2013). In addition, the reliability determined would depend on what criteria are used to define and identify failure (the emergence of localised vs overall yielding; the a loss of stability; exceedance of a displacement threshold).

8.4   Final Comments

The work in this thesis has illustrated that probabilistic reliability based design provides a viable alternative to the established partial factor limit states design framework. What is primarily illustrated is the additional utility offered by reliability analysis, regardless of the framework used in obtaining the original design.

Both pRBD and pfLSD have a reliability basis (Figure 1.1), so that both techniques require similar statistical parameters to execute successfully. Practitioners can therefore supplement partial factor based designs with reliability analyses with minimal additional effort.

Limit states partial factor design is an established design framework which is routinely used in practice. Instead of requiring practitioners to choose between pfLSD and pRBD, providing a framework within which reliability analysis can be combined with pfLSD may be more useful. In this sense, initial designs are determined using pfLSD, and then optimised and refined based on reliability analysis where this is justified.

List of References

AASHTO:2002 (2002). *LRFD Highway Bridge Design Specifications.* American Association of State Highway and Transportation Officials, Washington, DC.

Ang, A.H. and Tang, W.H. (1984). *Probability Concepts in Engineering Planning and Design: Volume II Decision, Risk, and Reliability.* 1st edn. John Wiley and Sons, New York.

ASCE 7:2002 (2002). *Minimum Design Loads for Buildings and Other Structures.* American Society of Civil Engineers, Reston, VA.

Au, S. and Wang, Y. (2014). Engineering risk assessment with subset simulation.

Baecher, G.B. and Christian, J.T. (2003). *Reliability and Statistics in Geotechnical Engineering.* 1st edn. John Wiley and Sons, New York.

Barratt, B.J. and Day, P.W. (2016). Geotechnical design using sans 10160: A comparison with current practice. In: Jacobsz, S.W. (ed.), *Proceedings of the 1st Southern African Geotechnical Conference.* CRC Press, London.

Bond, A. and Harris, A. (2008). *Decoding Eurocode 7.* Taylor and Francis, London.

Borja, R.I. (2013). *Plasticity: Modeling & Computation.* 1st edn. Springer, Berlin.

Box, G.E.P. and Tiao, G.C. (1973). *Bayesian Inference in Statistical Analysis.* 1st edn. Addison-Wesley, Reading, MA.

Bucher, C.G. and Bourgund, U. (1990). A fast and efficient response surface approach for structural reliability problems. *Structural Safety*, vol. 7, no. 1, pp. 571–66.

Butterfield, R. and Gottardi, G. (1994). A complete three-dimensional failure envelope for shallow footings on sand. *Geotechnique*, vol. 44, no. 1, pp. 181–184.

Cao, Z., Wang, Y. and Li, D. (2016). Quantification of prior knowledge in geotechnical site characterization. *Engineering Geology*, vol. 203, pp. 107–116.

CHBDC CSA S6:2000 (2000). *Canadian Highway Bridge Design Code (CHBDC).* Canadian Standards Association, Mississauga, ON.

Chen, J.R. (2004). Axial behavior of drilled shafts in gravelly soils. ph.d. dissertation. Tech. Rep., Cornell University, Ithaca, NY.

144

Ching, J., Chen, J.-R., Yeh, J.-Y. and Phoon, K.K. (2012). Updating uncertainties in friction angles of clean sands. *Journal of Geotechnical and Geoenvironmental Engineering*, vol. 138, pp. 217–229.

Ching, J., Lin, G.-H., Chen, J.-R. and Phoon, K.K. (2017). Transformation models for effective friction angle and relative density calibrated based on generic database of coarse-grained soils. *Canadian Geotechnical Journal*, vol. 54, pp. 481–501.

Ching, J. and Phoon, K.K. (2011). A quantile-based approach for calibrating reliability-based partial factors. *Structural Safety*, vol. 33, pp. 275–285.

Ching, J. and Phoon, K.K. (2013). Mobilized shear strength of spatially variable soils under simple stress states. *Structural Safety*, vol. 41, pp. 20–28.

Christian, J.T. (2004). Geotechnical engineering reliability: How well do we know what we are doing? *Journal of Geotechnical and Geoenvironmental Engineering*, vol. 130, no. 10, pp. 985–1003.

Christian, J.T., Ladd, C.C. and Baecher, G.B. (1994). Reliability applied to slope stability analysis. *Journal of Geotechnical Engineering*, vol. 120, no. 12, pp. 2180–2207.

Clayton, C.R.I., Simons, N.E. and Matthews, M.C. (1995). *Site Investigation*. Wiley, New York.

Day, P.W. (2017*a*). Results of survey. Geotechnical Design Codes Meeting, SAICE Geotechnical Division, 2 November 2017.

Day, P.W. (2017*b*). Terzaghi oration – challenges and shortcomings in geotechnical engineering practice in the context of a developing country. In: Lee, W., Lee, J.-S., Kim, H.-K. and Kim, D.-S. (eds.), *Proceedings of the 19th International Conference on Soil Mechanics and Geotechnical Engineering, Seoul*, pp. 11–34. Korea Geotechnical Society, Seoul, Republic of Korea.

De Koker, N. and Day, P.W. (2017). Assessment of reliability based design for a spectrum of geotechnical design problems. *Proceedings of the ICE - Geotechnical Engineering*, vol. in press.

DeGroot, M.H. (1970). *Optimal Statistical Decisions*. 1st edn. McGraw-Hill, New York.

Der Kiureghian, A. (1998). Measures of structural safety under imperfect states of knowledge. *Journal of Structural Engineering*, vol. 115, no. 5, pp. 1119–1140.

Der Kiureghian, A. (2008). Analysis of structural reliability under parameter uncertainties. *Probabilistic Engineering Mechanics*, vol. 23, pp. 351–358.

Der Kiureghian, A. and Ditlevsen, O. (2008). Aleatory or epistemic? does it matter? *Structural Safety*, vol. 31, pp. 105–112.

Dithinde, M., Phoon, K.K., Ching, J., Zhang, L. and Retief, J. (2016). Statistical characterisation of model uncertainty. In: Phoon, K.K. and Retief, J.V. (eds.), *Reliability of Geotechnical Structures in ISO2394*, pp. 127–154. CRC Press, London, UK,.

Ditlevsen, O. (1994). Distribution arbitrariness in structural reliability. In: Schueller, G.I., Shinozuka, M. and Yao, J.T.P. (eds.), *Proceedings of the 6th International Conference on Structural Safety & Reliability (ICOSSAR'93)*, pp. 1241–1247. Balkeman, Rotterdam.

Ditlevsen, O. and Madsen, H.O. (1996). *Structural Reliability Methods.* 1st edn. John Wiley and Sons, Chichester.

Duncan, J.M. (2000). Factors of safety and reliability in geotechnical engineering. *Journal of Geotechnical and Geoenvironmental Engineering*, vol. 126, pp. 307–316.

Duncan, J.M. and Wright, S.G. (2005). *Soil Strength and Slope Stability.* 2nd edn. John Wiley and Sons, New York.

Ellingwood, B., Galambos, T.V., MacGregor, J.G. and Cornell, C.A. (1980). *Development of a Probability Based Load Criterion for American National Standard A58 - Building Code Requirements for Minimum Design Loads in Buildings and Other Structures.* US Department of Commerce, Washington.

EN 1990:2002 (2002). *Eurocode - Basis of Structural Design.* European Committee for Standardization, Brussels.

EN 1991-1-4:2005 (2005). *Eurocode 1 - Actions on structures - Part 1-4: General actions - Wind actions.* European Committee for Standardization, Brussels.

EN 1991:2002 (2002). *Eurocode 1 - Actions of Structures.* European Committee for Standardization, Brussels.

EN 1997-1:2004 (2004). *Eurocode 7: Geotechnical Design - Part 1: General Rules.* European Committee for Standardization, Brussels.

EN 1997-2:2007 (2007). *Eurocode 7: Geotechnical Design - Part 2: Ground Investigation and Testing.* European Committee for Standardization, Brussels.

EN 1997:2004 (2004). *Eurocode 7 - Geotechnical Design.* European Committee for Standardization, Brussels.

Fenton, G.A., Naghibi, F., Dundas, D., Bathurst, R.J. and Griffiths, D.V. (2016). Reliability-based geotechnical design in 2014 canadian highway bridge design code. *Canadian Geotechnical Journal*, vol. 53, no. 2, pp. 236–251.

Forrest, W.S. and Orr, T.L.L. (2011). The effect of model uncertainty on the reliability of spread foundations. In: Vogt, N., Schuppener, B., Straub, D. and Braü, G. (eds.), *Geotechnical Safety and Risk*, pp. 401–408. Bundesanstalt für Wasserbau, Karlsruhe.

Frank, R., Bauduin, C., Driscoll, R., Kavvadas, M., Krebs Ovesen, N., Orr, T. and B., S. (2004). *Designers Guide to EN 1997-1, Eurocode 7: Geotechnical design Part 1: General rules.* Thomas Telford, London.

Freudenthal, A.M. (1947). The safety of structures. *ASCE Transactions*, vol. 112.

Freudenthal, A.M. and Gumbel, E.J. (1953). On the statistical interpretation of fatigue tests. *Proceedings of the Royal Society of London A: Mathematical, Physical and Engineering Sciences*, vol. 216, pp. 309–332.

Galilei, G. (1638). *Dialogues Concerning Two New Sciences (Translated from the Italian and Latin by Henry Crew and Alfonso de Salvio.).* 1st edn. Macmillan, 1914, New York.

Gibson, W. (2011). Probabilistic methods for slope analysis and design. *Australian Geomechanics*, vol. 46, pp. 1–12.

Goh, A., Phoon, K. and Kulhawy, F. (2009). Reliability analysis of partial safety factor design method for cantilever retaining walls in granular soils. *Journal of Geotechnical and Geoenvironmental Engineering*, vol. 135, no. 5, pp. 616–622.

Gulvanessian, H. (2010). Eurocode: Basis of structural design. In: Roberts, J. (ed.), *The essential guide to Eurocodes transition.* British Standards Institution, London.

Gulvanessian, H. and Holicky, M. (2005). Eurocodes: using reliability analysis to combine action effects. *Proceedings of the Institution of Civil Engineers - Structures and Buildings*, vol. 158, no. 4, pp. 243–252.

Hald, A. (1952). *Statistical Theory with Engineering Applications.* 1st edn. John Wiley & Sons, New York.

Harr, M.E. (1987). *Reliability-Based Design in Civil Engineering.* 1st edn. McGraw-Hill, New York.

Harris, A. and Bond, A. (2010). Eurocode 7: Geotechnical design. In: Roberts, J. (ed.), *The essential guide to Eurocodes transition.* British Standards Institution, London.

Hasofer, A.M. and Lind, N.C. (1974). Exact and invariant second-moment code format. *Journal of the Engineering Mechanics Division, ASCE*, vol. 100, pp. 111–121.

Haukaas, T. and Der Kiureghian, A. (2005). Parameter sensitivity and importance measures in nonlinear finite element reliability analysis. *Journal of Engineering Mechanics*, vol. 131, no. 10, pp. 1013–1026.

Holicky, M. and Retief, J.V. (2005). Reliability assessment of alternative eurocode and south african load combination schemes for structural design. *Journal of the South African Institution of Civil Engineering*, vol. 47, pp. 15–20.

Holicky, M., Retief, J.V. and Dunaiski, P.E. (2010). The reliability basis of eurocode. Background to SANS 10160 - Basis of structural design and actions for buildings and industrial structures, pp. Ch.1–4. African Sun Media, Stellenbosch.

Honjo, Y. (2008). Monte carlo simulation in reliability analysis. In: Phoon, K.K. (ed.), *Reliability-Based Design in Geotechnical Engineering: Computations and Applications*, pp. 169–191. Taylor & Francis, New York.

Honjo, Y., Kikuchi, Y. and Shirato, M. (2010). Development of the design codes grounded on the performance-based design concept in japan. *Soils & Foundations*, vol. 50, no. 6, pp. 983–1000.

Husein Malkawi, A.I., Hassan, W.F. and Abdulla, F.A. (2000). Uncertainty and reliability analysis applied to slope stability. *Structural Safety*, vol. 22, pp. 161–187.

ISO 2394:2015 (2015). *General principles on reliability for structures.* International Organization for Standardization, Geneva.

ISO/IEC CD 14882:2013 (2013). *Programming Languages – C++.* International Organization for Standardization, Geneva.

JCSS (2008*a*). *Probabilistic Model Code.* Joint Committee on Structural Safety, available at http://www.jcss.ethz.ch/.

JCSS (2008*b*). *Risk Assessment in Engineering: Principles, System Representation & Risk Criteria.* Joint Committee on Structural Safety, available at http://www.jcss.ethz.ch/.

Jonkman, S.N. and Schweckendiek, T. (2015). Developments in levee reliability and flood risk analysis in the netherlands. In: Schweckendiek, T., Van Tol, A.F., Pereboom, D., Van Staveren, M.T. and Cools, P. (eds.), *Geotechnical Safety and Risk*.

Kirsten, H.A.D. (1983). Significance of the probability of failure in slope engineering. *The Civil Engineer in South Africa*, vol. 25, pp. 17–23.

Länsivaara, T. and Poutanen, T. (2013). Safety concepts for slope stability. In: L'Heureux, J., Locat, A., Leroueil, S., Demers, D. and Locat, J. (eds.), *Landslides in Sensitive Clays: From Geosciences to Risk Management*, pp. 395–407. Springer, Dortrecht.

Lesny, K., Akbas, S., Bogusz, W., Burlon, S., Vessia, G., Phoon, K., Tang, C. and Zhang, L. (2018). Chapter 2 - evaluation and consideration of model uncertainties in reliability based design. In: Phoon, K.K. and Simpson, B. (eds.), *Joint TC205/TC304 Working Group on 'Discussion of Statistical/Reliability Methods for Eurocodes'*, pp. 127–154. ISSMGE, London, UK,.

Li, D.-Q., Zheng, D., Cao, Z.-J., Tang, X.-S. and Phoon, K.-K. (2016). Response surface methods for slope reliability analysis: Review and comparison. *Engineering Geology*, vol. 203, pp. 3–14.

Liu, P.-L. and Der Kiureghian, A. (1991). Finite element reliability of geometrically nonlinear uncertain structures. *Journal of Engineering Mechanics*, vol. 117, no. 8, pp. 1806–1825.

Low, B.K. (2008). Practical reliability approach using spreadsheet. In: Phoon, K.K. (ed.), *Reliability-Based Design in Geotechnical Engineering: Computations and Applications*, pp. 134–168. Taylor & Francis, New York.

Low, B.K., Gilbert, R.B. and Wright, S.G. (1998). Slope reliability analysis using generalized method of slices. *Journal of Geotechnical and Geoenvironmental Engineering*, vol. 124, no. 4, pp. 350–362.

Low, B.K. and Phoon, K.K. (2015). Reliability-based design and its complementary role to eurocode 7 design approach. *Computers and Geotechnics*, vol. 65, pp. 30–44.

Low, B.K. and Tang, W.H. (2007). Efficient spreadsheet algorithm for first-order reliability method. *Journal of Engineering Mechanics*, vol. 133, no. 12, pp. 1378–1387.

Marques, S.H. (2017). Discussion on robustness in the context of eurocode 7 partial factor design. In: Huang, J., Fenton, G.A., Zhang, L. and Griffiths, D.V. (eds.), *Geo-Risk 2017: Reliability-Based Design and Code Developments*, pp. 425–435.

MATLAB (2018). *version 9.4.0 (R2018a)*. The MathWorks Inc., Natick, Massachusetts.

Mayne, P.W., Christopher, B.R. and DeJong, J. (2001). *Report FHWA-NHI-01-031: Subsurface Investigations*. National Highway Institute, Washington, D.C.

McQuarrie, D.A. (2003). *Mathematical Methods for Scientists and Engineers*. University Science Books, Sausalito, CA.

Melchers, R. (1999). *Structural Reliability Analysis and Prediction*. John Wiley & Sons, New York.

Meyerhof, G.G. (1976). Bearing capacity and settlement of pile foundations. *Journal of the Geotechnical Engineering Division, ASCE*, vol. 102, pp. 195–228.

Meyerhof, G.G. (1995). Development of geotechnical limit state design. *Canadian Geotechnical Journal*, vol. 32, no. 1, pp. 128–136.

Montgomery, D.C. and Runger, G.C. (2014). *Applied Statists and Probability for Engineers*. 6th edn. John Wiley & Sons, New York.

Murphy, K.P. (2007). Conjugate bayesian analysis of the gaussian distribution. Tech. Rep., University of British Columbia.

NA to BS EN 1990:2002 (2004). *UK National Annex for Eurocode 0 - Basis of Structural Design*. British Standards Institution, London.

NA to BS EN 1997:2004 (2007). *UK National Annex for Eurocode 7 - Geotechnical Design.* British Standards Institution, London.

O'Hagan, A. (1994). *Kendall's Advanced Theory of Statistics, Volume 2B: Bayesian Inference.* 1st edn. Arnold, London.

Orr, T.L.L., Bergdahl, U., Frank, R., Scarpelli, G. and Simpson, B. (2005). Evaluation of eurocode 7: Geotechnical design. In: Orr, T.L.L. (ed.), *Proceedings of the International Workshop on the Evaluation of Eurocode 7.*

Peck, R.B. (1969). Advantages and limitations of the observational method. *Geotechnique*, vol. 19, no. 2, pp. 171–187.

Pereira, C. and Caldeira, L. (2011). Shallow foundation design through probabilistic and deterministic methods. In: Vogt, N., Schuppener, B., Straub, D. and Braü, G. (eds.), *Geotechnical Safety and Risk*, pp. 199–207. Bundesanstalt für Wasserbau, Karlsruhe.

Petroski, H. (1994). *Design Paradigms Case Histories of Error and Judgment in Engineering.* 1st edn. Cambridge University Press, Cambridge, UK.

Phoon, K.K. (2008*a*). Numerical recipes for reliability analysis - a primer. In: Phoon, K.K. (ed.), *Reliability-Based Design in Geotechnical Engineering: Computations and Applications*, pp. 1–75. Taylor & Francis, New York.

Phoon, K.K. (2008*b*). *Reliability-Based Design in Geotechnical Engineering: Computations and Applications.* Taylor & Francis, New York.

Phoon, K.K. (2016*a*). Reliability as a basis for geotechnical design. In: Phoon, K.K. and Retief, J.V. (eds.), *Reliability of Geotechnical Structures in ISO2394*, pp. 1–25. CRC Press, London, UK,.

Phoon, K.K. (2016*b*). Role of reliability calculations in geotechnical design. *Georisk: Assessment and Management of Risk for Engineered Systems and Geohazards, doi: 10.1080/17499518.2016.1265653.*

Phoon, K.K. and Ching, J. (2013*a*). Beyond coefficient of variation for statistical characterization of geotechnical parameters. In: Coutinho, R.W. and Mayne, P.W. (eds.), *Geotechnical and Geophysical Site Characterization*, pp. 113–130. Taylor & Francis, New York.

Phoon, K.K. and Ching, J. (2013*b*). Is site investigation an investment or expense? – a reliability perspective. In: Leung, C.F., Goh, S.H. and Shen, R.F. (eds.), *Advances in Geotechnical Infrastructure*, pp. 25–43. Geotechnical Society of Singapore, Singapore.

Phoon, K.K. and Ching, J. (2015). *Risk and Reliability in Geotechnical Engineering.* CRC Press, London, UK,.

Phoon, K.K., Ching, J. and Chen, J.R. (2011). How reliable are reliability-based multiple factor code formats? In: Vogt, N., Schuppener, B., Straub, D. and Braü, G. (eds.), *Geotechnical Safety and Risk*, pp. 85–104. Bundesanstalt für Wasserbau, Karlsruhe.

Phoon, K.K. and Kulhawy, F.H. (1999). Characterization of geotechnical variability. *Canadian Geotechnical Journal*, vol. 36, pp. 612–624.

Phoon, K.K., Kulhawy, F.H. and Grigoriu, M.D. (1995). *Report TR-105000: Reliability-Based Design of Foundations for Transmission Line Structures*. Electric Power Research Institute, Palo Alto, CA.

Phoon, K.K., Kulhawy, F.H. and Grigoriu, M.D. (2003). Development of a reliability-based design framework for transmission line structure foundations. *Journal of Geotechnical and Geoenvironmental Engineering*, vol. 129, no. 9, pp. 798–806.

Potgieter, J. and Jacobsz, S.W. (2018). Finite element versus limit equilibrium methods for analysis of lateral support. *Civl Engineering - Siviele Ingenieurswese*, vol. 26, no. 6, pp. 42–48.

Poulos, H.G. and Davis, E.H. (1980). *Pile Foundation Analysis and Design*. Series in geotechnical engineering. John Wiley and Sons, New York.

Press, W.H., Teukolsky, S.A., Vetterling, W.T. and Flannery, B.P. (2007). *Numerical Recipes: The Art of Scientific Computing*. 3rd edn. Cambridge University Press, Cambridge.

Pugsley, A. (1955). Report on structural safety. *Structural Engineer*, vol. 33, pp. 141–149.

Rackwitz, R. and Fiessler, B. (1978). Structural reliability under combined random load sequences. *Computers and Structures*, vol. 9, pp. 484–494.

Reissner, H. (1924). Zum erddruckproblem. In: *Proceedings, First International Conference on Applied Mechanics*. Delft.

Retief, J.V., Dithinde, M. and Phoon, K.K. (2016). General principles on reliability according to iso2394. In: Phoon, K.K. and Retief, J.V. (eds.), *Reliability of Geotechnical Structures in ISO2394*, pp. 33–48. CRC Press, London, UK,.

Retief, J.V. and Dunaiski, P.E. (2010). The limit states basis of structural design for sans 10160-1. Background to SANS 10160 - Basis of structural design and actions for buildings and industrial structures, pp. Ch.1–2. African Sun Media, Stellenbosch.

SAICE (2010). *Site Investigation Code of Practice*. South African Institution of Civil Engineering - Geotechnical Division, Johannesburg.

SANS 10160-1:2010 (2010). *Basis of structural design and actions for buildings and industrial structures, Part 1: Basis of structural design*. South African Bureau of Standards, Pretoria.

SANS 10160:2010 (2010). *Basis of structural design and actions for buildings and industrial structures, Parts 1-8.* South African Bureau of Standards, Pretoria.

Santamarina, J.C., Altschaeffl, A.G. and Chameau, J.L. (1992). Reliability of slopes: Incorporating qualitative information. *Transportation Research Record*, vol. 1343, pp. 1–5.

Schneider, H.R. (1997). Panel discussion: Definition and determination of characteristic soil properties. In: *Proceedings of the Fourteenth International Conference on Soil Mechanics and Foundation Engineering. Proceedings*, vol. 4, pp. 2271–2274. Hamburg.

Simpson, B. (2007). Approaches to uls design - the merits of design approach 1 in eurocode 7. In: *Proceedings of the First International Symposium on Geotechnical Safety and Risk, Shanghai, China*, pp. 527–538.

Simpson, B., Pappin, J.W. and Croft, D.D. (1981). An approach to limit state calculations in geotechnics. *Ground Engineering*, vol. 14, pp. 21–28.

Skempton, A.W. (1951). The bearing capacity of clays. *Proceedings of the Building Research Congress*, vol. 1, pp. 180–189.

Sklar, A. (1959). Fonctions de répartition à n dimensions et leurs marges. *Publications de l'Institut de statistique de l'Université de Paris*, vol. 8, pp. 229–231.

Spencer, E. (1967). A method of analysis of the stability of embankments assuming parallel inter-slice forces. *Géotechnique*, vol. 17, no. 1, pp. 11–26.

Straub, D. and Papaioannou, I. (2015). Bayesian analysis for learning and updating geotechnical parameters and models with measurements. In: Phoon, K.K. and Ching, J. (eds.), *Risk and Reliability in Geotechnical Engineering*, pp. 221–264. CRC Press, London, UK,.

Sudret, B. (2015). Polynomial chaos expansions and stochastic finite-element methods. In: Phoon, K.K. and Ching, J. (eds.), *Risk and Reliability in Geotechnical Engineering*, pp. 265–300. CRC Press, London, UK,.

Vanmarcke, E.H. (1977). Probabilisitic modeling of soil profiles. *Journal of the Geotechnical Engineering Division, ASCE*, vol. 103, no. GT11.

Vesic, A.S. (1967). A study of bearing capacity of deep foundations. In: *Final Report, Project B-189*, pp. 2271–2274. School of Civil Engineering, Georgia Inst. Tech., Atlanta, Ga.

Vogt, N. and Schuppener, B. (2006). Implementation of eurocode 7-1 geotechnical design in germany. In: *Proceedings of the International Symposium on New Generation Design Codes for Geotechnical Engineering Practice, Taipei, Taiwan*, pp. 1–12.

Wang, Y., Schweckendiek, T., Gong, W., Zhao, T. and Phoon, K.K. (2016). Direct probability-based design methods. In: Phoon, K.K. and Retief, J.V. (eds.), *Reliability of Geotechnical Structures in ISO2394*, pp. 193–226. CRC Press, London, UK.

Wen, Y.K. and Chen, H.C. (1987). On fast integration for time variant structural reliability. *Probabilistic Engineering Mechanics*, vol. 2, no. 3, pp. 156–162.

Wong, F.S. (1985). Slope reliability and response surface method. *Journal of Geotechnical Engineering*, vol. 111, no. 1, pp. 32–53.
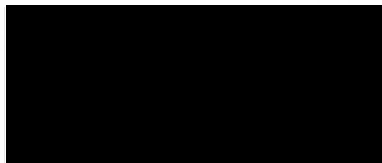
Declaration by the candidate (Chapter 3):

The scope of the candidate's contribution to Chapter 3 of this thesis, "*Assessment of Reliability Based Design for a Spectrum of Geotechnical Design Problems*", which has been published in the *Proceedings of the Institution of Civil Engineers -- Geotechnical Engineering,* was as follows:

Nature of contribution	Extent of contribution
Conceptualized and wrote manuscript	90 %
Modeling and calculations	
Review of existing literature	

The following co-authors contributed to Chapter 3 of this thesis:

Name	E-mail address	Nature of contribution	Extent of contribution
P. W. Day	day@jaws.co.za	Contributed to writing of the manuscript	10%

Signature of the candidate: ███████████

Date: _19 JuLY 2018_

Declaration by co-authors (Chapter 3):

The undersigned hereby confirm that:
1. The declaration above accurately reflects the nature and extent of the contribution of the candidate and the co-authors to Chapter 3 of this thesis,
2. No other author contributed to Chapter 3 of this thesis, and
3. Potential conflicts of interest have been revealed to all interested parties, and that the necessary arrangements have been made to use the material in Chapter 3 of this thesis.

	Signature	Date	Affiliation
P.W. Day	███████████	19 July 2018	University of Stellenbosch

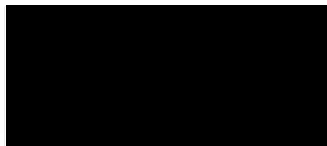## Declaration by the candidate (Chapter 4):

The scope of the candidate's contribution to Chapter 4 of this thesis, "*Reliability Analysis of EN1997 Design Approaches for Eccentrically Loaded Footings*", which has been published in the *Proceedings of the Institution of Civil Engineers -- Geotechnical Engineering,* was as follows:

Nature of contribution	Extent of contribution
Conceptualized and wrote manuscript	90 %
Modeling and calculations	
Review of existing literature	

The following co-authors contributed to Chapter 4 of this thesis:

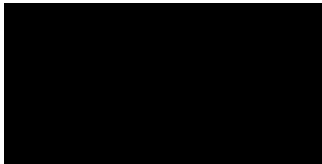| Name	E-mail address	Nature of contribution	Extent of contribution
P. W. Day	day@jaws.co.za	Contributed to writing of the manuscript	10%

Signature of the candidate:

Date: 19 July 2018

Declaration by co-authors (Chapter 4):

The undersigned hereby confirm that:
1. The declaration above accurately reflects the nature and extent of the contribution of the candidate and the co-authors to Chapter 4 of this thesis,
2. No other author ccontributed to Chapter 4 of this thesis, and
3. Potential conflicts of interest have been revealed to all interested parties, and that the necessary arrangements have been made to use the material in Chapter 4 of this thesis.

	Signature	Date	Affiliation
P.W. Day		19 July 2018	University of Stellenbosch

Declaration by the candidate (Chapter 5):

The scope of the candidate's contribution to Chapter 5 of this thesis, "*Assessment of Reliability Based Design of Stable Slopes*", which has been published in the *Canadian Geotechnical Journal*, was as follows:

Nature of contribution	Extent of contribution
Conceptualized and wrote manuscript	85 %
Modeling and calculations	
Review of existing literature	

The following co-authors contributed to Chapter 5 of this thesis:

Name	E-mail address	Nature of contribution	Extent of contribution
P. W. Day	day@jaws.co.za	Contributed to writing of the manuscript	5%
A.S. Zwiers	andy.zwiers@stantec.com	Contributed to literature review and writing of the manuscript	10%

Signature of the candidate: ███████████

Date: *17 July 2018*

Declaration by co-authors (Chapter 5):

The undersigned hereby confirm that:
1. The declaration above accurately reflects the nature and extent of the contribution of the candidate and the co-authors to Chapter 5 of this thesis,
2. No other author contributed to Chapter 5 of this thesis, and
3. Potential conflicts of interest have been revealed to all interested parties, and that the necessary arrangements have been made to use the material in Chapter 5 of this thesis.
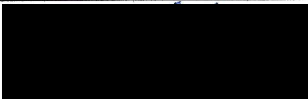
	Signature	Date	Affiliation
P.W. Day	███████	17 July 2018	University of Stellenbosch
A.S. Zwier	███████	17/07/2018	University of Stellenbosch

UNIVERSITEIT·STELLENBOSCH·UNIVERSITY
jou kennisvennoot • your knowledge partner

Plagiaatverklaring / Plagiarism *Declaration*

1   Plagiaat is die oorneem en gebruik van die idees, materiaal en ander intellektuele eiendom van ander persone asof dit jou eie werk is.
Plagiarism is the use of ideas, material and other intellectual property of another's work and to present is as my own.

2   Ek erken dat die pleeg van plagiaat 'n strafbare oortreding is aangesien dit 'n vorm van diefstal is.
I agree that plagiarism is a punishable offence because it constitutes theft.

3   Ek verstaan ook dat direkte vertalings plagiaat is.
I also understand that direct translations are plagiarism.

4   Dienooreenkomstig is alle aanhalings en bydraes vanuit enige bron (ingesluit die internet) volledig verwys (erken). Ek erken dat die woordelikse aanhaal van teks sonder aanhalingstekens (selfs al word die bron volledig erken) plagiaat is.
Accordingly all quotations and contributions from any source whatsoever (including the internet) have been cited fully. I understand that the reproduction of text without quotation marks (even when the source is cited) is plagiarism.

5   Ek verklaar dat die werk in hierdie skryfstuk vervat, behalwe waar anders aangedui, my eie oorspronklike werk is en dat ek dit nie vantevore in die geheel of gedeeltelik ingehandig het vir bepunting in hierdie module/werkstuk of 'n ander module/werkstuk nie.
I declare that the work contained in this assignment, except where otherwise stated, is my original work and that I have not previously (in its entirety or in part) submitted it for grading in this module/assignment or another module/assignment.

████████████	████████████
Studentenommer / *Student number*	Handtekening / *Signature*
N P J DE KOKER	18 JULY 2018
Voorletters en van / *Initials and surname*	Datum / *Date*

ICE Publishing is part of the Institution of Civil Engineers

ICE Virtual Library
essential engineering knowledge

Cart   Mobile   Help   S

Home   Journals   Books   Subjects   Information   News   ICE 200   About   Contact

Enter words / phrases / DOI / ISBN / authors / keywords / etc.

Anywhere ▾   Search

Home

Permissions and Copyright

Use our below tool to find out how to share your article, re-use it elsewhere, apply to use part of someone else's article, or ask a question about copyright.

What are my rights as an author?

How can I use / share my published article?

Activity	Subscriber content	Gold open access
Post the accepted version on open, unrestricted websites or deposit it in an institutional repository, with a link to the version of record 12 months after the publication of your article. Your accepted article is the peer-reviewed version that has been accepted (not the page proof or final PDF). The version of record is the final PDF. For further information on open access click here.	Y	Y
Share your article directly with up to 50 colleagues	Y	Y
Share your article's title and abstract with a weblink to the version of record (final PDF) on the ICE Virtual Library, via social media, or in a second party mailing (such as an electronic newsletter)	Y	Y
Explain the impact of your work and share it using www.growkudos.com	Y	Y
--		
Post the version of record (final PDF) of your article on an open website, social sharing sites (such as Mendeley, ResearchGate, Academia.edu), via social media, or in a second party mailing (such as an electronic newsletter)	N	Y
Print a commercial number of copies (greater than 50). If you require more than 50 hardcopies, we offer a professional printing service	N	Y
Use the PDF for commercial (fee-earning) purposes	N	Y
Make further changes to the published article (the version of record). This includes online ahead of print (AoP) publication	N	Dependent on licence chosen by author

Copyright transfer form

Asking to use our content

Using other people's content in your article for us

Find out more

Author home

Writing Master Cla
Part 1 of our writing gu
help on getting your pa

Writing Master Cla
Part 2 of our guide give
outstanding articles

Submitting your ar
Find out what you nee
submitting your article

Preparing your ma
Learn more about prep
article for publication

After acceptance
Discover how we prep
for publication

Author ethics
ICE Publishing adheres
of conduct in all its wo

Best Paper Award
Explore our award winn
free to access

Frequently asked
Our FAQ answers prov
and guidance

Increase the impa
Use the free tools avail
Kudos author commun
platform

No recently viewed arti

Resources:

> Home   > For Librarians
> Journals   > Help and FAQs
> Books   > About ICE Publishing

Subjects:

> Buildings and structures

> Coastal and offshore engineering

> Development, planning and urban engineering

> Energy

> Geology, geotechnical and ground engineering

> Health and safety

> Law and contracts

> Leadership and management

> Professional developme

> Science

> Transportation

> Water engineering and management

Powered by Atypon® Literatum

Powered by Atypon® Literatum

Canadian Science Publishing

Home   About Us   Journals   Books   Compilations   Open Access   Authors   Librarians   Societies   Blog   Contact   Français

Services

Submissions

Just-IN

Reprints & permissions

Video abstracts

Plain language summaries

How to Deposit to Tspace or Another Institution Repository

Publishing Toolkit for authors

License to publish forms (copyright agreements for publishing)

Permission forms

Your responsibilities as an author (Publishing Policy)

Files and graphics

Authors' rights

General ethical guidelines

English-improvement services

Successful publishing strategies for authors

Authors' rights

As of 2009, copyright of all articles in NRC Research Press journals remains with the authors. Copyright of all articles published prior to 2009 is held by Canadian Science Publishing (operating as NRC Research Press) or its licensors (also see our Copyright and Reuse of Content information).

Under the terms of the license to publish granted to NRC Research Press, authors retain the following rights:

1. To post a copy of their submitted manuscript (pre-print) on their own website, an institutional repository, a preprint server, or their funding body's designated archive (no embargo period). Publication on a preprint server prior to submitting to an NRC Research Press journal does not constitute "prior publication".

2. To post a copy of their accepted manuscript (post-print) on their own website, an institutional repository, a preprint server, or their funding body's designated archive (no embargo period). Authors who archive or self-archive accepted articles are asked to provide a hyperlink from the manuscript to the Journal's website.

3. Authors, and any academic institution where they work at the time, may reproduce their manuscript for the purpose of course teaching.

4. Authors may reuse all or part of their manuscript in other works created by them for non-commercial purposes, provided the original publication in an NRC Research Press journal is acknowledged through a note or citation.

These authors' rights ensure that NRC Research Press journals are compliant with open access policies of research funding agencies, including the Canadian Institutes of Health Research, the Natural Sciences and Engineering Research Council of Canada, the US National Institutes of Health, the Wellcome Trust, the UK Medical Research Council, l'Institut national de la santé et de la recherche médicale in France, and others.

In support of authors who wish or need to sponsor open access to their published research articles, NRC Research Press also offers a Gold Open Access (OpenArticle) option.

The above rights do not extend to copying or reproduction of the full article for commercial purposes. Authorization to do so may be obtained by clicking on the "Reprints & Permissions" link in the Article Tools menu of the article in question or under license by Access Copyright. The Article Tools menu is accessible through the full-text article or abstract page.

Connect With Us   ✉ Alerts   CSP Blog   f Facebook   Twitter   YouTube   in Linked In   RSS

research4life   COUNTER   RSC SRC The Royal Society of Canada / La Société royale du Canada   RightsLink®

crossref   cross check   PRESERVED IN CLOCKSS   COPE   PORTICO   readcube